Bupropion's Bioinequivalence: Patient Variability, Absorption, and Metabolism

by

Jamie Nicole Connarn

A dissertation submitted in partial fulfillment
of the requirements for the degree of
Doctor of Philosophy
(Pharmaceutical Sciences)
in the University of Michigan
2015

Doctoral Committee:

      Professor Duxin Sun, Chair
      Professor Gordon L. Amidon
      Professor Vicki L. Ellingrod
      Professor David E. Smith

Dedication

To my family for all their love, prayers, and support; especially my Mom.

together in Ann Arbor. A special thanks to two of my best friends who helped me through many times over years; Melissa Benham and Maryann Oram.

Finally, I would like to thank *all of my family* especially; my parents Leslie Persin and Jim Connarn and my sister Jennifer and Jessica Connarn for their love and support.

TABLE OF CONTENTS

List of Figures

List of Tables

List of Appendices

List of Abbreviations

ANDA: Abbreviated new drug application

AUC: Area under the curve

CE: Collision energy

CL_{int}: Intrinisic clearance

BE: Bioequivalence

BUP: Bupropion

CHIP: C- terminus of HSC70- Interacting Protein

CI: Confidence intervals

CR: Carbonyl reductase

CYP: Cytochrome P450

CYP2B6: Cytochrome P450 2B6

DAT: Dopamine transporter

DP: Declustering potential

DRC: Dose response curves

E-BUP: Erythrohydrobupropion

EP: Entrance potential

ESI: Electron spray ionization

FDA: Food and Drug Administration

GI: Gastrointestinal

H-BUP: Hydroxybupropion

HOP: Hsp70- Hsp90 Organizing Protein

HSP: Heat shock protein

IR: Immediate release

IS: Internal standard

LC: Liquid chromatography

LLOQ: Lower limit of quantification

MDD: Major depressive disorder

Min: Minutes

MR: Modified release

MRM: Multiple reaction monitoring

MS: Mass spectrometry

NET: Norepinephrine transporter

PK: Pharmacokinetics

PPI: Protein-protein interactions

T-BUP: Threohydrobupropion

XL or ER: Extended release

Abstract

Bupropion is a clinically available drug product, marketed as Wellbutrin and Zyban. Bupropion is a norepinephrine/dopamine reuptake inhibitor used for major depressive disorder, seasonal affective disorder, and smoking cessation. A single dose bioequivalence (BE) study was performed for generic versions of bupropion and the name brand product, Wellbutrin. Due to dose related seizures associated with the 300 mg dose, BE studies with the 150 mg dose was extrapolated to the 300 mg dose. However, after complaints of lack of efficacy and adverse effects, the FDA conducted a pilot study on one generic (Budeprion 300 XL) with Wellbutrin 300 XL where it was found that some of the 300 mg generic formulations were bioinequivalent. Therefore, the purpose of these studies was to understand how absorption, metabolism/ metabolic enzymes expression, and patient variability influenced bupropion's pharmacokinetics. Bupropion produced three active metabolites via two separate pathways, cytochrome P450 2B6 and carbonyl reductase. We compared the relative contribution of the two metabolic pathways of bupropion (by cytochrome P450 2B6 and carbonyl reductase) in the subcellular fractions of liver and intestine, investigated the difference of bupropion's metabolism in both liver and intestines, and identified which carbonyl reductases might be responsible for bupropion's metabolism. Secondly, we looked at healthy individuals to see how differences in both enzyme expression (such as polymorphisms in cytochrome P450 2B6) and various formulations (immediate, sustained, or extended release) can affect the pharmacokinetics of bupropion and metabolites in humans.

Chapter 1
Background and Introduction

1.1 Introduction to Bupropion

Bupropion HCl is a clinically approved drug that is used for treatment of major depressive disorder (MDD), smoking cessation, and seasonal affective disorder. Bupropion was first marketed as Wellbutrin in the late 1980's by GlaxoSmithKline [1]. Bupropion, a non-tricyclic antidepressant, is a nonselective inhibitor of dopamine (DAT) and norepinephrine (NET) transport [2]. It is also thought that bupropion is an antagonist of the neuronal nicotinic acetylcholine receptor (nAChR) which contributes to its use as a smoking cessation drug [3]. Currently, over 11 million prescriptions of bupropion have been issued annually [4, 5]. Bupropion was initially released as an immediate release product that was dosed 3 times daily. In 1996, a sustained release formulation (dosed twice daily) and in 2003 an extended release formulation (dosed once daily) were approved [6]. One risk that is associated with bupropion is dose related seizures, particularly it was thought to start at doses of 300 mg and higher [7]. In addition to seizures, other side effects have been associated such as headaches, dry mouth, and insomnia [8].

1.2 Pharmacology

Bupropion is a free base with a molecular weight of 239.74 g/mole (bupropion HCl, 276.2 g/mol). The logP of bupropion HCl at 37 ºC in n-octanol water solution at pH 7 is 3.4 and the pKa of bupropion is 7.9. Bupropion is highly soluble in water at 312 mg/mL.

There has been some debate on bupropion's true mechanism [9]. It has been proposed that bupropion is a nonselective inhibitor of DAT and NET transporters [2]. Based on studies using positron emission tomography, bupropion and its metabolites have been shown to act on the DAT in the brain. However, the occupancy was found to be low (6-22%) for DAT; this has raised questions whether therapeutic levels can be reached for efficacy or whether another mechanism of action is involved [10]. Other studies have revealed that bupropion may act as a noncompetitive nicotinic antagonist, which would explain the efficacy as smoking cessation agent [11, 12]. However, unlike many antidepressants that are typically selective serotonin reuptake inhibitors, bupropion has been associated with less severe side effects including; sexual dysfunction, suicidal depression, fatigue, and sleepiness [13-15]; which makes it a popular choice.

Due to the metabolism of bupropion, it has been found that bupropion has potential drug interactions with ritonavair, efavirenz, and nelfinavir [16]. It has also been shown that bupropion is a strong CYP2D6 inhibitor and therefore should be avoided when taking other drugs that may be metabolized by CYP2D6 [17]. Therefore, one should be cautious about dosing bupropion with multiple medications as it might have a drug-drug interaction or drug-enzyme interaction.

1.3 Pharmacokinetics of Bupropion

Bupropion is rapidly absorbed after oral administration [18]. For the immediate release formulation, the mean T_{max} for bupropion is ~1.5 hours. For the sustained release and the extended release, the absorption is prolonged to having an estimated T_{max} of about ~3 and ~5 hours respectively [19]. The mean elimination half-life of bupropion is 21 ± 9 hours [20]. Bupropion is vastly distributed throughout the body; the volume of distribution at steady state is 19 L/kg and it has an estimated total clearance of 36 mL/min/kg. The protein binding of bupropion to human plasma is about 82-88% [19].

Bupropion goes through extensive first pass metabolism to form 3 primary active metabolites; hydroxybupropion, threohydrobupropion, and erythrohydrobupropion. The metabolites exhibit less protein binding compared to the parent drug bupropion; hydroxybupropion 77% and threohydrobupropion 42% [21]. Hydroxybupropion has an elimination half-life is on the same order as bupropion (~20 hours) [20]. However, both threohydrobupropion and erythrohydrobupropion have a longer half-life of ~33 and ~35 hours respectively [20]. For more details on the metabolism, see the metabolism section below.

For multiple doses of bupropion, it takes about 7-10 days to reach steady state. Bupropion is mainly excreted in urine via metabolites. In fact, 87% of bupropion is eliminated in urine but only 0.5% is unchanged [19]. Similarly, 10% of bupropion is eliminated in feces but <0.1% is unchanged [18]. One study looked at elimination of bupropion in urine after a single dose, they found that of the total recovery, bupropion consisted of 0.6% and hydroxybupropion consisted of 2.8%; in total these two analytes

3

constituted 3.6% of total drug recovered (threohydrobupropion or erythrohydrobupropion were not quantified in this study) [22]. This suggests that the three major metabolites may further be metabolized before elimination, but studies have yet to confirm this. Studies on hepatic or renal impairment have been investigated, yet the clinical implications of these have not been fully translated. For renal impairment, one study suggested patients should be administered a lower dose of bupropion. Reasons for this have yet to be completely understood however, one hypothesis was due to CYP2B6 metabolism activity, yet this would further need to be explored [23]. In rats, they found that hepatic impairment lead to bupropion exhibiting a C_{max} 3 times higher than control, an AUC increase of 4-5 times compare to control, and the half-life twice a long [24]. Again, translating this to humans would need to be investigated.

1.4 Metabolites

Bupropion forms three primary active metabolites by CYP450 2B6 (CYP2B6) and carbonyl reductase (CR). Hydroxybupropion is formed by CYP2B6 metabolism via hydroxylation of the tert-butyl group and threo/ erythrohydrobupropion are formed when bupropion is metabolized by CR. Using an *in vitro* microsome assay, the major metabolite has been reported to be hydroxybupropion [22, 25]. Additional kinetics studies evaluating metabolite formation (hydroxybupropion, threohydrobupropion, and erythrohydrobupropion) in liver fractions have been performed [26, 27].

The metabolism of this drug has been very important to consider in terms of clinical efficacy since all 3 of these metabolites are thought to be active and have shown to have as much 25-50% activity of the parent drug using an animal model [28, 29]. In addition, hydroxybupropion and threohydrobupropion have shown to have higher plasma concentrations compared to bupropion after a single oral dose (and therefore, higher AUC) [20].

The diastereomers, threohydrobupropion and erythrohydrobupropion have not been fully characterized in terms of formation (*in vitro*), activity, or potency. However, for both *in vitro* studies and *in vivo* plasma samples, threohydrobupropion formation/ concentration were shown to be higher than erythrohydrobupropion; in fact erythrohydrobupropion concentration in plasma is very low. Likewise, stereochemistry may play an important role for hydroxybupropion. Hydroxybupropion can exist as (2S, 3S) or (2R, 3R) (typically (2S, 3R) or (2R, 3S) does not exist due to steric hindrance). One group looked at the clearance of the enantiomer of hydroxybupropion in urine and plasma; in plasma, 95% of total hydroxybupropion existed as the R,R form and of the

total hydroxybupropion in urine, 72% existed in the R,R form [30]. In a different study, they evaluated the formation of enantiomers of hydroxybupropion *in vitro*. Using human liver microsome and recombinant CYP450's, studies revealed a 3 fold higher formation rate of the S,S hydroxybupropion compared to R,R hydroxybupropion [22]. Although these studies conflict, it is important to recognize and to keep in mind because of the impact it might play clinically.

1.4.1 Metabolic Enzymes Review
Cytochrome P450 2B6

CYP2B6 has emerged as an important metabolic enzyme in the liver in the past several years. In fact, it is now thought that CYP2B6 might account for 2-10% of total hepatic metabolism [31]. Similar to most CYP enzymes, CYP2B6 is primarily expressed in the liver and contributes to first pass metabolism. It has also been suggested that CYP2B6 might be expressed in brain, kidney, intestine, endometrium, skin, and others [32-34]. However, the degree at which they are expressed (if at all) and whether they exhibit any activity to contribute to the metabolism of CYP2B6 substrates is unknown. Like previously mentioned, this enzyme is an important for metabolizing bupropion to form hydroxybupropion.

CYP2B6 is highly polymorphic, showing over 20-250 fold variability in expression and activity [31]. Moreover, several *in vitro* studies looked at the various formation of hydroxybupropion using liver microsome; they saw a 45-80 fold change in metabolite formation and a 100 fold difference in the corresponding protein expression of CYP2B6 [35, 36]. Many studies also indicated that drug-drug interactions might affect CYP2B6

metabolism and thus hinder formation of hydroxybupropion [25]. Therefore, this inhibition could potentially cause too much toxicity from additional exposure of the bupropion. CYP2B6 variants have started to be investigated over the past decade; however, the functions of these variants on metabolism have still not been fully characterized. It has been proposed that CYB2B6 *4 and *22 might be high metabolizer whereas CYP2B6 *5 and *6 might be poor metabolizers [37]. The literature has tried to unravel what might cause inter-patient variability in CYP2B6. For instances, it has been shown that ethnicity and gender can impact the variants an individual expresses. In Asians, CYP2B6 has been shown to have higher frequency compared to the African American population [38]. Additionally, sex differences have been observed where females have a high protein expression (1.7 fold) and activity (1.6 fold) of CYP2B6 *4 compared to males [39]. In fact, one study looked at the pharmacokinetics of bupropion in 75 adolescents after a single dose of a sustained release formation and found that adolescent females had higher formation of hydroxybupropion compared to adolescent males [40].

In conclusion, many factors can contribute to the genetic and environmental factors that influence the CYP2B6 metabolism of bupropion. Moreover, there have been studies that suggest that other CYP isoforms might have roles in the metabolism of bupropion (particularly forming hydroxybupropion) including CYP2E1, and CYP3A4 [41]. However, it's unclear to date if these have any impact *in vivo.*

Carbonyl Reductase

7

CR also play a big role in the metabolism of bupropion. To date, it's not clear which carbonyl reductase enzyme(s) is (are) involved in this metabolism. CR enzymes have been divided into two families that encode for CR genes; aldo-keto reductases (AKR) and the short-chain dehydrogenases/reductases (SDR) where there are about 6-7 different enzymes in each family [42, 43]. Combined, these two families have a total of 12 enzymes involved in the reductive metabolism of carbonyl compounds [42]. These reactions are typically carried out in an NAD(P)(H)- dependent state and majority of these enzymes are localized in the cytoplasm [42]. To date, very little is known about this enzymatic pathway and its role in bupropion's metabolism. Recently one study looked at the role these enzymes have on bupropion *in vitro* using liver microsomes and cytosolic fractions. The study proposed that CR can catalyze microsome liver fraction to form erythrohydrobupropion at K_m=149 ± 24 µM (V_{max}=30.2 ± 1.2 pmol/mg of protein/min) and threohydrobupropion at K_m 62 ± 7µM (V_{max}=756.2 ± 17.9 pmol/mg of protein/min). However, their kinetic data contradicts much of literature, by showing that threohydrobupropion forms at nearly 7 fold higher than hydroxybupropion. They also suggest that the following CR enzymes; 11 β-hydroxysteroid dehydrogenase1, AKR1C1, AKR1CS, AKR1C3, and CBR1 might participate in the reduction of bupropion *in vitro* using recombinant forms of cytosolic CR enzymes [27], however, this needs to further be confirmed.

1.5. *In vitro* systems for studying drug metabolism

There are various organs in the body such as liver, kidney, lungs, or intestines responsible for drug metabolism. The biotransformation of compounds typically occur as 1) phase 1 metabolism (including oxidation, reduction, and hydroxylation) or 2) phase 2 reaction (including conjugation). The purpose of these reactions are to make compounds more hydrophilic (water soluble) so that they can be eliminated [44]. Although, drug metabolism can occur in various tissues, the liver is the primary organ for metabolism [45]. *In vitro* drug metabolism has been highly important in preclinical drug development due to the high throughput (compared to *in vivo*) and the vast information that can be studied *in vitro* (metabolism identification, metabolite kinetics, etc) [46]. Once centrifugation technique were available, it was possible to separate organelles to measure metabolism; particularly one popular technique has become microsomes stability assays. Microsomes are vesicles that reform from pieces of the endoplasmic reticulum that contain many phase 1 metabolism enzymes (making xenobiotics more polar), including Cytochrome P450's (CYP450). Microsome stability assays have been a cheap, reproducible, and easy way to evaluate xenobiotic metabolism [47, 48]. However, phase II metabolism typically occurs at a lesser extent compared to CYP metabolism and these enzymes are not always localized in microsomes but rather cytosolic, mitochondria, or other organelles. For measuring this metabolism, cytosolic fraction or S9 fraction might be useful. S9 fraction, which is a post mitochondrial supernatant fraction, contains both microsomes and cytosolic fraction (**Figure 1**). This fraction contains both phase I and phase II metabolites. Typically reactions seen in microsomes will also occur in S9 fraction but at a lesser

degree; this is because it is thought that CYP activity in S9 fraction is 20-25% of that in microsomes [49]. In addition to these subcellular *in vitro* assays, hepatocytes (cellular organelle) are a common way to measure metabolism. It has been observed that there is a good correlation between metabolism between *in vitro* hepatocyte studies and *in vivo*, likely due to the fact that the cells are intact [50]. Hepatocytes are more ideal system because they contain all metabolism enzymes and transporters. However, they also present more challenges such as low through put, harder to culture, and are typically expensive.

1.7. Bioequivalence

In order for generic drugs to become approved, manufactures must file an abbreviated new drug application (ANDA). For generics to be approved, bioequivalence studies (BE) are performed to ensure that the generic and name brand drug are equivalent. The Food and Drug Administration (FDA) defines bioequivalences as "the absence of a significant difference in the rate and extent to which the active ingredient or active moiety in pharmaceutical equivalents or pharmaceutical alternatives becomes available at the site of drug action when administered at the same molar dose under similar conditions in an appropriately designed study" [52]. A typical study for BE to be approved by FDA includes a test (generic drug) to reference (name brand drug) single dose cross-over study design [53]. In order to be approve to sell to market, the test product must stay within a 90% confidence interval of 80-125% for both the area under the curve (AUC) and C_{max}. The FDA Guidance for Industry: Bioavailability and Bioequivalence Studies for Orally Administered Drug Products highlights some biowaiver criteria to be exempt from testing at the highest strength for ANDA. These include linear elimination kinetics over a therapeutic dose range, test and reference shows similar dissolution, and the higher strength of the test and reference products are proportionally similar to the lower strengths. For BE testing, there has been concern whether this criteria is strict enough to ensure similar therapeutic equivalences, particularly relating to narrow therapeutic index drugs and capturing the rate of absorption [54-58]. In fact, it is thought that with modified release products, current BE standards fail to reproduce therapeutic equivalence. One study highlighted this using two drug products, methylphenidate and nifedipine. They showed by using an extra

metric, partial AUC, differences were seen using a plasma concentration vs time profile where no differences were observed using current standards [59]. The partial AUC is calculated by looking at the plasma concentration vs time profile from time 0 to the median time to reach T_{max} and applying the same 90% CI interval of 80-125% between test and reference product [60]. To date, partial AUC is not a requirement for approval of generic drugs (for either IR or MR) but highly recommended. In some circumstances such as vast differences in the shape of the concentration vs time profile, the FDA may recommend partial AUC.

1.8. Regulation issues

When Wellbutrin came off patent, many generics were approved by the FDA including the following manufactures; ANCHEN Pharms, EDGEMONT Pharms, IMPAX Labs, Mylan, Sandoz, Sun Pharma Global, Valeant Intl, Watson Labs, Wockhard Ltd, and Apotex Inc at doses ranging from 75-300 mg in either, IR, SR, or ER [61]. These generics were approved using BE standards comparing bupropion generics to Wellbutrin. In order for these generic products to be BE, the 90% confidence interval of the pharmacokinetic parameters C_{max} and AUC of the generic to name brand means need to be within 80-125%.

Since there was concern that bupropion at a 300 mg dose had a greater risk for seizures, BE studies for the ER generics were conducted at the 150 mg ER in healthy volunteers. The data was extrapolated from the 150 mg dose to the 300 mg dose based on the criteria for biowaivers. The 150 mg dose were BE and approved to sell and based on the extrapolated data the 300 mg ER generics were also passed BE and were approved to sell to market.

Shortly after, many generics of bupropion came to market including one, Budeprion 300 mg XL (Impax Labs distributed by Teva). After some patients switched to a few of these generics, the FDA received many complaints in regards to adverse events, loss of antidepressant effects, headaches, gastrointestinal disorder, fatigue, and anxiety particularly with Budeprion 300 mg ER starting in 2006. Following this, the FDA conducted a pilot study consisting of a crossover with Budeprion ER 300 and Wellbutrin 300 mg ER with 24 health individuals. Their findings revealed that Budeprion 300 mg ER and Wellbutrin 300 mg ER showed differences that did not meet BE standards. The

studies indicated that the mean AUC of Budeprion ER was 86% of Wellubtrin with a 90% CI of 77-96% and the C_{max} for Budeprion XL was 75% of Wellbutrin with a 90% CI of 65-87% (**Figure 2**) [62]. After these studies, Impax Labs voluntarily withdrew Budeprion 300 mg XL from the market. In addition, all other manufactures were no longer able to sell the 300 mg ER formulations until appropriate BE studies were conducted at that corresponding dose. After further review, dose-related seizures typically only happened in about 1 in 1000 patients and at the 450 mg dose (300 mg dose was considered a safe dose) [63].

1.9 Research Objectives

These regulatory issues have sparked many questions about bupropion and the bioinequivalence issues with some of the generics at the 300 mg ER formulation. Are these differences in BE due to the release mechanisms of the formulation? Was there a problem with *in vitro* dissolution data that might have been used for extrapolation of the 150 mg dose? Is there a saturation of enzymes that might be occurring with a higher dose or region GI metabolism that might be influencing the metabolism? What role dose pharmacogenomics play in terms of polymorphs in metabolism enzymes that might influence plasma concentrations? Although there are probably multiple factors that are involved in this issue, we sought to address some of these questions, particular relating to metabolism, saturation of metabolic enzyme, absorption, and pharmacogenomics (patient variability).

The central hypothesis for this thesis work is that generic versions of bupropion have delayed release may change absorption and metabolism profiles of bupropion to cause bioinequivalence of controlled release bupropion drug products.

Aim 1: Metabolism of Bupropion by Carbonyl Reductases in Liver and Intestine.

Aim 2: Method Development, Validation, and Sample Analysis of Bupropion HCl in Human Plasma.

Aim 3: Investigate Different Release Mechanism that May Alter Absorption, Metabolism, and Pharmacogenomics of Bupropion.

References

1. Fava, M., et al., *15 years of clinical experience with bupropion HCl: from bupropion to bupropion SR to bupropion XL.* Prim Care Companion J Clin Psychiatry, 2005. **7**(3): p. 106-13.
2. Stahl, S.M., et al., *A Review of the Neuropharmacology of Bupropion, a Dual Norepinephrine and Dopamine Reuptake Inhibitor.* Prim Care Companion J Clin Psychiatry, 2004. **6**(4): p. 159-166.
3. Dwoskin, L.P., et al., *Review of the pharmacology and clinical profile of bupropion, an antidepressant and tobacco use cessation agent.* CNS Drug Rev, 2006. **12**(3-4): p. 178-207.
4. Desmarais, J.E., L. Beauclair, and H.C. Margolese, *Switching from brand-name to generic psychotropic medications: a literature review.* CNS Neurosci Ther, 2011. **17**(6): p. 750-60.
5. Reese, M.J., et al., *An in vitro mechanistic study to elucidate the desipramine/bupropion clinical drug-drug interaction.* Drug Metab Dispos, 2008. **36**(7): p. 1198-201.
6. Dhillon, S., L.P. Yang, and M.P. Curran, *Spotlight on bupropion in major depressive disorder.* CNS Drugs, 2008. **22**(7): p. 613-7.
7. Rissmiller, D.J. and T. Campo, *Extended-release bupropion induced grand mal seizures.* J Am Osteopath Assoc, 2007. **107**(10): p. 441-2.
8. Settle, E.C., et al., *Safety profile of sustained-release bupropion in depression: results of three clinical trials.* Clin Ther, 1999. **21**(3): p. 454-63.
9. Foley, K.F., K.P. DeSanty, and R.E. Kast, *Bupropion: pharmacology and therapeutic applications.* Expert Rev Neurother, 2006. **6**(9): p. 1249-65.
10. Meyer, J.H., et al., *Bupropion occupancy of the dopamine transporter is low during clinical treatment.* Psychopharmacology (Berl), 2002. **163**(1): p. 102-5.
11. Arias, H.R., *Is the inhibition of nicotinic acetylcholine receptors by bupropion involved in its clinical actions?* Int J Biochem Cell Biol, 2009. **41**(11): p. 2098-108.
12. Richmond, R. and N. Zwar, *Review of bupropion for smoking cessation.* Drug Alcohol Rev, 2003. **22**(2): p. 203-20.
13. Cooper, J.A., V.L. Tucker, and G.I. Papakostas, *Resolution of sleepiness and fatigue: a comparison of bupropion and selective serotonin reuptake inhibitors in subjects with major depressive disorder achieving remission at doses approved in the European Union.* J Psychopharmacol, 2014. **28**(2): p. 118-24.
14. Grunebaum, M.F., et al., *SSRI versus bupropion effects on symptom clusters in suicidal depression: post hoc analysis of a randomized clinical trial.* J Clin Psychiatry, 2013. **74**(9): p. 872-9.
15. Safarinejad, M.R., *The effects of the adjunctive bupropion on male sexual dysfunction induced by a selective serotonin reuptake inhibitor: a double-blind placebo-controlled and randomized study.* BJU Int, 2010. **106**(6): p. 840-7.
16. Hesse, L.M., et al., *Ritonavir, efavirenz, and nelfinavir inhibit CYP2B6 activity in vitro: potential drug interactions with bupropion.* Drug Metab Dispos, 2001. **29**(2): p. 100-2.
17. Kotlyar, M., et al., *Inhibition of CYP2D6 activity by bupropion.* J Clin Psychopharmacol, 2005. **25**(3): p. 226-9.

18. Schroeder, D.H., *Metabolism and kinetics of bupropion.* J Clin Psychiatry, 1983. **44**(5 Pt 2): p. 79-81.

19. Findlay, J.W., et al., *{Coles, 2008 #3}.* Eur J Clin Pharmacol, 1981. **21**(2): p. 127-35.

20. Jefferson, J.W., J.F. Pradko, and K.T. Muir, *Bupropion for major depressive disorder: Pharmacokinetic and formulation considerations.* Clin Ther, 2005. **27**(11): p. 1685-95.

21. LLC, G. *Wellbutrin-bupropion hydroxhloride tablet, film coated.* DAILYMED Updated 2014; Available from: http://dailymed.nlm.nih.gov/dailymed/drugInfo.cfm?setid=60525754-0d2b-4ba4-918a-1c9d3eff89b2.

22. Coles, R. and E.D. Kharasch, *Stereoselective metabolism of bupropion by cytochrome P4502B6 (CYP2B6) and human liver microsomes.* Pharm Res, 2008. **25**(6): p. 1405-11.

23. Turpeinen, M., et al., *Effect of renal impairment on the pharmacokinetics of bupropion and its metabolites.* Br J Clin Pharmacol, 2007. **64**(2): p. 165-73.

24. Kaka, J.S., K.I. Al-Khamis, and M.O. Tanira, *Effect of hepatic and renal dysfunction on disposition of bupropion in rats.* Eur J Drug Metab Pharmacokinet, 1988. **13**(3): p. 149-53.

25. Hesse, L.M., et al., *CYP2B6 mediates the in vitro hydroxylation of bupropion: potential drug interactions with other antidepressants.* Drug Metab Dispos, 2000. **28**(10): p. 1176-83.

26. Molnari, J.C. and A.L. Myers, *Carbonyl reduction of bupropion in human liver.* Xenobiotica, 2012. **42**(6): p. 550-61.

27. Skarydova, L., et al., *Deeper insight into the reducing biotransformation of bupropion in the human liver.* Drug Metab Pharmacokinet, 2013.

28. Bondarev, M.L., et al., *Behavioral and biochemical investigations of bupropion metabolites.* Eur J Pharmacol, 2003. **474**(1): p. 85-93.

29. Damaj, M.I., et al., *Enantioselective effects of hydroxy metabolites of bupropion on behavior and on function of monoamine transporters and nicotinic receptors.* Mol Pharmacol, 2004. **66**(3): p. 675-82.

30. Coles, R. and E.D. Kharasch, *Stereoselective analysis of bupropion and hydroxybupropion in human plasma and urine by LC/MS/MS.* J Chromatogr B Analyt Technol Biomed Life Sci, 2007. **857**(1): p. 67-75.

31. Wang, H. and L.M. Tompkins, *CYP2B6: new insights into a historically overlooked cytochrome P450 isozyme.* Curr Drug Metab, 2008. **9**(7): p. 598-610.

32. Ding, X. and L.S. Kaminsky, *Human extrahepatic cytochromes P450: function in xenobiotic metabolism and tissue-selective chemical toxicity in the respiratory and gastrointestinal tracts.* Annu Rev Pharmacol Toxicol, 2003. **43**: p. 149-73.

33. Gervot, L., et al., *Human CYP2B6: expression, inducibility and catalytic activities.* Pharmacogenetics, 1999. **9**(3): p. 295-306.

34. Janmohamed, A., et al., *Quantification and cellular localization of expression in human skin of genes encoding flavin-containing monooxygenases and cytochromes P450.* Biochem Pharmacol, 2001. **62**(6): p. 777-86.

35.	Faucette, S.R., et al., *Validation of bupropion hydroxylation as a selective marker of human cytochrome P450 2B6 catalytic activity.* Drug Metab Dispos, 2000. **28**(10): p. 1222-30.

36.	Hesse, L.M., et al., *Pharmacogenetic determinants of interindividual variability in bupropion hydroxylation by cytochrome P450 2B6 in human liver microsomes.* Pharmacogenetics, 2004. **14**(4): p. 225-38.

37.	Zanger, U.M. and K. Klein, *Pharmacogenetics of cytochrome P450 2B6 (CYP2B6): advances on polymorphisms, mechanisms, and clinical relevance.* Front Genet, 2013. **4**: p. 24.

38.	Zanger, U.M., et al., *Polymorphic CYP2B6: molecular mechanisms and emerging clinical significance.* Pharmacogenomics, 2007. **8**(7): p. 743-59.

39.	Lamba, V., et al., *Hepatic CYP2B6 expression: gender and ethnic differences and relationship to CYP2B6 genotype and CAR (constitutive androstane receptor) expression.* J Pharmacol Exp Ther, 2003. **307**(3): p. 906-22.

40.	Stewart, J.J., et al., *Single-dose pharmacokinetics of bupropion in adolescents: effects of smoking status and gender.* J Clin Pharmacol, 2001. **41**(7): p. 770-8.

41.	Faucette, S.R., et al., *Evaluation of the contribution of cytochrome P450 3A4 to human liver microsomal bupropion hydroxylation.* Drug Metab Dispos, 2001. **29**(8): p. 1123-9.

42.	Matsunaga, T., S. Shintani, and A. Hara, *Multiplicity of mammalian reductases for xenobiotic carbonyl compounds.* Drug Metab Pharmacokinet, 2006. **21**(1): p. 1-18.

43.	Malatkova, P., E. Maser, and V. Wsol, *Human carbonyl reductases.* Curr Drug Metab, 2010. **11**(8): p. 639-58.

44.	S., W.B.a.N., *Common Biotransformation Reactions.* Mass Spectrometry in Drug Metabolism and Disposition: Basic Principles and Applications, 2011.

45.	Alavijeh, M.S., et al., *Drug metabolism and pharmacokinetics, the blood-brain barrier, and central nervous system drug discovery.* NeuroRx, 2005. **2**(4): p. 554-71.

46.	Wen, B. and M. Zhu, *Applications of mass spectrometry in drug metabolism: 50 years of progress.* Drug Metab Rev, 2015: p. 1-17.

47.	Ekins, S., et al., *Present and future in vitro approaches for drug metabolism.* J Pharmacol Toxicol Methods, 2000. **44**(1): p. 313-24.

48.	Jancova, P., P. Anzenbacher, and E. Anzenbacherova, *Phase II drug metabolizing enzymes.* Biomed Pap Med Fac Univ Palacky Olomouc Czech Repub, 2010. **154**(2): p. 103-16.

49.	Jia, L. and X. Liu, *The conduct of drug metabolism studies considered good practice (II): in vitro experiments.* Curr Drug Metab, 2007. **8**(8): p. 822-9.

50.	Gebhardt, R., et al., *New hepatocyte in vitro systems for drug metabolism: metabolic capacity and recommendations for application in basic research and drug development, standard operation procedures.* Drug Metab Rev, 2003. **35**(2-3): p. 145-213.

51.	Jackson, K.A. and S.E. Rosenbaum, *The application of population pharmacokinetics to the drug development process.* Drug Dev Ind Pharm, 1998. **24**(12): p. 1155-62.

52. Zhang, X., et al., *Innovative approaches for demonstration of bioequivalence: the US FDA perspective.* Ther Deliv, 2013. **4**(6): p. 725-40.

53. Van Peer, A., *Variability and impact on design of bioequivalence studies.* Basic Clin Pharmacol Toxicol, 2010. **106**(3): p. 146-53.

54. Aarons, L., *Assessment of rate of absorption in bioequivalence studies.* J Pharm Sci, 1987. **76**(10): p. 853-5.

55. Jackson, A.J. and M.L. Chen, *Application of moment analysis in assessing rates of absorption for bioequivalency studies.* J Pharm Sci, 1987. **76**(1): p. 6-9.

56. Jiang, W., et al., *A Bioequivalence Approach for Generic Narrow Therapeutic Index Drugs: Evaluation of the Reference-Scaled Approach and Variability Comparison Criterion.* AAPS J, 2015.

57. Khoo, K.C., M. Gibaldi, and R.K. Brazzell, *Comparison of statistical moment parameters to Cmax and tmax for detecting differences in in vivo dissolution rates.* J Pharm Sci, 1985. **74**(12): p. 1340-2.

58. Veng-Pedersen, P. and L.G. Tillman, *Center of gravity of drug level curves: a model-independent parameter useful in bioavailability studies.* J Pharm Sci, 1989. **78**(10): p. 848-54.

59. Endrenyi, L. and L. Tothfalusi, *Do regulatory bioequivalence requirements adequately reflect the therapeutic equivalence of modified-release drug products?* J Pharm Pharm Sci, 2010. **13**(1): p. 107-13.

60. Chen, M.L., et al., *Using partial area for evaluation of bioavailability and bioequivalence.* Pharm Res, 2011. **28**(8): p. 1939-47.

61. Chen, M.L., et al., *Challenges and opportunities in establishing scientific and regulatory standards for assuring therapeutic equivalence of modified release products: workshop summary report.* AAPS J, 2010. **12**(3): p. 371-7.

62. Woodcock, J., M. Khan, and L.X. Yu, *Withdrawal of generic budeprion for nonbioequivalence.* N Engl J Med, 2012. **367**(26): p. 2463-5.

63. Davidson, J., *Seizures and bupropion: a review.* J Clin Psychiatry, 1989. **50**(7): p. 256-61.
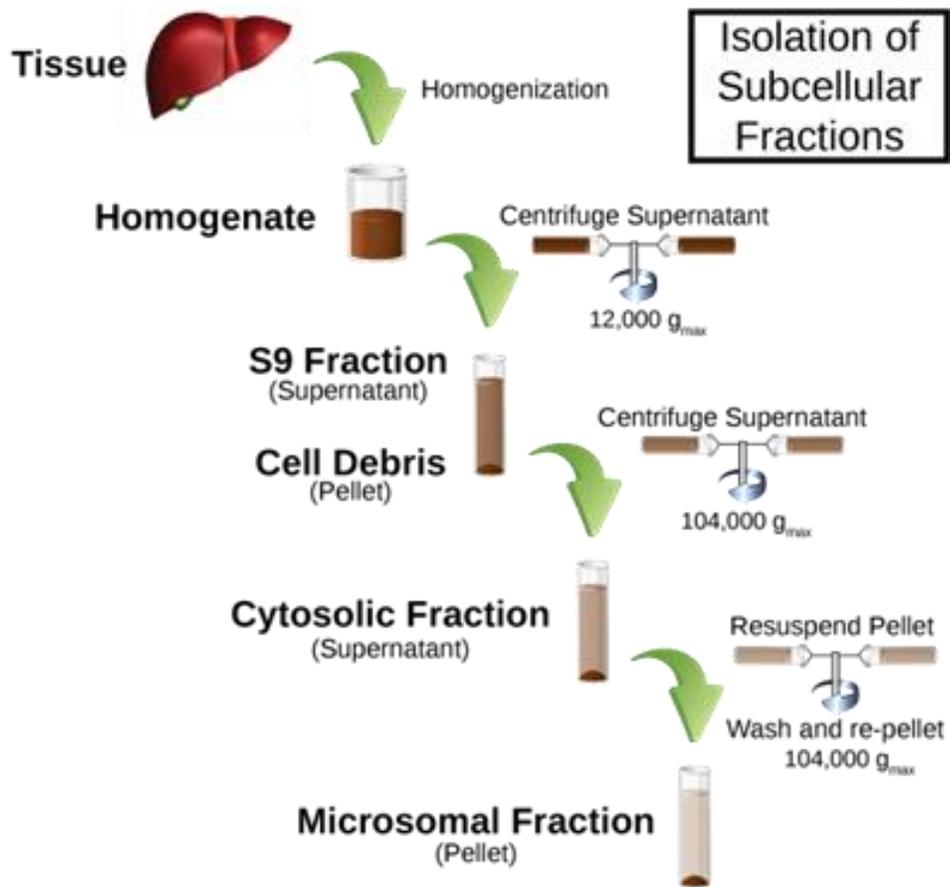
Figure 1-1. **Subcellular Fractions.** This figure depicts the subcellular fraction isolation from tissue for metabolism studies.

(Adapted: http://www.xenotechllc.com/products/subcellular-fractions)
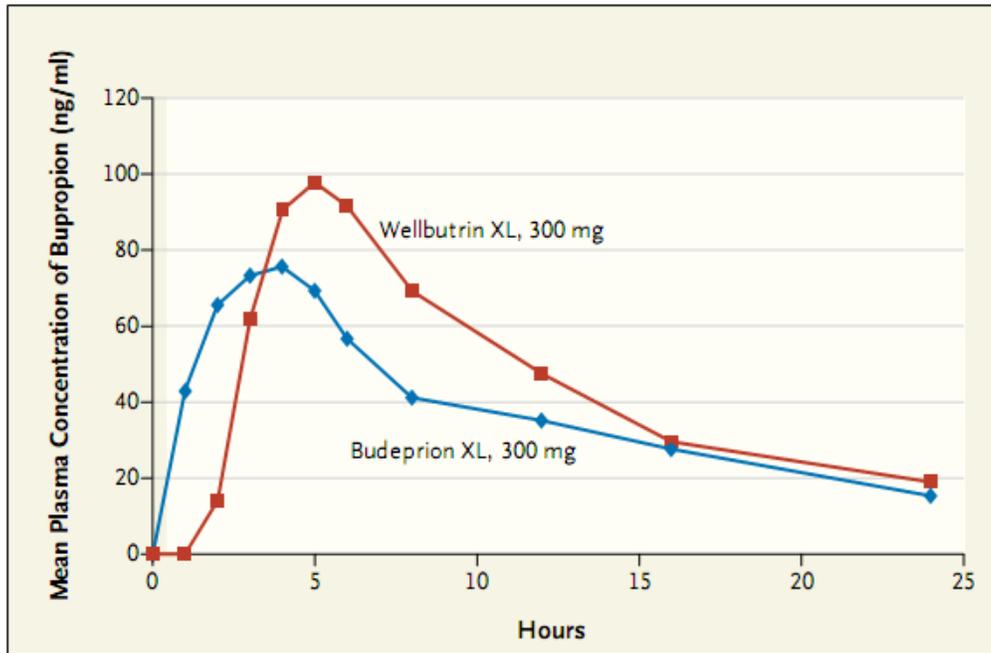
Mean Plasma Concentration of Bupropion (Budeprion XL and Wellbutrin XL) as a Function of Time in 24 Fasting Healthy Volunteers.

Figure 1-2. **Generics Failed BE Standards**. Comparing one generic, Budeprion ER 300 to Wellbutrin ER 300, both AUC and C_{max} fell out of an 80-125% using a 90% confidence interval.

(Adapted from: Woodcock, J., M. Khan, and L.X. Yu, *Withdrawal of generic budeprion for nonbioequivalence.* N Engl J Med, 2012. **367**(26): p. 2463-5)

Chapter 2
Metabolism of Bupropion by Carbonyl Reductases in Liver and Intestine

Abstract

Bupropion's metabolism to form hydroxybupropion in the liver by cytochrome P450 2B6 (CYP2B6) has been extensively studied; however, the metabolism to form erythro/threohydrobupropion in the liver and intestine by carbonyl reductases (CR) has not been well characterized. The purpose of this investigation was to compare the relative contribution of the two metabolic pathways of bupropion (by CYP2B6 and CR) in the subcellular fractions of liver and intestine and to identify the CRs responsible for erythro/threohydrobupropion formation in the liver and the intestine. The results showed that liver microsomes generated the highest amount of hydroxybupropion (V_{max}= 131 pmol/min/mg, K_m = 87 µM). In addition, liver microsomes and S9 fractions produced similar levels of threohydrobupropion by CR (V_{max}= 98-99 pmol/min/mg and K_m =186-265 µM). Interestingly, the liver has similar capability to form hydroxybupropion (by CYP2B6) and threohydrobupropion (by CR). In contrast, none of the intestinal fractions generated hydroxybupropion, suggesting that the intestine does not have fuctional CYP2B6 available for metabolism of bupropion. However, intestinal S9 fractions formed threohydrobupropion at 25% of the amount of threohydrobupropion formed by liver S9 fractions. Enzyme inhibition studies and Western blots identified that the 11β-dehydrogenase isozyme 1 in liver

microsomal fractions was mainly responsible for the formation of

threohydrobupropion, while AKR7 in the intestine may also be responsible for

producing the same metabolite formation. These quantitative comparisons of

bupropion metabolism by CR in the liver and intestine may provide new insight on the

efficacy and side effects of bupropion dosing.

Introduction

Bupropion is a norepinephrine/ dopamine reuptake inhibitor [1], which is clinically used for treatment of major depressive disorder (MDD) and smoking cessation [2]. Currently, over 11 million prescriptions annually of bupropion have been issued to over 40 million patients [3, 4]. Bupropion hydrochloride (HCl) extended release (ER) tablets, which is marketed as Wellbutrin XL by Biovail, has many generics manufacturers such as Teva/Impax, Mylan, Actavis, and Par Pharmaceuticals which used the current bioequivalence (BE) standard based on Cmax and AUC. The original approvals of the 300-mg generic bupropion HCl ER tablets were based on the demonstration of *in vivo* BE of the 150-mg generic bupropion HCl ER tablets to the brand name product and other *in vitro* criteria. However, a follow-up *in vivo* BE study on 300-mg Budeprion (bupropion HCl) ER tablets, manufactured by Impax Laboratories and distributed by Teva Pharmaceuticals, showed that the 300 mg strength failed to demonstrate BE [5]. It is not clear if the failure of extrapolating the BE conclusion from 150-mg to 300-mg tablets was related to changes of metabolism of bupropion in the liver and intestine between different formulations and different strengths of bupropion. Therefore, it is important to study in detail the bupropion metabolism mechanism in the liver and intestine.

Bupropion is rapidly (T_{max} 1.3-1.9 hours) absorbed and extensively distributed throughout the body (V_d = 19 L/kg), and less than 1% of the parent compound is eliminated in urine [6, 7]. The majority of bupropion is eliminated by metabolism. It is well known that bupropion forms three primary metabolites: hydroxybupropion (by

CYP2B6) and the diastereoisomers, threohydrobupropion and erythrohydrobupropion (by CR) [8] **(Figure 1)**. Different metabolites of bupropion pose significant impact for its efficacy since these metabolites have 25-50% potency as compared to bupropion based on antidepressant screening tests in an animal model [9, 10]. In addition, the plasma levels of hydroxybupropion are 5-10 fold higher than the parent drug bupropion after oral administration of bupropion HCl [6, 9-12].

The metabolism of bupropion by CYP2B6 in the liver to form hydroxybupropion, the major metabolite of bupropion, has been extensively studied. Studies have shown that the kinetic formation of hydroxybupropion in liver microsome can form at a high extent with a V_{max} ranging from 85-254 pmol/mg/min and a K_m ranging from 103-198 µM [13-15]. However, the metabolism of bupropion by CR has not been well characterized. For example, what metabolic pathways (CYP2B6 and CR) play a more important role in the liver and intestine for bupropion metabolism? Which subcellular fraction in the liver and intestine are responsible for metabolism of bupropion? Are there any differences in how bupropion is metabolized in the liver and in the intestines? Which CR is responsible for bupropion metabolism in the liver and the intestine?

To date, there are 11 known CR enzymes, which are categorized into two superfamilies: short-chain dehydrogenase/reductase (SDR) and aldo-keto reductase (AKR) [16, 17]. SDR family has 5 CR enzymes: CBR1, CBR3, 11 β-dehydrogenase isozyme 1 (11β-HSD), DHRS4, and L- Xylulose reductase. AKR family has 6 CR enzymes: AKR7A2, AKR7A3, AKR1C1, AKR1C2, AKR1C3, and AKR1C4. The

subcellular locations of most CR enzymes are in the cytoplasm, except for 11β-HSD which is localized in the microsomes [16].

In this study we investigated the metabolism of bupropion in subcellular fractions (microsome, cytosolic, and S9 fractions) of the liver and intestine to compare the extent of formation of all three metabolites in the different subcellular fractions of the liver and intestine. In addition, we conducted inhibition studies with these subcellular fractions to determine which CR enzymes are important for bupropion metabolism.   These results confirm that CYP2B6 in microsome is mainly responsible for hydroxybupropion.   In comparison, the liver microsome and S9 fraction formed similar levels of threohydrobupropion by CR, which was similar to hydroxybupropion's formation. This suggests that the metabolism of bupropion by CYP2B6 and CR in the liver is equally important. In contrast, none of the intestinal fractions detected hydroxybupropion, which suggests that the intestines didn't contribute to the CYP2B6 metabolism of bupropion. Intestinal S9 fraction indeed generated threohydrobupropion. In fact, the formation of threohydrobupropion in the intestinal S9 fraction is 25% the amount that formed from liver S9 fraction. Furthermore, the enzyme inhibition studies and Western blotting assay suggest that 11β-HSD is responsible for the formation of threohydrobupropion in the liver microsome, while ARK7 may be responsible for the same metabolite in the intestine. These results quantitatively compare bupropion metabolism by CR in the liver and intestine, which may provide new insight on its efficacy by these metabolites.

Materials and Methods

Chemicals/ Reagents:

Bupropion HCl and venlafaxine HCl (internal standard; IS) were purchased from Sigma (St. Louis, MO). Hydroxybupropion was purchased from Caymen Chemicals (Ann Arbor, MI) and a racemic mixture of both erythrohydrobupropion and threohydrobupropion were purchased from Toronto Research Chemicals (Toronto, Canada). β- Nicotinamide adenine dinucleotide 2'phosphate (NADPH) was also purchased from Sigma. Acetonitrile (HPLC grade) and methanol (HPLC grade) were purchased from Fisher Scientific (Pittsburgh, PA, USA). Water was purified with a Milli-Q water system (Bedford, MA). Mix Gender Pooled Human microsomes, cytosolic and S9 fractions for both liver and intestines (duodenum and jejunum) were purchased from Xenotech (Lenexa, KS). The following CR inhibitors were purchased from Sigma (St. Louis, MO); rutin, fluefenamic acid, and carbenozolone. The following antibodies were used in the western blot; AKR1C1/2 (Abcam (Cambridge, England) Cat # ab131375), carbonyl reductase 1/2/3 (Santa Cruz Cat # sc-292143), 11β-Hydroxysteroid Dehydrogenase (Type 1) (Cayman Chemical Cat # 10004303), AKR7A antibody (Santa Cruz Cat # sc-32944), CYP2B6 antibody (Santa Cruz Cat # sc-67224), Goat Anti-Mouse secondary antibody (Santa Cruz Cat # sc2005), and Anti-rabbit IgG antibody (Cell Signal Cat # 7074).

LC-MS/MS Method

The LC-MS/MS analysis was conducted using an Agilent 1200 HPLC system coupled to an API 3200 mass spectrometer (Applied Biosystems, MDS Sciex Toronto,

Canada) equipped with an API electrospray ionization (ESI) source. Quantitative analysis was accomplished on a Supelco C18 (150 x 4.6 mm I.D., 5 µm). The mobile phases used were purified water + 0.04% formic acid (A) and methanol + 0.04% formic acid (B). The LC was ran at isocratic at 35% methanol +0.04% and a flow rate of 0.8 mL/min. The LC-MS/MS was operated at positive ESI ionization. The MRM transitions and collision energies were determined for bupropion, hydroxybupropion, threohydrobupropion, erythrohydrobupropion and venlafaxine. The analytical data was processed by Analyst software (version 1.2; Applied Biosystems, Foster City, CA, USA). The quantitation of bupropion, hydroxybupropion, threohydrobupropion, and erythrohydrobupropion in these *in vitro* assay were performed by multiple reaction monitoring (MRM) of the $[M-H]^+$ ion, using an internal standard (IS) to establish peak area ratios. The method development was derived and optimized from previous studies that monitored bupropion and metabolites by HPLC or LC-MS/MS [8, 18-20].

Subcellular Kinetic Assay:

Liver and intestinal microsome, cytosolic, and S9 fraction were conducted with concentrations of bupropion as the substrate from 1-4000 µM dissolved in PBS (3.3 mM MgCl2 + 100 mM K_2HP0_4+ 100 mM KH_2HPO_4 buffer pH=7.4) (no organic solvent was used in this system). The master mix consisted of microsome, cytosolic, or S9 fraction at a final concentration of 1 mg/mL, 4 µL of corresponding substrate, and PBS (3.3 mM MgCl2 + 100 mM K_2HP0_4+ 100 mM KH_2HPO_4 buffer pH=7.4). A fresh sample of the cofactor nicotinamide adenine dinucleotide phosphate (NADPH) was prepared at 16.7 mg/mL in PBS buffer. Both master mix and NADPH was heated for

3 minutes at 37⁰C. Following, NADPH was added to master mix to initiate reaction. Sample was collected at 30 minutes; sample was spiked into ice cold methanol containing 500 nM of internal standard (venlafaxine).

Hepatocytes Study

Hepatocytes were ordered from Xenotech hepatosure (HCP100.H15), all reagents were included in kit expect for the K2500 media (50 mL). Bupropion was added to cells at a final concentration of 5-1000 µM. All reagents (tube A and B that are supplied with hepatocytes and K2500 media) were warmed to 37 ⁰C in a water bath for 15 minutes. Hepatocytes were removed from liquid nitrogen and warmed in a 37 ⁰C water bath for ~80 seconds. The pellet in the hepatocyte vial was added to tube A and the hepatocyte vial was rinses with tube B media and added to tube A. Tube A was centrifuged for 5 minutes at 100 g at 4 ⁰C. The cells were re-suspended in K2500 media and the cell density was measured using a hemocytometer. Cells were diluted so that the final concentration was 1 *10^6 cells/mL. Using a clear 96 well plate, each well had 136 µL of K2500 media, 2 µL of 100X desired bupropion concentration, and 62 µL of cells after they were dethawed and diluted. Reactions started when cells were added to each well, and were terminated at 0, 30, 60, 90, 120 minutes by spiking 50 µL of sample into methanol with organic solvent + 500 nM of internal standard. Reactions were ran in triplicate per concentration per time point. All samples were sonicated to break the cells and centrifuged at 15,000 rpm. The supernatant was then analyzed by LC-MS/MS to quantify bupropion and metabolites concentration.

Carbonyl Reductase Inhibition Study

For inhibition studies, bupropion substrate was used at the corresponding K_m for threohydrobupropion (since this was the dominant metabolite formed by CR) determined from the subcellular kinetic analysis (liver microsome = 186 µM, liver S9 = 265 µM, liver cytosolic = 90 µM, intestinal microsome = 150 µM, intestinal cytosolic = 5.6 µM, and intestinal S9 = 573 µM). The master mix consisted of microsome, cytosolic, or S9 at a final concentration of 1 mg/mL, bupropion, PBS (3.3 mM MgCl2 + 100 mM potassium phosphate buffer pH=7.4), and CR inhibitor at 3 fold higher than the IC_{50} (the $3XIC_{50}$ values were; rutin 6.1 µM, flufenamic acid 60 µM, and carbenoxolone 250 nM). A fresh sample of the cofactor NADPH was prepared at 16.7 mg/mL in PBS buffer. Both master mix and NADPH was heated for 3 minutes at 37ºC. Following, NADPH was added to master mix to initiate reaction. Sample was collected at 0, 30, 60, and 90 minutes; sample was spiked into ice cold methanol containing 500 nM of internal standard (venlafaxine).

Standards and Sample Preparation

Stock solutions of bupropion, hydroxybupropion, threohydrobupropion, or erythrohydrobupropion at 2 mg/mL were prepared in methanol to generate a working solution of 100 µg/mL. An aliquot of this solution was diluted in 1(MeOH):1(Milli-Q water) to get a series of working standard solutions of 5, 10, 25, 50, 100, 250, 500, 1000, 2500, and 5000 ng/mL. Internal standard (IS) solution was prepared by diluting the stock solution of venlafaxine to yield a final concentration of 500 nM in 1(MeOH):1(Milli-Q water). After preparation of working standards, 50 µL of the

appropriate concentrations of analyte was added to 150 µL of IS solution (500 nM of

venlafaxine in in 1(MeOH):1(Milli-Q water)), and 50 µL of PBS. Fifty µL of sample

from microsome, cytosolic, or S9 reaction at each time point was spiked into 150 µL

of IS solution (500 nM of venlafaxine in in 1(MeOH):1(Milli-Q water)) and 50 µL

1(MeOH):1(Milli-Q water). Samples were vortex for 1 min, followed by centrifugation

for 15 min at 14,000 rpm in an Eppendorf centrifuge. The supernatant was transfer to

vials and 5 µl was injected for LC-MS/MS analysis.

Western Blot

Subcellular fraction; liver and intestinal microsome, S9, and cytosolic fractions were

lysed using radioimmunoprecipitation assay buffer ((RIPA: 50 mM Tris-HCL, 150 mM

NaCl, 1% NP-40, 0.5% sodium deoxycholate, and 0.1% SDS, pH 7.4± 0.2) (Boston

BioProducts, BP-115)) with 1% protease inhibitor and 1% EDTA. Approximately 200 µL

of RIPA buffer was used to resuspend each subcellular fraction which was incubated on

ice for 30 minutes. Following, each sample was centrifuged at 14,000 rpm for 15

minutes at 4ºC. The protein concentration of the supernatant of each sample was

quantified using Pierce BCA Protein Assay Kit (23225). All samples were diluted to

have a protein concentration of 750 µg/mL. Laemmli sample buffer (BIO-RAD 161-

0737) was used according to protocol; mix 950 µL of sample buffer with 50 µL of β-

mercaptoethanol. Each sample was prepped by using 50 µL of protein sample with 25

µL of sample buffer and boiled samples at 95 ºC for 10 minutes. All samples were

loaded on an SDS-PAGE gel (25 µL) and ran at 200 V for about 2 hours. The ladder

see-blue (Life Technologies LC5625) was used to determine the proteins molecular

weight. The running buffer for the SDS-Page gel consist of 3.0 g of tris base, 14.4 g of

glycine, and 1 g of SDS with ddH20 to 1 L. A wet transfer was performed using transfer

buffer (3.03 g of tris base, glycine 14.4 g, 200 µL of methanol, and ddH20 to 1 L). The

transfer was done using a PVDF immune-blot membrane (BIO-RAD 162-0177) at 250

mV for 3 hours. The membrane was blocked for 1.5 hours using 5% of milk in Tris-

Buffered Saline and Tween 20 (TBST buffer) (TBST buffer: 2.4 g of tris, 8 g of NaCl

adjust pH to 7.6 with HCl, 0.1% tween 20 (v/v), and 1L of ddH2O). Primary antibody

was added to membrane at various dilutions according to manufacturer's protocol;

AKR1C1/2 antibody (dilution 1:500), CRB1/2/3 (dilution 1:500), 11β hydroxysteroid

dehydrogenase (dilution 1:200), AKR7 (dilution 1:200), and CYP2B6 (1:200) (dilutions

were used as suggested by manufactures) and incubated at 4ºC overnight. Membrane

was washed with TBST (3X) before the corresponding secondary antibody was added;

AKR1C1/2 (dilution 1:2000), CRB1/2/3 (dilution 1:2000), 11β hydroxysteroid

dehydrogenase (dilution 1:5000), AKR7 (dilution 1:5000), and CYP2B6 (dilution 1:5000)

for 1.5 hours at room temperature. The membrane was washed again with TBST (3X).

Stripping buffer (Thermo Scientific 21059) was used to remove previous antibody, we

confirmed that the antibody was washed out each time. Proteins were detected using

X-ray development; 5 mL of substrate (2.5 mL of reagent 1 and 2.5 mL of reagent 2)

was added to the membrane before detection (thermo cat #'s 1859701 and 1859698).

Data Analysis

For microsome, cytosolic, and S9 kinetics, all data was converted into pmol/min/mg

and plotted against concentration of bupropion. Graphpad Prism5 was used to

simulate the K_m and V_{max} using the Michaelis-Menten model using the following equation.

(1)

$$Y = \frac{Vmax * [substrate]}{(Km + [substrate])}$$

The intrinisic cleareance for S9 formation of each metabolite was calculated using the following equation.

(2)

$$CLint = (\frac{Vmax}{Km})$$

For statistical analysis, R version 3.0.3 was ran with a t-test.

Results

LC-MS/MS development for bupropion and metabolites

An LC-MS/MS method was developed in order to quantify bupropion, hydroxybupropion, erythrohydrobupropion, and threohydrobupropion. Since the fragmentations of the diastereoisomers (threohydrobupropion and erythrohydrobupropion) are the same and bupropion also had very similar fragmentation, it was necessary for all analytes to be separated by LC. **Figure 2A** shows the MRM chromatograms of the successful separation of all analytes. The MS parameters are highlighted in **figure 2B** for each analyte**.**

Calibration curves for each analyte were performed in order to quantify samples in later studies. A wide linear range was achieved for each analyte (**figure 2C**). In addition, the coefficient of determination for each analyte was greater than or equal to 0.99. The lower limit of detection was either 5 or 10 ng/mL (noted in figure 2C) depending on which analyte was being monitored.

Metabolism in Liver Subcellular fractions

To begin with, we used liver microsome, cytosolic, and S9 fractions to look at bupropion's metabolism. Bupropion was used as the substrate at concentrations ranging from 1-4000 µM. Samples were analyzed by LC-MS/MS to establish the kinetics, and bupropion, hydroxybupropion, threohydrobupropion, and erythrohydrobupropion were monitored. **Figure 3A-C** shows the formation of hydroxybupropion in liver microsome, S9 fraction, and cytosolic fraction respectively. Hydroxybupropion was formed at the highest extent in liver microsome (K_m = 87.98 ±

20.2 µM and V_{max} = 131.2 ± 5.6 pmol/min/mg), which was expected since

microsomes typically contain concentrated amounts of CYP's. In the S9 fraction,

hydroxybupropion formation was still apparent but the formation occurred at a lower

of extent (K_m = 99.53 ±18.91 µM and V_{max} = 51.45 ± 1.9 pmol/min/mg).

Hydroxybupropion formation in the cytosolic fraction was almost negligible (K_m =

71.35 ± 127 µM and V_{max} = 1.594 ± 0.52 pmol/min/mg). These results suggest that

CYP enzymes which are subcellularly localized in microsomes are responsible for the

formation of hydroxybupropion in the liver.

Threohydrobupropion was also formed in all subcellular liver fractions (**Figure 4A-C**). The extent of formation in both microsome and S9 fractions were about the

same; however, the affinity differed slightly (microsome: K_m = 186.3 ± 53.48 µM and

V_{max} = 98.37 ± 6.6 pmol/min/mg; S9: K_m = 265.7 ± 77.79 µM and V_{max} = 99 ±7.5

pmol/min/mg). In the cytosolic fraction, threohydrobupropion was formed at a lesser

extent (V_{max}: 14.56 ± 0.714 pmol/min/mg and K_m: 89.82 ± 22 µM). These results

suggested that the CR enzyme which is subcellularly localized in the microsomes,

11β hydroxysteroid dehydrogenase, plays a major role in the conversion of bupropion

to threohydrobupropion. In addition, since the cytosolic fraction still forms

threohydrobupropion to some extent, this suggested there may be multiple CR

enzymes responsible for this metabolism.

Finally, we saw that erythrohydrobupropion was also formed in liver microsome,

S9, and cytosolic fractions (**figure 5A-C**, respectively); however, the extent of

formation was very small in all subcellular fractions (microsome: K_m = 41.45 ± 26.62

µM and V_{max} = 2.649 ± 0.3 pmol/min/mg; cytosolic: K_m= 274.4 ± 254 µM and V_{max} =

3.654± 1.2 pmol/min/mg; S9: K_m = 107 ± 32.14 µM and V_{max} = 4.23 ± 0.286

pmol/min/mg). These results suggest that hydroxybupropion and

threohydrobupropion is the dominant metabolite in the liver subcellular fraction. Yet,

similar to threohydrobupropion, since formation of erythrohydrobupropion occurred in

both the microsome and cytosolic fractions, this again suggested that multiple CR

enzymes may be involved in erythrohydrobupropion's formation. A summary of the

liver kinetics are summarized in **table 1A**.

Using the Michaelis-Menten kinetic parameters (Vmax and Km) we were able to

calculate the intrinsic clearance for each metabolite using the S9 fraction (since this

contains both microsome and cytosolic fractions) in the liver (**Table 2**). After adding

each metabolite intrinsic clearance, we calculated the liver contributes a CL_{int} of

931.8 µL/min/mg.

Metabolism in Intestinal Subcellular fractions

We continued to evaluate the metabolism of bupropion using intestinal

microsome, cytosolic, and S9 fractions. Similar to the liver metabolism, we used

bupropion at concentrations from 1-4000 µM and analyzed samples by LC-MS/MS to

establish the kinetics of hydroxybupropion, erythrohydrobupropion, and

threohydrobupropion. However, unlike the liver fractions where all metabolites were

detected, the only metabolite that formed through the intestinal metabolism was

threohydrobupropion. Both hydroxybupropion and erythrohydrobupropion were

undetectable in both intestinal microsome, cytosolic, and S9 fraction. This suggested

that CYP2B6 metabolism does not occur in the intestines since hydroxybupropion was unable to form.

The extent in which threohydrobupropion was formed was smaller compared to its formation in the liver (**figure 6 A-C**) (microsome: K_m = 149.9 ± 28.8 µM and V_{max} = 5.55 ±0.4 pmol/min/mg; cytosolic: K_m = 569 ± 64.89 µM and V_{max} = 5.649 ± 0.214 pmol/min/mg and S9: K_m = 573.4 ± 188.9 µM and V_{max} = 25.87 ± 2.8 pmol/min/mg). The formation of threohydrobupropion was 25% of the formation that which occurred in the liver S9 fraction. Similar to the formation in the liver, these data suggest that multiple CR enzymes are involved in the formation of this metabolite. A summary of the intestinal S9 kinetics formation of each metabolite is summarized in **Table 1B**.

Similarly to the liver, using the Michaelis-Menten kinetic parameters (V_{max} and K_m) we were able to calculate the intrinsic clearance for threohydrobupropion using the S9 fraction in the intestines (**Table 2**). This was about 20 fold lower than the liver CL_{int} clearance since two of the metabolites did not form in the intestines and threohydrobupropion formations was 25% of the formation in the liver S9 fraction. Nevertheless, the CL_{int} in the intestines S9 fraction was estimated to be 45 µl/min/mg.

Metabolite inhibition by Carbonyl Reductase Inhibitors

Next we went on to evaluate which CR enzymes are important for the reduction of bupropion and whether there might be multiple enzymes involved in this process. Using the microsome, cytosolic, and S9 fraction assay, we added various CR inhibitors and analyzed the reduction of metabolite formation. The inhibitors that were chosen were the following: rutin, which has been shown to target the CRB

family of CR at an IC_{50} of 2.1 µM; flufenamic acid, which has been reported to inhibit AKR family 67% at concentrations of 20 µM; and carbenoxolone, which targets the microsomal CR 11β hydroxysteroid dehydrogenase at an IC_{50} values in the nM range [21-23]. We monitored all metabolite formation with each inhibitor and compared these results to a control with no inhibitor.

For the formation of hydroxybupropion, none of the three inhibitors had a significant effect compared to control on any liver subcellular fraction (**figure 7A**), as expected since formation of this metabolite occurs via CYP2B6. In addition, this metabolite was again not detected in any intestinal fraction. These results suggested no CRs are involved in formation of hydroxybupropion.

However, for threohydrobupropion formation, inhibition was observed in both the liver and intestinal subcellular fractions. In the liver, carbenoxolone, the inhibitor of 11β hydroxysteroid dehydrogenase, showed as much as 82.4% inhibition compared to control in the liver microsome. Flufenamic acid was shown to have about a 40% inhibition on threohydrobupropion formation in liver cytosolic fraction (**Figure 7B**). These results suggested that in the liver, 11β hydroxysteroid dehydrogenase was the dominant enzyme in the liver for reduction of bupropion to threohydrobupropion.

However, in the intestinal subcellular fractions, carbenozolone seemed to have no significant effect on inhibiting threohydrobupropion formation. Furthermore, flufenamic acid showed inhibition on intestinal fractions ranging from 57.8-78.7% of threohydrobupropion formation (**Figure 7B**). Minor inhibition was seen with rutin, implicating minor involvement of the CRB family of CR enzymes in the formation of

threohydrobupropion. All together, the liver and intestinal data for the formation of threohydrobupropion suggest that both 11β hydroxysteroid dehydrogenase and the AKR family of CR enzymes are the major CR enzymes responsible for threohydrobupropion formation.

In the same way, erythrohydrobupropion formation was inhibited by both carbenoxolone and flufenamic acid (**Figure 7C**). Carbenoxolone inhibited the formation of erythrohydrobupropion by 95% in liver microsome and 91.6% in liver S9 fraction yet had no effect on liver cytosolic fraction. Flufenamic acid showed about 67-88% inhibition in the liver S9 and cytosolic fractions. These results suggested that 11β hydroxysteroid dehydrogenase and AKR family are the dominant enzymes that form erythrohydrobupropion in the liver.

Hepatocyte Kinetics

We measured the kinetics of the metabolite formation using hepatocytes. Hepatocytes have scaling factors that can translate into CL hepatic unlike S9 fraction. We were only able to detect the formation of hydroxybupropion and threohydrobupropion using hepatocytes, no erythrohydrobupropion was able to be detected (**supplemental figure 1**). The affinity for both hydroxybupropion and threohydrobupropion were both much higher than previous in vitro systems used. **Supplemental table 1A** shows that the CL_{int} calculated from the hepatocytes kinetics. A previous paper showed that the conversion between cell to kg can calculate by $99*10^6$ cell/ gram of liver and 21 gram liver/ kg of body weight [24]. Using this we scaled the intrinsic clearance to *in vivo,* 45.67 mL/min/kg **supplemental table 1B**.

Finally, we showed that the hepatic clearance was 5.4 mL/min/kg (**supplemental 1C**) assuming fraction unbound is 0.16 and the human blood flow is 20.7 ml/min/kg.

Western Blot

Finally, we went on to confirm whether these enzymes of various CR enzymes are expressed in the different subcellular fraction. Analysis of protein expression was performed using an immunoblot after separation by SDS-Page gel (**Figure 8**). Both liver and intestinal microsome, cytosolic, and S9 fraction was examined for CYP2B6, 11β hydroxysteroid dehydrogenase, CRB1/2/3, AKR7 family, and AKR1A family.

It was observed that CYP2B6 was primarily only expressed in liver microsome with minor expression in the liver S9 fraction (lane 1 & 2). CYP2B6 was absent in liver cytosolic (lane 3) and all intestinal fractions (lane 4-6). This is consistent with the metabolite formation data suggested that hydroxybupropion predominantly formed in liver microsome and S9 and does not participate in intestinal metabolism of bupropion. 11β hydroxysteroid dehydrogenase was highly expressed in liver microsome and S9 fraction (lanes 1 & 2); its expression in the intestines was almost non-existing, supporting our results with the inhibition datathat 11β hydroxysteroid dehydrogenase activity is dominant in the liver. The CRB1/2/3 enzymes were primarily found to be expressed in both liver and intestinal S9 and cytosolic fractions (lanes 2, 3, 5, 6); however, these enzymes may not be important in bupropion's metabolism, as suggested by the inhibition data. The AKR1A family had very little expression in any of the subcellular fractions except minor expression in liver S9 and liver cytosolic (lanes 2 & 3). Finally, the AKR7 family enzymes were found to be

expressed in all subcellular fractions. This supported the CR inhibition data seen by flufenamic acid in both liver and intestines. All together, the enzyme expression data verified the results seen in the formation and inhibition studies as those enzymes were expressed in the corresponding subcellular fraction.

Discussion

In our studies, we show that the contribution of hydroxybupropion and threohydrobupropion formation in the liver (microsome and S9 fractions) occur at similar levels. In addition, we showed that no CYP2B6 expression or metabolism to form hydroxybupropion in the intestines occurs. However, the only metabolite that forms in the intestines is threohydrobupropion. Its formation in the intestinal S9 fraction is 25% of that seen in the liver S9 fraction. Furthermore, inhibition studies prove that there are multiple CR enzymes that are involved in the metabolism of bupropion to threohydrobupropion; and the CR activity may have a gastrointestinal (GI) regional dependency which influences the metabolism of the parent compound. Western blots confirmed that the CR enzymes important for metabolizing bupropion are expressed in the corresponding subcellular fractions.

Previous studies have shown that CYP450 2B6 metabolism of bupropion forms hydroxybupropion [13, 25-28]. In addition, studies have also suggested that other CYPs such as CYP2C19, CYP2E1, and CYP3A4 might have a minor roles in the hydroxybupropion formation but still need to be confirmed [29]. Therefore, based off of liver microsome stability assays, it was thought that hydroxybupropion was the major metabolite. Several studies failed to realize that the CR pathway to form

threehydrobupropion and erythrohydrobupropion may not occur extensively in liver microsomes since most of these enzymes are subcellularly located within the cytosol [13, 30].

Therefore, examining all subcellular fractions; microsome, cytosolic, and S9 fraction will help to explain more broadly which enzymes are responsible for bupropion's metabolism and at what rate these metabolites are formed. Typically, CYP enzymes are localized in the microsomes. On the other hand, most other CR are subcellularly located in cytosolic fractions, expect for 11β-HSD, one of the only CR enzymes that is subcellularly localized in microsomes. Using an S9 fraction, which contains both cytosolic and microsomes, allowed us to compare metabolite formations across the three metabolites. We found that in the S9 fractions threehydrobupropion has a 2-fold higher formation compared to hydroxybupropion suggesting that many CR enzymes have been under looked for bupropion's metabolism Although hydroxybupropion formation in microsomes is slightly higher than S9 fraction, this difference in activity between microsome and S9 fraction is normal since microsomes are concentrated CYP, where S9 fraction contain both CYP and cytosolic fraction [31, 32].

In Molnari et al [14], the authors found that threehydrobupropion was the major metabolite in *liver microsome*, which disagrees with many previous studies that identified hydroxybupropion as the major metabolite and the results presented here. Although, in our studies, threehydrobupropion was the major metabolite formed in liver S9 fraction, hydroxybupropion still forms at the highest extent in liver microsomes. Moreover, the authors saw no change with flufenamic acid in inhibition

studies in the liver where we did. However, this inhibitor seemed to have a larger effect on intestinal fraction, which was not pursued in the Molnari study.   Likewise, in Meyers et al. 2013 [30] the authors showed the 11 β-HSD was the CR enzyme important for metabolizing bupropion to form threohydrobupropion. While our data agrees with this, a more thorough analysis of subcellular fractions could have been explored. In this study, the authors only examine liver microsomes and in which case only 11 β-HSD activity would be observed. Therefore, cytosolic fractions were needed to be examined to see if there were multiple CR enzymes that contribute to bupropion metabolism.

Our results suggest that both hydroxybupropion and threohydrobupropion are important metabolites to consider for the metabolism of bupropion. This is consistent with *in vivo* studies which looked at the pharmacokinetic levels of bupropion and metabolites and that both hydroxybupropion and threohydrobupropion showed higher plasma concentration than the parent drug, bupropion (erythrohydrobupropion concentration was minor or undetectable) [33]. In addition, this is consistent with our hepatocyte studies. Although are $CL_{hepatic}$ is a little overestimated considered the reported CL_{total} is 36 mL/min/kg whereas our $CL_{hepatic}$ was 45.6 mL/hr/kg. It has been noted that is common to over or under estimate $CL_{hepatic}$ using *in vitro* systems compare to the true *in vivo* hepatic clearance [34].

To the best of our knowledge, no authors have studied the formation of bupropion's metabolites in any intestinal fractions. The intestines have been shown to be involved in both phase I and phase II metabolism, which might influence the metabolism of bupropion. Although CYP enzyme expression is typically less in the

intestines compared to the liver (20 pmol/mg of microsome compared to 300 pmol/mg of microsome) [35], metabolism in this region of the GI tract should still be investigated. Likewise, the expression of CR enzymes has been found to be highly concentrated in both liver and small intestines [35, 36]. We did not observe any hydroxybupropion (CYP2B6 metabolism) in the intestines, this finding is consistent with another study that looked for various CYP expression in intestinal microsomes and similarly saw no CYP2B6 present [37]. However, in this study threohydrobupropion metabolized by CR was able to form in all three subcellular intestinal fractions (microsome, S9, and cytosolic) again showing how studies have discounted the CR pathway for metabolism of bupropion. The intestinal subcellular fractions used in these studies were taken from the duodenum and jejunum. The intestinal metabolism is an important concept to understand since these metabolites are active. One hypothesis for the failure of extrapolating BE from lower strength to higher strength, as discussed in the introduction, could be that we have discounted the CR metabolism particularly in the intestines and these enzymes were saturating. However, a more thorough analysis would be needed to disapprove/approve the hypothesis and this is also true *in vivo*.

In conclusion, these results suggest that depending on the subcellular localization of the bupropion and tissue type, the metabolism can be different forming different metabolites by multiple enzymes (both CYP and CR).

References

1. Stahl, S.M., et al., *A Review of the Neuropharmacology of Bupropion, a Dual Norepinephrine and Dopamine Reuptake Inhibitor.* Prim Care Companion J Clin Psychiatry, 2004. **6**(4): p. 159-166.
2. Fava, M., et al., *15 years of clinical experience with bupropion HCl: from bupropion to bupropion SR to bupropion XL.* Prim Care Companion J Clin Psychiatry, 2005. **7**(3): p. 106-13.
3. Desmarais, J.E., L. Beauclair, and H.C. Margolese, *Switching from brand-name to generic psychotropic medications: a literature review.* CNS Neurosci Ther, 2011. **17**(6): p. 750-60.
4. Reese, M.J., et al., *An in vitro mechanistic study to elucidate the desipramine/bupropion clinical drug-drug interaction.* Drug Metab Dispos, 2008. **36**(7): p. 1198-201.
5. Woodcock, J., M. Khan, and L.X. Yu, *Withdrawal of generic budeprion for nonbioequivalence.* N Engl J Med, 2012. **367**(26): p. 2463-5.
6. Jefferson, J.W., J.F. Pradko, and K.T. Muir, *Bupropion for major depressive disorder: Pharmacokinetic and formulation considerations.* Clin Ther, 2005. **27**(11): p. 1685-95.
7. Schroeder, D.H., *Metabolism and kinetics of bupropion.* J Clin Psychiatry, 1983. **44**(5 Pt 2): p. 79-81.
8. Loboz, K.K., et al., *HPLC assay for bupropion and its major metabolites in human plasma.* J Chromatogr B Analyt Technol Biomed Life Sci, 2005. **823**(2): p. 115-21.
9. Bondarev, M.L., et al., *Behavioral and biochemical investigations of bupropion metabolites.* Eur J Pharmacol, 2003. **474**(1): p. 85-93.
10. Damaj, M.I., et al., *Enantioselective effects of hydroxy metabolites of bupropion on behavior and on function of monoamine transporters and nicotinic receptors.* Mol Pharmacol, 2004. **66**(3): p. 675-82.
11. Damaj, M.I., et al., *Effects of hydroxymetabolites of bupropion on nicotine dependence behavior in mice.* J Pharmacol Exp Ther, 2010. **334**(3): p. 1087-95.
12. Zhu, A.Z., et al., *CYP2B6 and bupropion's smoking-cessation pharmacology: the role of hydroxybupropion.* Clin Pharmacol Ther, 2012. **92**(6): p. 771-7.
13. Coles, R. and E.D. Kharasch, *Stereoselective metabolism of bupropion by cytochrome P4502B6 (CYP2B6) and human liver microsomes.* Pharm Res, 2008. **25**(6): p. 1405-11.
14. Molnari, J.C. and A.L. Myers, *Carbonyl reduction of bupropion in human liver.* Xenobiotica, 2012. **42**(6): p. 550-61.
15. Skarydova, L., et al., *Deeper insight into the reducing biotransformation of bupropion in the human liver.* Drug Metab Pharmacokinet, 2014. **29**(2): p. 177-84.
16. Matsunaga, T., S. Shintani, and A. Hara, *Multiplicity of mammalian reductases for xenobiotic carbonyl compounds.* Drug Metab Pharmacokinet, 2006. **21**(1): p. 1-18.
17. Rosemond, M.J. and J.S. Walsh, *Human carbonyl reduction pathways and a strategy for their study in vitro.* Drug Metab Rev, 2004. **36**(2): p. 335-61.

18.   Borges, V., et al., *High-throughput liquid chromatography-tandem mass spectrometry determination of bupropion and its metabolites in human, mouse and rat plasma using a monolithic column.* J Chromatogr B Analyt Technol Biomed Life Sci, 2004. **804**(2): p. 277-87.

19.   Cooper, T.B., R.F. Suckow, and A. Glassman, *Determination of bupropion and its major basic metabolites in plasma by liquid chromatography with dual-wavelength ultraviolet detection.* J Pharm Sci, 1984. **73**(8): p. 1104-7.

20.   Wang, X., et al., *Simultaneous quantitative determination of bupropion and its three major metabolites in human umbilical cord plasma and placental tissue using high-performance liquid chromatography-tandem mass spectrometry.* J Pharm Biomed Anal, 2012. **70**: p. 320-9.

21.   Carlquist, M., T. Frejd, and M.F. Gorwa-Grauslund, *Flavonoids as inhibitors of human carbonyl reductase 1.* Chem Biol Interact, 2008. **174**(2): p. 98-108.

22.   Rosemond, M.J., et al., *Enzymology of a carbonyl reduction clearance pathway for the HIV integrase inhibitor, S-1360: role of human liver cytosolic aldo-keto reductases.* Chem Biol Interact, 2004. **147**(2): p. 129-39.

23.   Su, X., et al., *Inhibition of human and rat 11beta-hydroxysteroid dehydrogenase type 1 by 18beta-glycyrrhetinic acid derivatives.* J Steroid Biochem Mol Biol, 2007. **104**(3-5): p. 312-20.

24.   Barter, Z.E., et al., *Scaling factors for the extrapolation of in vivo metabolic drug clearance from in vitro data: reaching a consensus on values of human microsomal protein and hepatocellularity per gram of liver.* Curr Drug Metab, 2007. **8**(1): p. 33-45.

25.   Benowitz, N.L., et al., *Influence of CYP2B6 genetic variants on plasma and urine concentrations of bupropion and metabolites at steady state.* Pharmacogenet Genomics, 2013. **23**(3): p. 135-41.

26.   Ilic, K., et al., *The influence of sex, ethnicity, and CYP2B6 genotype on bupropion metabolism as an index of hepatic CYP2B6 activity in humans.* Drug Metab Dispos, 2013. **41**(3): p. 575-81.

27.   Kharasch, E.D., D. Mitchell, and R. Coles, *Stereoselective bupropion hydroxylation as an in vivo phenotypic probe for cytochrome P4502B6 (CYP2B6) activity.* J Clin Pharmacol, 2008. **48**(4): p. 464-74.

28.   Kirchheiner, J., et al., *Bupropion and 4-OH-bupropion pharmacokinetics in relation to genetic polymorphisms in CYP2B6.* Pharmacogenetics, 2003. **13**(10): p. 619-26.

29.   Chen, Y., et al., *The in vitro metabolism of bupropion revisited: concentration dependent involvement of cytochrome P450 2C19.* Xenobiotica, 2010. **40**(8): p. 536-46.

30.   Meyer, A., et al., *Formation of threohydrobupropion from bupropion is dependent on 11beta-hydroxysteroid dehydrogenase 1.* Drug Metab Dispos, 2013. **41**(9): p. 1671-8.

31.   Brandon, E.F., et al., *An update on in vitro test methods in human hepatic drug biotransformation research: pros and cons.* Toxicol Appl Pharmacol, 2003. **189**(3): p. 233-46.

32.   Jia, L. and X. Liu, *The conduct of drug metabolism studies considered good practice (II): in vitro experiments.* Curr Drug Metab, 2007. **8**(8): p. 822-9.

33.   Laizure, S.C., et al., *Pharmacokinetics of bupropion and its major basic metabolites in normal subjects after a single dose.* Clin Pharmacol Ther, 1985. **38**(5): p. 586-9.

34.   Houston, J.B. and D.J. Carlile, *Prediction of hepatic clearance from microsomes, hepatocytes, and liver slices.* Drug Metab Rev, 1997. **29**(4): p. 891-922.

35.   Peters, W.H. and P.G. Kremers, *Cytochromes P-450 in the intestinal mucosa of man.* Biochem Pharmacol, 1989. **38**(9): p. 1535-8.

36.   Gervot, L., et al., *Human CYP2B6: expression, inducibility and catalytic activities.* Pharmacogenetics, 1999. **9**(3): p. 295-306.

37.   Paine, M.F., et al., *The human intestinal cytochrome P450 "pie".* Drug Metab Dispos, 2006. **34**(5): p. 880-6.
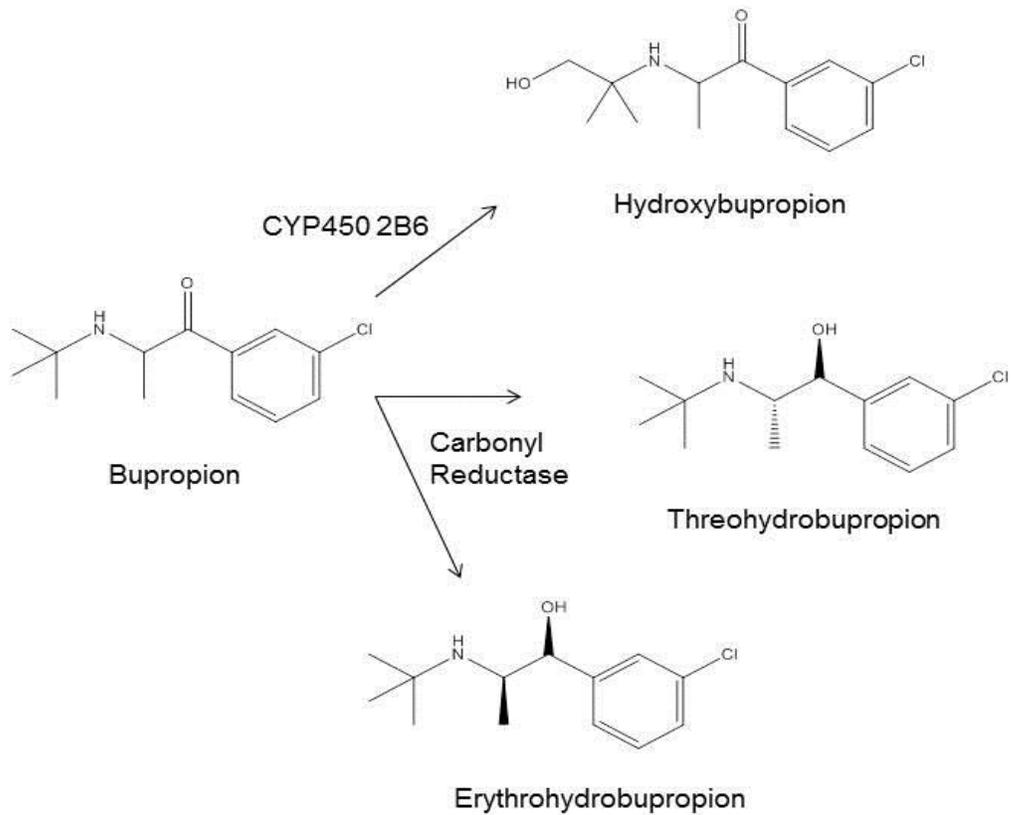
Figure 2-1. **Bupropion and Metabolism.** Bupropion is metabolized by Cytochrome P450 2B6 to form hydroxybupropion and by Carbonyl Reductase to form the diasterisomers, threohydrobupropion and erythrohydrobupropion.

(A)
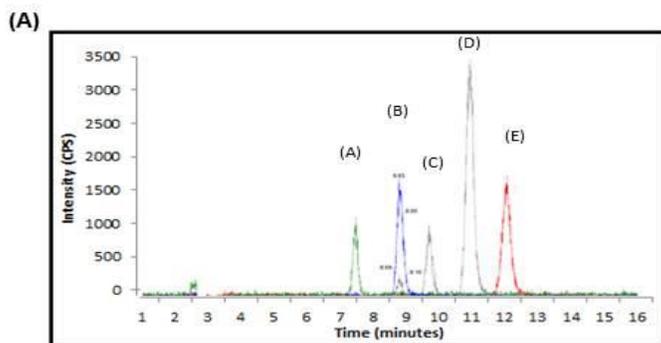
(B)

Peaks	Compound	Rentention time (minutes)	Q1 Mass	Q3 Mass	CE	DP	EP	CXP
(B)	**Bupropion**	8.8	240.1	184	10	50	10	3
(A)	**Hydroxybupropion**	7.3	256	238	12	50	10	3
(D)/(C)	**Threo /Erythrohydrobupropion**	9.96/11.2	242	168.1	5	50	10	3
(E)	**Venlafaxine**	12.5	278	260	10	50	10	3

(C)

Analyte	Linear Range	Linear equation	R^2	LLOQ
Bupropion	5-5000 ng/mL	Y=0.0136X+0.0194	0.9975	5 ng/mL
Hydroxybupropion	10-5000 ng/mL	Y=0.0085X+0.0975	0.9900	10 ng/mL
Threohydrobupropion	5-5000 ng/mL	Y=0.0546X+0.0012	0.9948	5 ng/mL
Erythrohydrobupropion	10-5000 ng/mL	Y=0.0286+0.0652	0.9966	10 ng/mL

Figure 2-2. **Method Development for Bupropion and Metabolites.** (A) Separation of Bupropion and metabolite for detections using LC-MS/MS. (B) LC/MS parameters for bupropion and metabolites. (C) Validation with Standards for bupropion and metabolites. All analytes had a good linear range with acceptable coefficient of determination. CE: collision energy, DP: declustering potential, EP: entrance potential, CXP: collision cell exit potential.
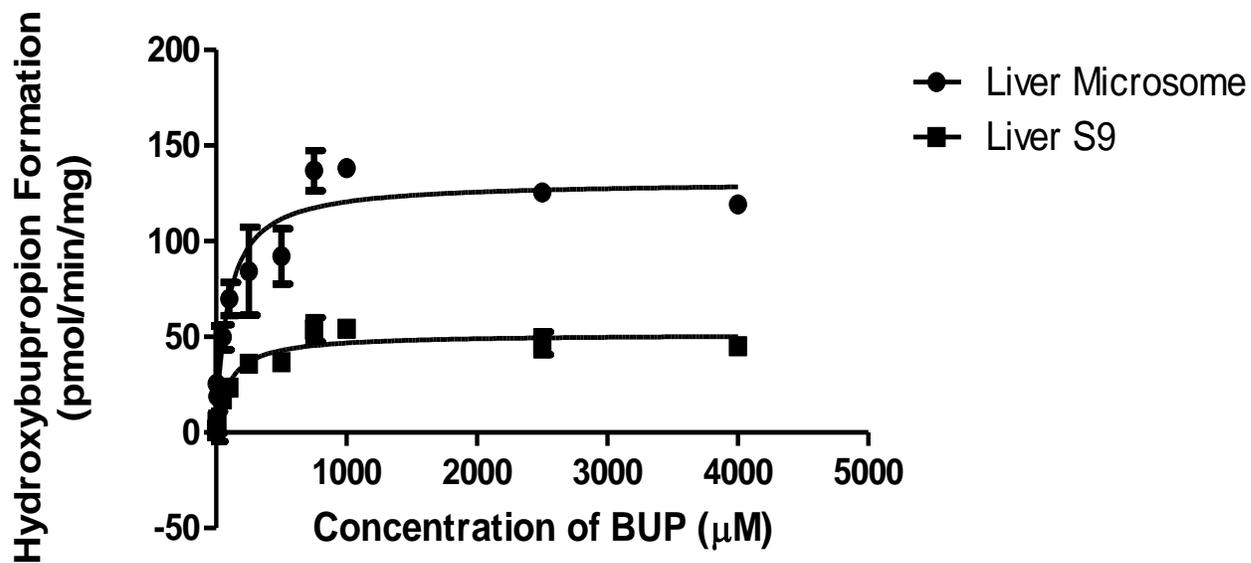
Figure 2-3. **Hydroxybupropion Metabolite Formation in Liver Subcellular Fractions.** Hydroxybupropion formation is indicated in Liver Microsome and Liver S9. No formation occurred in Liver Cytosolic. Data are presented as mean ± S.D. ($n = 3$).
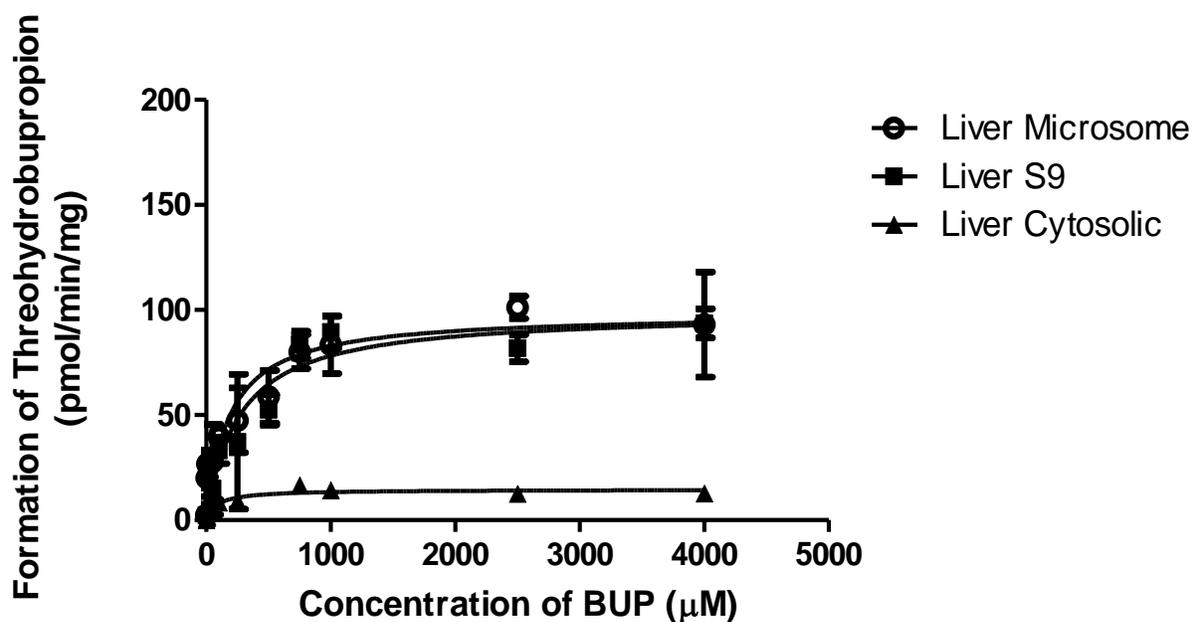
Figure 2-4. **Threohydrobupropion Metabolite Formation in Liver Subcellular Fractions.** Threohydrobupropion formation is indicated in Liver Microsome, Liver S9, and Liver Cytosolic. Data are presented as mean ± S.D. ($n = 3$).
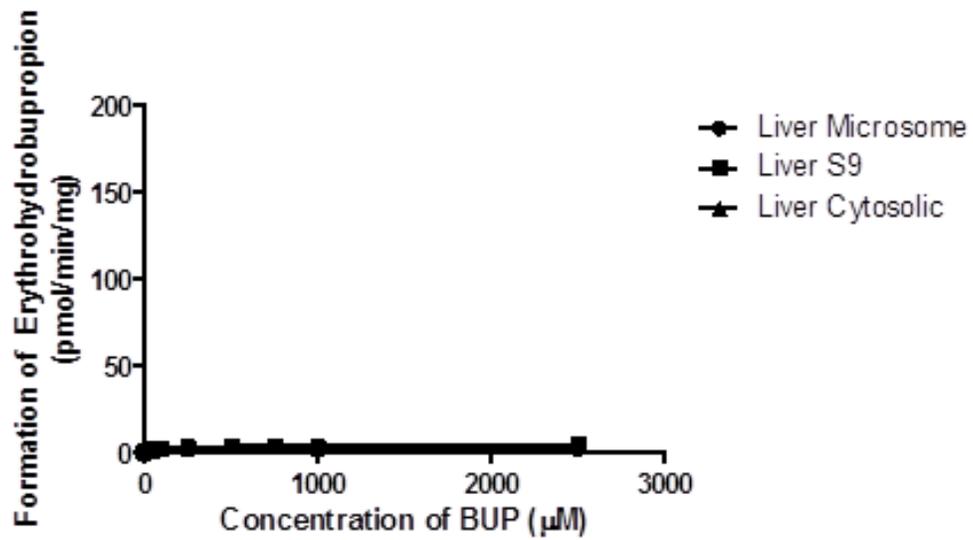
Figure 2-5. **Erythrohydrobupropion Metabolite Formation in Liver Subcellular Fractions.** Erythohydrobupropion formation is indicated in Liver Microsome, Liver S9, and Liver Cytosolic. Data are presented as mean ± S.D. ($n = 3$).
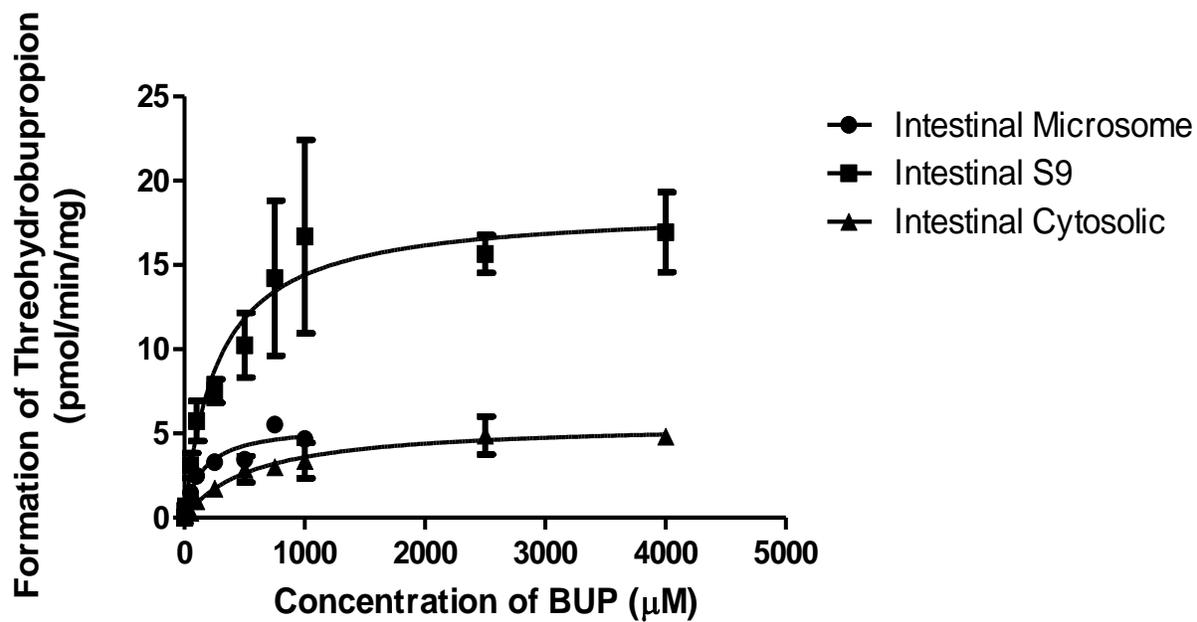
Figure 2-6. **Threohydrobupropion Metabolite Formation in Intestinal Subcellular Fractions.** Threohydrobupropion formatation is indicated in Intestinal Microsome, Intestinal S9, and Intestinal Cytosolic. Data are presented as mean ± S.D. (n = 3).
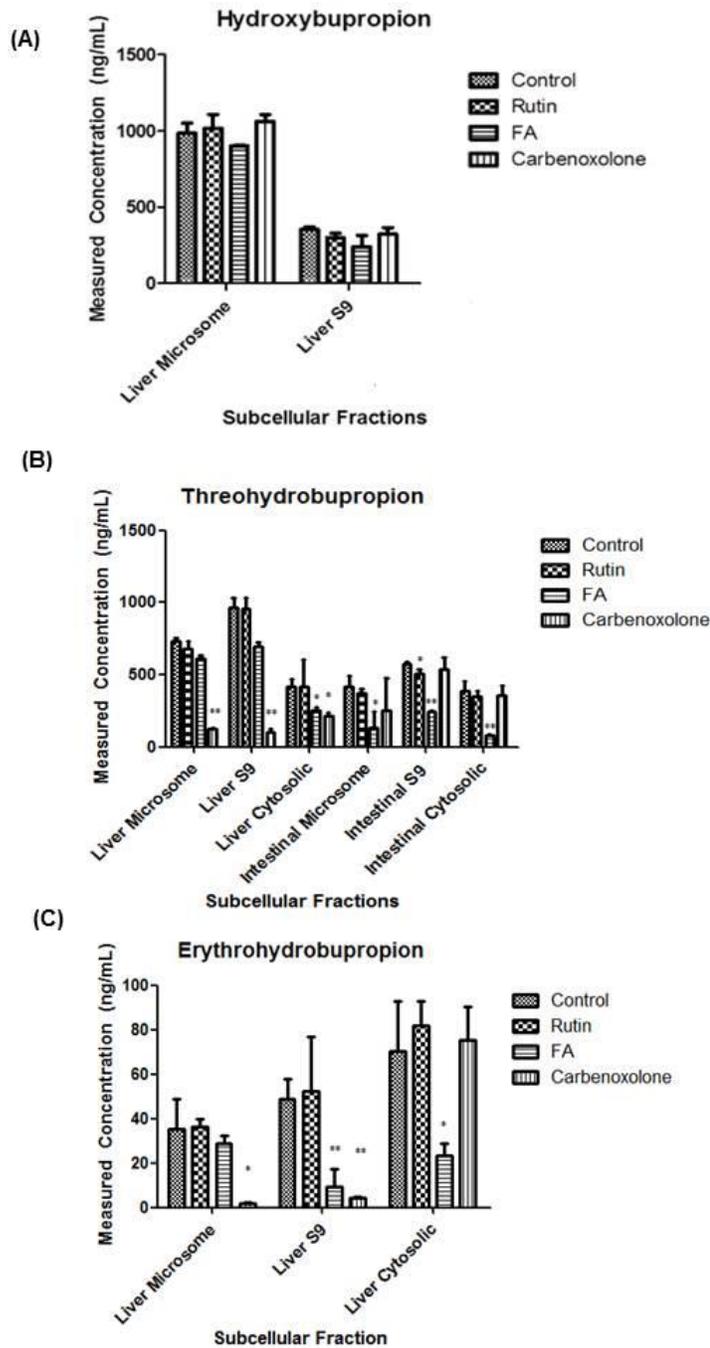
Figure 2-7. **Threohydrobupropion Metabolite Formation in Intestinal Subcellular Fractions.** Threohydrobupropion formatation is indicated in (A) Intestinal Microsome (B) Intestinal S9 (C) Intestinal Cytosolic. Data are presented as mean ± S.D. ($n = 3$). *$P<0.05$, **$P<0.01$.
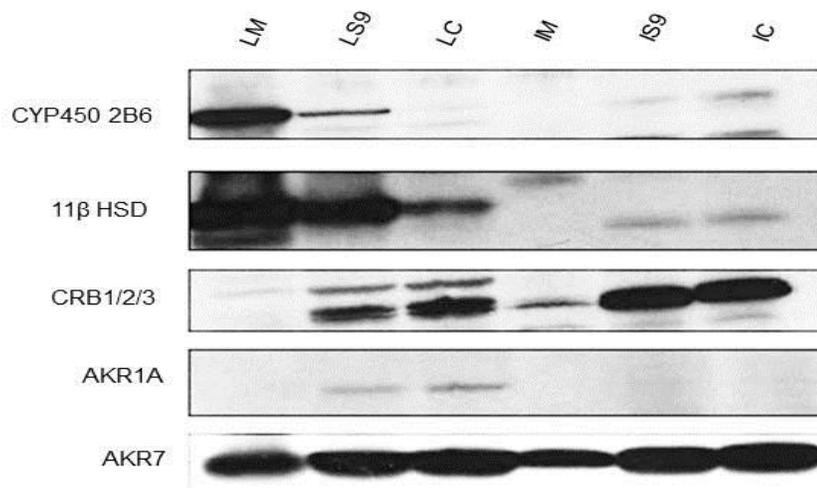
Figure 2-8. **Enzyme Expression in Human Subcellular Fractions.** Subceullar fractions were ran on an SDS-polyacrylamide gradient (4-12% W/V) gel to detect various carbonyl reductase enzyme and CYP2B6. Lane 1: Liver Microsome (LM). Lane 2: Liver S9 (LS9). Lane 3: Liver Cytosolic (LC). Lane 4: Intestinal Microsome (IM). Lane 5: Intestinal S9 (IS9). Lane 3: Intestinal Cytosolic (IC).

(A)

	Liver Microsome		Liver S9		Liver Cytosolic	
	Vmax (pmol/min/mg)	Km (µM)	Vmax (pmol/min/mg)	Km (µM)	Vmax (pmol/min/mg)	Km (µM)
HBUP	131.2 ± 5.8	87.9 ± 20.2	51.4 ± 1.9	99.5 ± 18.9	1.5 ± 0.5	71.3 ± 127
TBUP	98.4 ± 6.6	186.3 ± 53.5	99 ± 7.5	265.7 + 77.7	14.5 + 0.7	89.8 ± 22
EBUP	2.6 ± 0.3	41.4 ± 26.6	4.2 ± 0.28	107 ± 32.1	3.65 ± 1.2	274 ± 254

(B)

	Intestinal Microsome		Intestinal S9		Intestinal Cytosolic	
	Vmax (pmol/min/mg)	Km (µM)	Vmax (pmol/min/mg)	Km (µM)	Vmax (pmol/min/mg)	Km (µM)
HBUP	NF	NF	NF	NF	NF	NF
TBUP	5.55 ± 0.3	149.9 ± 28.8	25.87 ± 2.8	573.4 ± 188	5.6 ± 0.2	569 ± 64.8
EBUP	NF	NF	NF	NF	NF	NF

Table 2-1. **Summary of Subcellular Kinetics.** (A) The Vmax and Km are highlighted for each metabolite in liver microsome, S9, and cytosolic fraction. (B) The Vmax and Km are highlighted for threohydrobupropion metabolite in lintestinal microsome, S9, and cytosolic fraction. If no metabolite formation occurred in the corresponding fraction, this was denoted by NF. HBUP: hydroxybupropion, TBUP:threohydrobupropion, EBUP: erythrohydrobupropion.

Subcellular Fraction	Metabolite	Clint (1)
Liver S9 Fraction	Hydroxybupropion	519 µl/min/mg
	Threohydrobupropion	372 µl/min/mg
	Erythrohydrobupropion	39 µl/min/mg
	Total Clint from liver	**931.8 µl/min/mg**
Intestinal S9 Fraction	Hydroxybupropion	N/A
	Threohydrobupropion	45 µl/min/mg
	Erythrohydrobupropion	N/A
	Total Clint from Intestines	**45 µl/min/mg**
Total Contribution from Liver and Intestines S9 Fraction		976 µl/min/mg

Table 2-2. **Estimated Intrinsic Clearance.** Using equation (2) the intrinsic clearance for both liver and intestines S9 fraction was calculated based off the Michaelis Menten equation assuming the linear portion of the curve. The relative contribution for each metabolite in S9 liver or intestines is indicated in the table.

(A)
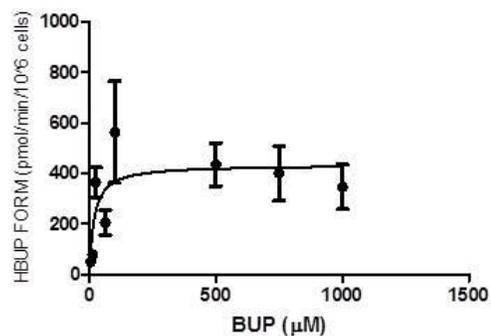
Km	46.2 ± 9.6 µM
Vmax	434.0 ± 46.2 pmol/min/10^6 cells

(B)
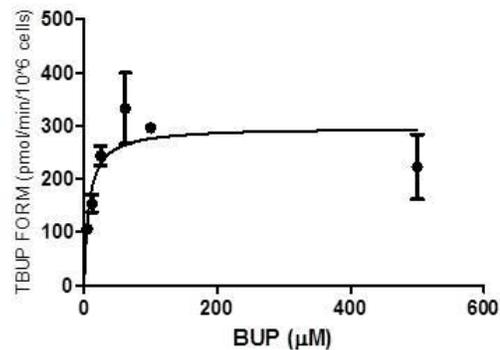
Km	7.67 ± 2.97 µM
Vmax	297.2 ± 23.7 pmol/min/10^6 cells

Supplemental Figure 2-1.. **Hepatocytes Kinetics**. The formation of (A)
hydroxybupropion and (B) threohydrobupropion were measured using hepatocytes at
concentrations of bupropion from 5-1000 µM. Data are presendted as mean ± S.D.
(n=3).

Subcellular Fraction	Metabolite	Cl$_{int}$ (1)
Liver hepatocytes	Hydroxybupropion	0.00947 mL/min/10^6cells
	Threohydrobupropion	0.0125 ml/min/10^6 cells
	Erythrohydrobupropion	n.a.
	Total Clint from liver	**0.02197 ml/min/10^6cells**

Assumptions
99 *10^6 cells/ gr liver
21 gram liver/kg bw

(B)

Metabolite	Intrinsic Clearance (CL$_{int}$) *in vivo* (mL/min/kg)
Hydroxybupropion	19.68
Threohydrobupropion	25.9
Erythrohydrobupropion	n.a.
Total *in vivo* intrinsic CL	**45.67**

$$CLhepatic = \frac{Q * Fu * CLint}{Q + Fu * CLint}$$

Q= 20.7 ml/min/kg
Fu=0.16

(C)

CL hepatic	~ 5.4 ml/min/kg
Extraction	~0.26

Supplemental Table 2-1. **Hepatocytes Kinetics Summary**. (A) Represents the instrinic clearance calculated based on the hepatocyte kinetics, using equation 1 (Vmax/Km). Assuming Scaling factors shown above (Barter 2007) data was scaled to *in vivo* CL intrinsic clearance (B). (C) Represents the hepatic CL and extraction ratio.

Chapter 3
Method Development, Validation, and Sample Analysis of Bupropion in Human Plasma.

Abstract

A liquid chromatography tandem with electrospray ionization mass spectrometry method was developed to quantify bupropion and the major metabolites (hydroxybupropion, threohydrobupropion, and erythrohydrobupropion) in human plasma. The analytes were extracting from the plasma using protein precipitation (main steps include addition of organic solvent (methanol), vortex, centrifugation, and analysis of supernatant by LC-MS/MS). The analytes were separated using a C18 Supelco column with an isocratic gradient at 35% methanol and 65% water (0.04% formic acid, v/v) for 17 minutes. Method development and validation was performed to ensure that the analytical procedure was appropriate for detection of bupropion and metabolites in plasma. After method validation met the standards of the FDA suggested Bioanalytical Methods Guidelines, samples obtained from the clinical trial were analyzed to quantify the concentration of bupropion and major metabolites in plasma samples over 96 hours.

Introduction

Bupropion HCl is a clinically available drug product that was first marketed as Wellbutrin in the 1980's as an immediate release product. Bupropion is used for major depressive disorder, smoking cessation, and seasonal depression. Over the last 25 years, various formulations have come to market (including a sustained and an extended release) in addition to generic bupropion products [1-3]. All generic products undergo bioequivalent (BE) testing to show that using a 90% confidence interval; the mean of both the rate (C_{max}) and extent (Area Under the Curve (AUC)) of the test and reference are within 80-125% [4]. Many generics for bupropion were approved from doses of 75-300 mg in 3 formulations. Due to dose related seizures, the BE studies for the extended release (ER) 300 mg, data was extrapolated using the results from the 150 mg BE study. Both the 150 mg and 300 mg ER for generics were approved for market. However, after addition studies, several generic products at the 300 mg dose failed to meet BE standards [5]. This has then sparked many questions trying to understand what is causing the difference in systemic exposure for both bupropion and metabolites. Bupropion is also extensively metabolized (as the primary route of elimination) to form three primary active metabolites; hydroxybupropion, threohydrobupropion, and erythrohydrobupropion [6, 7]. In an animal model it was shown that these metabolites may exhibit 25-50% potency [8, 9]. Although many *in vitro* studies have been perform to quantify the formation rate of these metabolites [7, 10-12], it is unknown if these active metabolites are causing any difference in efficacy. In addition, another question is whether gastrointestinal (GI) regional dependency might affect the absorption and/or metabolism of bupropion?

61

Therefore, a clinical study was designed to address some of these questions by running a single dose, 6 phase, crossover study (immediate release 75 & 100, sustained release 100 &150, and extended release 150 & 300 mg). The plasma from these samples were analyzed using liquid chromatography- mass spectrometry/ mass spectrometry (LC-MS/MS) The purpose of the following studies were to develop a sensitive, specific, and reproducible analytic method using LC-MS/MS to detect bupropion and it's major metabolites (hydroxybupropion, threohydrobupropion, and erythrohydrobupropion) in human plasma.

After the method was developed, we confirmed that the matrix effect had little influence on detection of bupropion and metabolites, our samples had less than 10% difference when comparing neat (organic solvent) to plasma samples. We also showed that the accuracy and precision for both inter- and intra-day was within 85-115% and %CV was less than 15% of the nominal concentration, respectively. There was very little carry over for all analytes including the internal standard (<0.1%) and the recovery was reproducible. Finally, we showed the samples were stable at room temperature (25⁰ C) for up to 16 hours. The bioanalytical method was developed based off *Guidance for Industry: Bioanalytical Method Validation* [13]. Following method validation, clinical samples were analyzed trying to unravel some of the issues that may be causing bioinequivalence for bupropion.

Materials/ Methods

Reagents

Bupropion HCl, venlafaxine HCl (internal standard; IS), and formic acid were purchased from Sigma (St. Louis, MO). Metabolites; hydroxybupropion was purchased from

Caymen Chemicals and both erythrohydrobupropion and threohydrobupropion were purchased from Toronto Research Chemicals. Methanol (HPLC grade) were purchased from Fisher Scientific (Pittsburgh, PA, USA). Water was purified with a Milli-Q water system (Bedford, MA). All other solvents and chemicals were analytical grade or better.

Liquid Chromatography/ Mass Spectrometry-Mass Spectrometry Optimization

The LC-MS/MS analysis was conducted using an Agilent 1200 HPLC system coupled to an API 3200 mass spectrometer (Applied Biosystems, MDS Sciex Toronto, Canada) equipped with an API electrospray ionization (ESI) source. Quantitative analysis was accomplished on a Supelco C18 (150 x 4.6 mm I.D., 5 µm). The mobile phases were 0.04% formic acid in purified water (A) and 0.04% formic acid in methanol (B). An isocratic was held constant at 35% and the flow rate was set at 0.8 mL/min for 17 minutes.

The LC-MS/MS was operated at positive ESI ionization. The MRM transitions and collision energies determined for bupropion, hydroxybupropion, threo/ erythrohydrobupropion and internal standard are listed in **Table 1**. The source parameters for the MS consisted of a curtain gas (CUR) of 45, collision gas (CAD) at medium, ionspray voltage at 5500, temperature (TEM) was 700, ion source gas (GS1 and GS2) were both 70 for bupropion and metabolites. The analytical data were processed by Analyst software (version 1.2; Applied Biosystems, Foster City, CA, USA).

The quantitation of bupropion, hydroxybupropion, threohydrobupropion and erythrohydrobupropion were performed by multiple reaction monitoring (MRM) of the

[M-H] $^+$ ion, using an internal standard (IS) to establish peak area ratios. The LC-MS/MS method was adapted and slightly modified from other studies [6, 14, 15].

Stock Solutions and Sample Prep

Bupropion, hydroxybupropion, threohydrobupropion, and erythrohydrobupropion solutions were made fresh at least every two weeks. All 4 compounds were dissolved in methanol at 2 mg/mL. Stock solutions for the standard curves were made at 10 µg/mL.

All samples contained 500 nM of internal standard in methanol (unless noted). Typical standard preparation consisted of 150 µL of internal standard, 50 µL of plasma, and 50 µL of methanol (if this was not a clinical sample or blank, analyte was dissolved in this methanol at the appropriate concentration). After all samples were vortex for at least one minute, centrifuged at 14,000 rpm, and the supernatant was transferred to an amber color HPLC vial for analysis on the LC-MS/MS.

Results

Method Development Selectivity & Specificity

In order to evaluate the selectivity, blank plasma samples were ran (n=3) to ensure no excess background signal was detected (**Figure 1**). The average noise was 50 CPS. This was done using 200 µL of methanol and 50 µL of plasma. In addition, we looked at specificity by looking at the internal standard alone (n=3) in the plasma matrix (**Figure 2**). There was no interference observed and the retention time was consistent. To evaluate the specificity for each analyte; bupropion, hydroxybupropion,

threohydrobupropion, or erythrohydrobupropion were ran at the corresponding LLOQ

(n=3/ analyte) (**Figure 3**). For each LLOQ we ensured that the signal to noise (S/N)

ratio was greater than 3.5 and the peak area for the LLOQ was at least 5 times the peak

area of the blank sample.

Calibration Curves

In order to quantify bupropion and its metabolites from the plasma samples obtained in

our clinical trial, we developed calibration curves for each analyte. **Table 2** shows the

linear range, linear equation, coefficient of determination (R^2), and LLOQ for each

analyte. Calibration curves consisted of at least 6 non- zero samples that covered the

linear range. The accuracy of the nominal concentration for each calibration curve

sample was within 80-120% and the R^2 for each curve was above .99 for each batch.

With each batch of clinical samples analyzed, a fresh calibration curve for each analyte

was made and quality control (QC) samples at low (10ng/mL), medium (50 ng/mL), and

high (2500 ng/mL) concentrations were used to validate the standard curves (two QC

per concentration per analyte). The QC needed to be within 85-115% of nominal

concentration with the exception of the LLOQ which was within 80-120%. At least 67%

(4/6) of QC samples needed to meet these criteria for it to be an acceptable run.

Matrix Effect

In order to examine whether the matrix had an effect on the detection signal, we

prepared samples in both plasma and organic solvent (neat). Each sample had 150 µL

of methanol containing internal standard (500 nM), 50 µL of sample at desired

concentration (10, 500, 2500 ng/mL), and 50 µL of plasma or methanol (neat). All

samples were vortex, centrifuged at 14,000 rpm, and the supernatant was transferred to an amber HPLC vial. In order to determine the matrix effect, the peak area ratio of the neat vs plasma sample was compared and was acceptable if the %CV was less than 15% of nominal concentration. **Table 3** showed that the plasma matrix had very little to no effect on quantifying analytes in each sample.

Accuracy/ Precision

At three different concentrations (10, 500, 2500 ng/mL) (n=5) for each day, the precision and accuracy was measured. Samples were prepared as normal by protein precipitation. The intra- and inter- day accuracy and precision was also evaluated. Each day we ran 5 samples per analyte for 3 days. The accuracy was within 15% of the nominal value and the precision had a %CV less than 15%. **Tables 4 & 5** shows that the method met acceptable criteria for both accuracy and precision.

Recovery

Using 3 different batches and 3 different concentrations (10, 500, 2500 ng/mL) for each analyte, the recovery was measured. For one set of samples, they were prepared as normal; each sample had 150 µL of methanol containing internal standard (500 nM), 50 µL of sample at the desired concentration, and 50 µL of plasma. All samples were vortex, centrifuged at 14,000 rpm, and the supernatant was transferred to an amber HPLC vial. For the second set, samples were prepared by only adding 180 µL of methanol containing internal standard (500 nM) and 60 µL of plasma followed by vortex and centrifugation. After centrifugation, 200 µL was taken from this sample was added with 50 µL of analyte at the desired concentration in methanol. The recovery was

calculated by comparing the peak area of the analyte between the two separate preparations. **Table 6** shows the recovery was acceptable since it was consistent and reproducible for each analyte for over a concentration range of 10-2500 ng/mL.

Short Term Stability

Bupropion and major metabolites short term stability at room temperature for 36 hours was analyzed using 2 concentrations (low at 10 ng/mL and high at 2500 ng/mL) (n=3/ each analyte/concentration). The same samples were analyzed at 0, 8, 16, 24, and 36 hours to see if the peak area concentrations were maintained over time. For the high concentrations, none of the analytes showed a significant decrease in peak area; bupropion stayed within 82% of the 0 hour peak area over 36 hours, hydroxybupropion stayed within 91-102% over 36 hours, threohydrobupropion stayed within 97-101% over 36 hours, and erythrohydrobupropion stayed within 99-101% over 36 hours. For the low concentrations; bupropion's peak area started to decrease at 16 hours (64% of 0 hour peak area), however, the other 3 analytes were able to maintain stable peak areas over 36 hours. Hydroxybupropion's peak area over 36 hours at low concentrations were within 93-101%, threohydrobupropion's peak area at low concentrations were within 85.5-102% over 36 hours, and erythrohydrobupropion's peak area at low concentrations were 87-92% over 36 hours. Therefore, for analyzing our clinical samples, no samples were allowed to be at room temperature for more than 8 hours due to degradation of bupropion at low concentrations.

Carryover

The upper limit of quantification (ULOQ) for each analyte (5000 ng/mL) was ran (n=3) followed by a blank plasma sample. The percent from the peak area of the blank sample to peak area of the ULOQ was calculated to ensure no carryover was occurring for any of the analytes(<20%). This was also performed with the internal standard where the carryover needed to be less than 5%. For our samples, the maximum carryover observed was <2% for each analyte and internal standard.

Clinical Sample Analysis

All clinical samples were stored at -80 ºC until sample analysis. Each sample was prepared with 50 µL of plasma, 50 µL of methanol, and 150 µL of internal standard (500 nM) in methanol. All samples were vortex for one minute, centrifuged, and supernatant was analyzed by LC-MS/MS. Runs were only considered acceptable if 67% of the QC samples were in the appropriate range (85-115% except the LLOQ acceptable range was 80-120%).

Conclusion

We were able to successfully develop and validate a sensitive, accurate, reproducible method to detect bupropion and major metabolites in human plasma using LC-MS/MS. We were able to use this method to detect bupropion and its major metabolites in our clinical trial to evaluate the concentration of bupropion and metabolites in plasma for the various formulations and doses.

References

1.	Dhillon, S., L.P. Yang, and M.P. Curran, *Bupropion: a review of its use in the management of major depressive disorder.* Drugs, 2008. **68**(5): p. 653-89.
2.	Dwoskin, L.P., et al., *Review of the pharmacology and clinical profile of bupropion, an antidepressant and tobacco use cessation agent.* CNS Drug Rev, 2006. **12**(3-4): p. 178-207.
3.	Jefferson, J.W., J.F. Pradko, and K.T. Muir, *Bupropion for major depressive disorder: Pharmacokinetic and formulation considerations.* Clin Ther, 2005. **27**(11): p. 1685-95.
4.	Galgatte, U.C., et al., *Study on requirements of bioequivalence for registration of pharmaceutical products in USA, Europe and Canada.* Saudi Pharm J, 2014. **22**(5): p. 391-402.
5.	Woodcock, J., M. Khan, and L.X. Yu, *Withdrawal of generic budeprion for nonbioequivalence.* N Engl J Med, 2012. **367**(26): p. 2463-5.
6.	Loboz, K.K., et al., *HPLC assay for bupropion and its major metabolites in human plasma.* J Chromatogr B Analyt Technol Biomed Life Sci, 2005. **823**(2): p. 115-21.
7.	Skarydova, L., et al., *Deeper insight into the reducing biotransformation of bupropion in the human liver.* Drug Metab Pharmacokinet, 2014. **29**(2): p. 177-84.
8.	Bondarev, M.L., et al., *Behavioral and biochemical investigations of bupropion metabolites.* Eur J Pharmacol, 2003. **474**(1): p. 85-93.
9.	Damaj, M.I., et al., *Enantioselective effects of hydroxy metabolites of bupropion on behavior and on function of monoamine transporters and nicotinic receptors.* Mol Pharmacol, 2004. **66**(3): p. 675-82.
10.	Coles, R. and E.D. Kharasch, *Stereoselective metabolism of bupropion by cytochrome P4502B6 (CYP2B6) and human liver microsomes.* Pharm Res, 2008. **25**(6): p. 1405-11.
11.	Kharasch, E.D., D. Mitchell, and R. Coles, *Stereoselective bupropion hydroxylation as an in vivo phenotypic probe for cytochrome P4502B6 (CYP2B6) activity.* J Clin Pharmacol, 2008. **48**(4): p. 464-74.
12.	Molnari, J.C. and A.L. Myers, *Carbonyl reduction of bupropion in human liver.* Xenobiotica, 2012. **42**(6): p. 550-61.
13.	Administration, F.a.D. *Guidance for Industry: Bioanalytical Method Validation.* 2013; Available from: http://www.fda.gov/downloads/drugs/guidancecomplianceregulatoryinformation/guidances/ucm368107.pdf.
14.	Borges, V., et al., *High-throughput liquid chromatography-tandem mass spectrometry determination of bupropion and its metabolites in human, mouse and rat plasma using a monolithic column.* J Chromatogr B Analyt Technol Biomed Life Sci, 2004. **804**(2): p. 277-87.
15.	Cooper, T.B., R.F. Suckow, and A. Glassman, *Determination of bupropion and its major basic metabolites in plasma by liquid chromatography with dual-wavelength ultraviolet detection.* J Pharm Sci, 1984. **73**(8): p. 1104-7.

Compound	Q1 Mass	Q3 Mass	Collision Energy (CE)	Declustering Potential (DP)	Entrance Potential (EP)	Collision Cell Exit Potential (CXP)
Bupropion	240.1	184	10	50	10	3
Hydroxybupropion	256	238	12	50	10	3
Threo/Erthrohydrobupropion	242	168.1	5	50	10	3
Venlafaxine	278	260	10	50	10	3

Table 3-1. **MRM Parameters.** The transitions for each analyte are shown in this table as well as the MS optimization for collision energy, declustering potential, entrance potential, and collision cell exit potential.

(A)

(B)

(C)
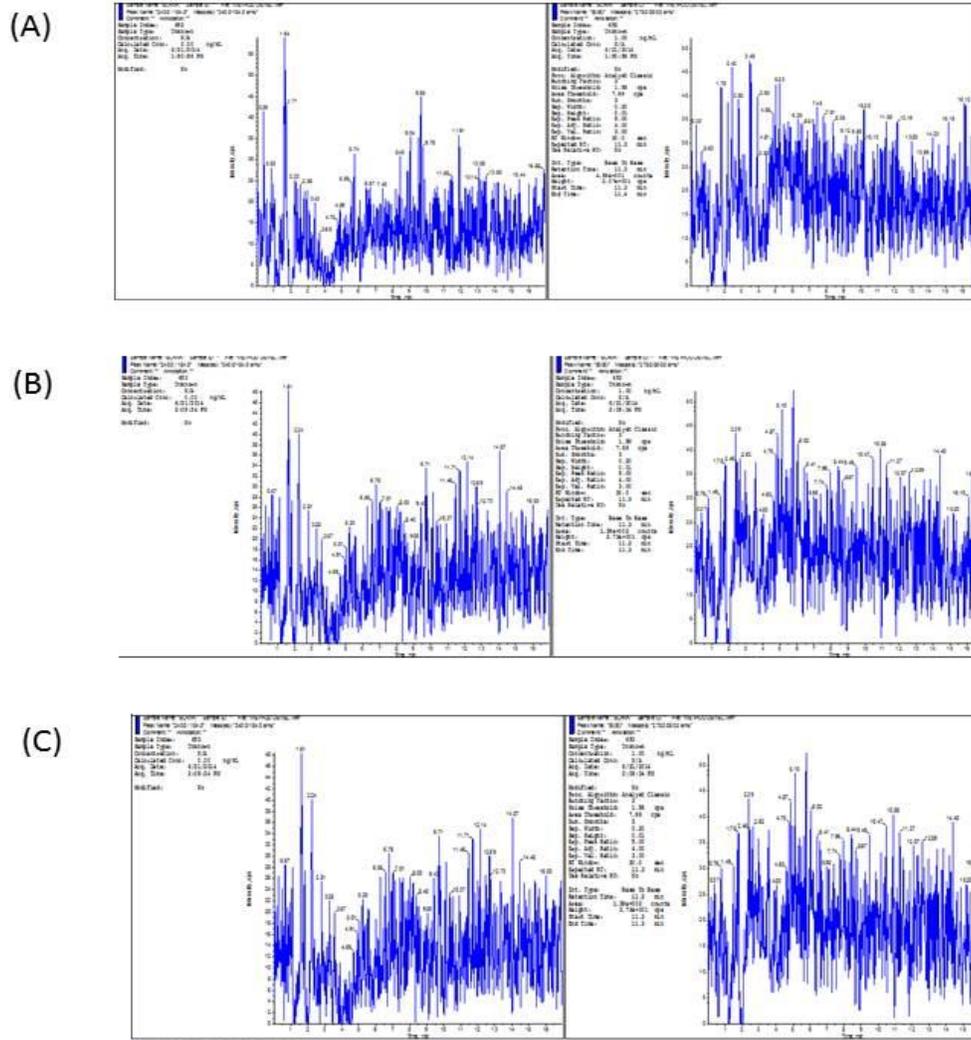
Figure 3-1. **MRM Chromatograms of Blank Plasma Samples for Selectivity.** The left side of the chromatogram represents no detections of analytes. The right side of the spectra represents no detections of internal standard. Average of noise =50 CPS. Data represents (n=3).

(A)

(B)

(C)
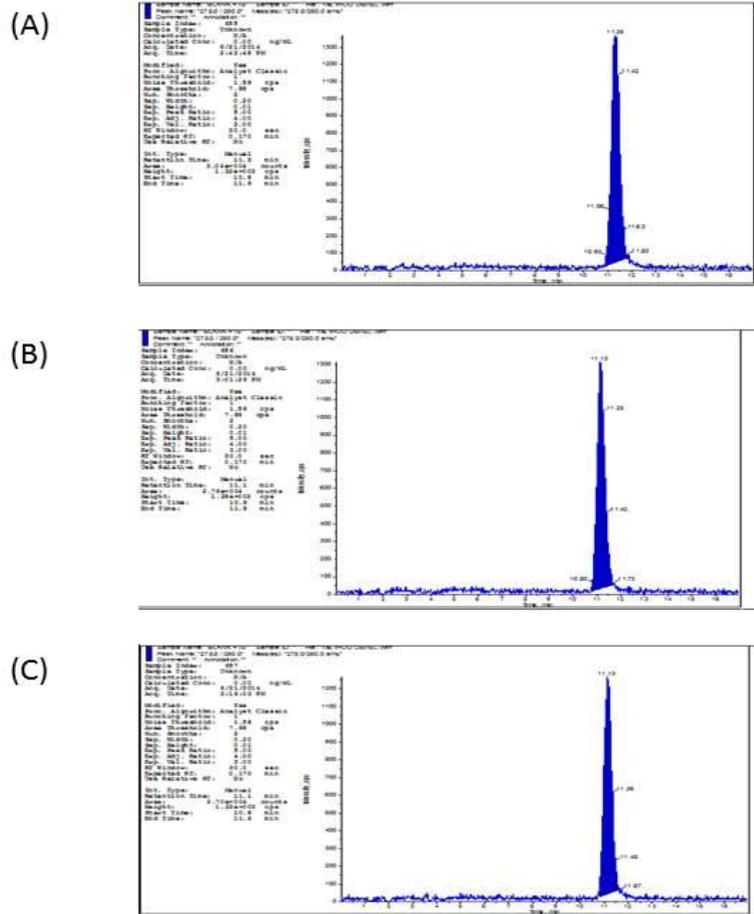
Figure 3-2. **MRM Chromatograms of Blank Samples with IS for Selectivity.** The chromatograms represent the detections of internal standard at 500 nM and no interference of analyte detection. Average Retention Time: 11.2±0.12 minutes. Average Peak Height: 1.5X10^3 CPS. Data represents (n=3).

(A)

(B)

(C)

(D)

(E)

Peak Area of the blank to Peak Area of LLOQ			
	Signal 1	Signal 2	Signal 3
Bupropion	2080	2410	2120
Hydroxybupropion	2060	2970	2010
Threohydrobupropion	15900	17400	16100
Erythrohydrobupropion	13200	12900	12600
Blank	133	127	222
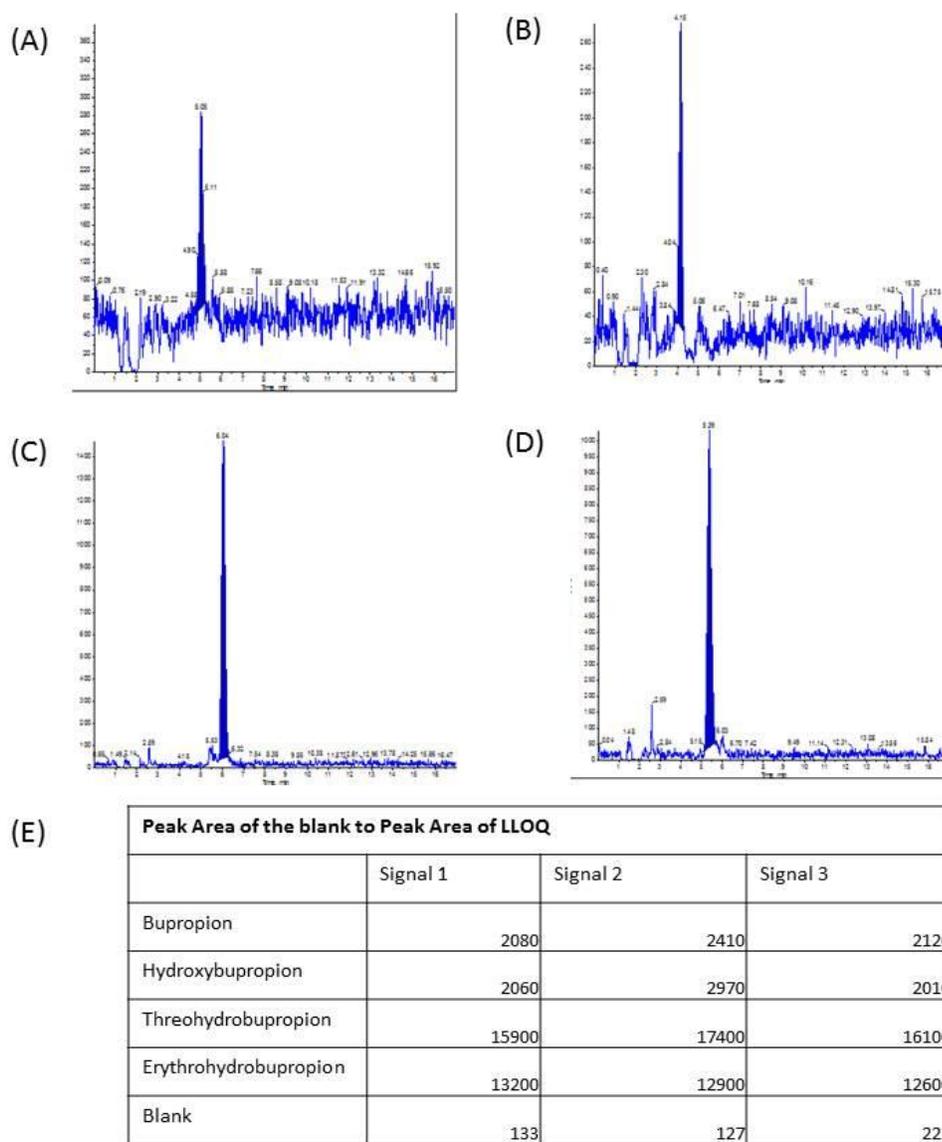
Figure 3-3. **Specificity for Bupropion and Metabolites.** One chromatogram for each analyte is shown; (A) bupropion (B) hydroxybupropion (C) threohydrobupropion (D) erythrohydrobupropion. The LLOQ was determined for each analyte. We ensured that both the S/N was less than 3 and (E) peak area of each analyte was at least 5X greater than blank.

Analyte	Linear Range (ng/mL)	Linear Equation	R^2	Lower Limit of Quantification (LLOQ) (ng/mL)
Bupropion	2.5-5000	Y=0.00251x+0.00723	0.9941	2.5
Hydrobupropion	5-5000	Y=0.00356x+0.0105	0.9904	5
Threohydrobupropion	5-5000	Y=0.00985x+0.00572	0.9910	5
Erythrohydrobupropion	5-5000	Y=0.00712X+0.0008	0.9902	5

Table 3-2. **Standard Curves for Bupropion and Metabolites**. Calibration curves for each analyte was ran for each batch of samples being analyzed. The linear range and LLOQ seen in the table was consistent with each batch. The coefficient of determination was 0.99 or greater for each batch.

Analyte	Nominal Concentration (ng/mL)	ME (%)
Bupropion	10	99.2
	500	95.9
	2500	95.2
Hydroxybupropion	50	96.8
	500	97.5
	2500	97.9
Threohydrobupropion	10	101
	500	99.2
	2500	101
Erythrohydrobupropion	10	99.6
	500	102
	2500	95.2

Table 3-3. **Matrix Effect Analysis.** The matrix effect was determined by comparing the neat sample (in organic solvent) to a post-extraction spiked plasma sample. The percentage of matrix effect (ME) was calculated by the peak area of post-extraction spiked sample divided by peak area of the neat sample (n=3). The matrix has no effect on the samples.

Analyte	Nominal Concentration (ng/mL)	Intra-day (n=5)			Inter-day over 3 days (n=30)		
		Average Conc Observed (ng/mL)	Standard Error	Average Accuracy (%)	Average Conc Observed (ng/mL)	Standard Error	Average Accuracy (%)
BUP	10 500 2500	11.0 444 2786	1.41 12.73 13.6	110 88.8 111.4	10 429.8 2817	1.25 14.99 50.0	100 85.9 112.6
H-BUP	10 500 2500	9.33 587 2220	0.29 1.41 28.28	93.3 117.5 88.8	10.2 578 2270	1.04 11.12 89	101.4 115.5 90.85
T-BUP	10 500 2500	10.8 544.5 2190	0.49 14.85 40	107.5 109 87.6	10.4 551 2323	0.8 23.3 115.4	104.5 110.1 92.2
E-BUP	10 500 2500	10.7 487.5 2564	1.89 27.58 94.2	106.7 97.4 102.5	10.8 495 2488	1.1 17.5 115.9	108.2 98.9 99.5

Table 3-4. **Accuracy.** The accuracy of bupropion and major metabolites were analyzed both intra- and inter- day (n=5) over 3 days. All analytes stayed with 85-115% of nominal concentration.

Analyte	Nominal Concentration (ng/mL)	Intra CV (%) (n=5)	Inter CV (%) over 3 days (n=30)
BUP	10	10.5	17.2
	500	1.45	12.2
	2500	2.7	1.77
H-BUP	10	10.7	13.35
	500	1.49	7.21
	2500	0.59	8.29
T-BUP	10	0.07	8.52
	500	0.009	8.42
	2500	8.2	4.97
E-BUP	10	0.15	8.0
	500	2.3	12.0
	2500	3.67	5.29

Table 3-5. **Precision.** The Precision for bupropion and major metabolite was monitor to ensure a %CV of 15 or less both intra and inter variability (n=5) over 3 days.

Sample #	Nominal Concentration (ng/mL)	BUP (%)	H-BUP (%)	T-BUP (%)	E-BUP (%)
1	10	97.5	78.8	114	91.1
2	10	90.9	67	116	97.4
3	10	109	73.5	100	98.3
1	500	87.8	103	97.2	100
2	500	88.7	99.0	102	99.2
3	500	94.3	98.5	101	94.8
1	2500	101	101	100	105
2	2500	107	103	106	95.2
3	2500	97.8	108	97.2	96.2

Table 3-6. **Recovery.** The recovery for bupropion and major metabolites were monitor to ensure reproducibility at low, medium, and high concentrations. The peak area of the analyte post-spike to normal preparation.
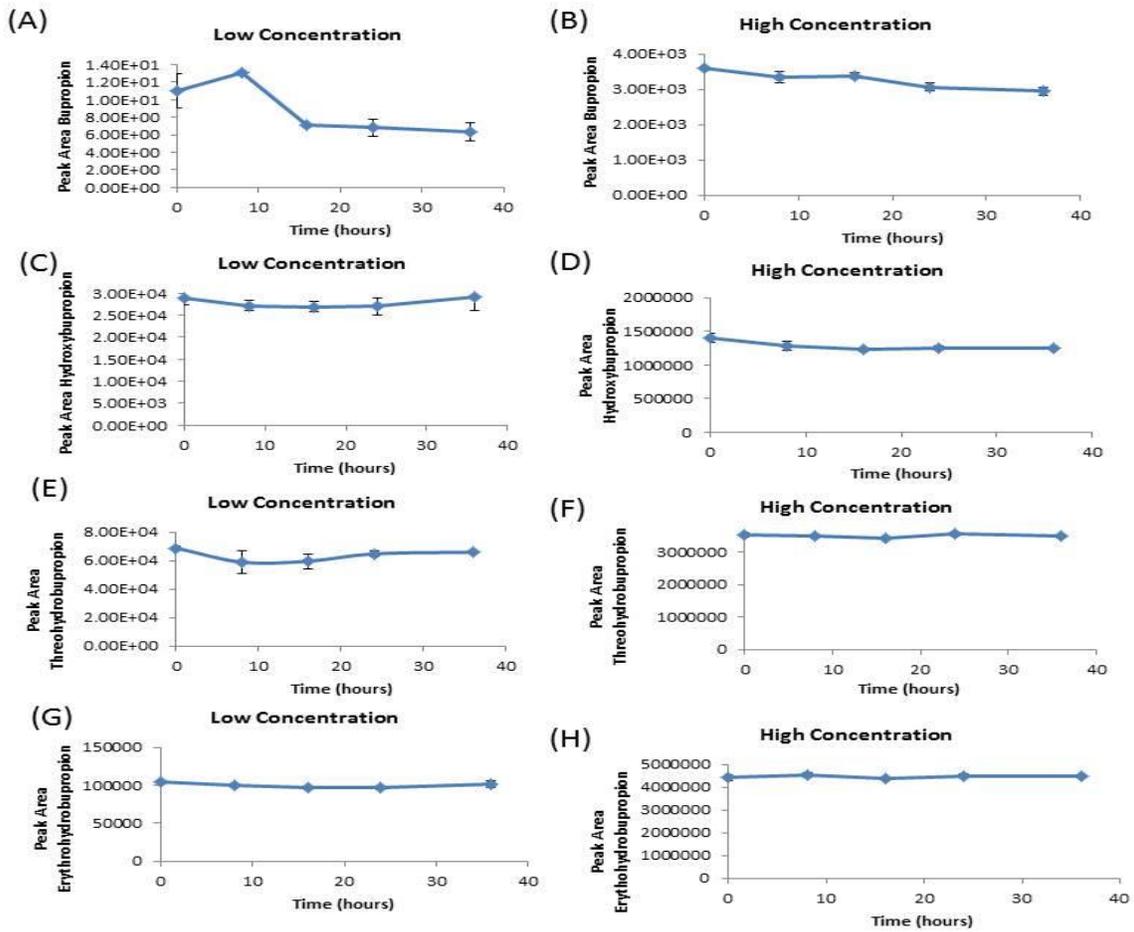
Figure 3-4. **Short term stability.** The short term stability was analyzed for each analyte by keeping samples at room temperature for 36 hours. Plots represent any decrease in peak area stability over this range of time. Bupropion was measured at (A) low and (B) high concentration, hydroxybupropion stability was measured at (C) low and (D) high concentration, threohydrobupropion was measured at (E) low and (F) high concentration, and erythrohydrobupropion was measured at (G) low and (H) high concentration. Low concentrations were 10 ng/mL and high concentrations were 2500 ng/mL.

(A)

sample #	% of analyte measured in blank(n=3)	% of IS measured in blank(n=3)
1	0.03%	0.50%
2	0%	0%
3	0.00%	0%

(B)

sample #	% of analyte measured in blank(n=3)	% of IS measured in blank(n=3)
1	0.008%	0%
2	0.029%	0%
3	0.029%	0.7%

(C)

sample #	% of analyte measured in blank(n=3)	% of IS measured in blank(n=3)
1	1.2%	0%
2	1.3%	0.71%
3	1.5%	0.44%

(D)

sample #	% of analyte measured in blank(n=3)	% of IS measured in blank(n=3)
1	0.57%	0.17%
2	0%	0%
3	0.71%	0.69%

Figure 3-5. **Carryover.** The ULOQ of each analyte was ran followed by blank sample. The percent from blank sample to ULOQ was calculated to determine if carryover existed. (A) bupropion; (B) hydroxybupropion; (C) threohydrobupropion; (D) erythrohydrobupropion.

Chapter 4
Investigate Different Release Mechanisms that May Alter Absorption, Metabolism, and Pharmacogenomics of Bupropion.

Abstract

The purpose of these studies was to evaluate whether different release mechanisms of bupropion changes absorption or metabolism of bupropion following immediate release, sustained release, and extended release formulations; and to estimate *in vivo* release and absorption rate of bupropion following modified release (MR) products. We performed a 6 phase cross-over study with healthy individuals and collected plasma samples to quantify bupropion and the major metabolites after being dosed by one of the various formulations. We observed that ER products showed a decrease in relative bioavailability compared to the reference IR products. When we compared the AUC (m)/ AUC (p), there were no differences among formulations for each of the ratios for any of the metabolites. Bupropion products showed high inter-subject pharmacokinetic variability, which may be amplified by different release rates. Using Weibull type absorption, we were able to describe the absorption rate of bupropion's MR products. When we looked at the systemic appearance of drug among the different formulations, the absorption of bupropion was complete by 2 hours for the immediate release formulations, 4-6 hours for the sustained release formulations, and 10 hours for the extended release formulations.

Introduction

Bupropion HCl is a clinically available drug product that was first marketed as an immediate release (IR) product and was approved in the 1980's; however, the IR formulation is dosed 3 times daily. To help with patient compliance, a sustained release (SR) (b.i.d.) and extended release (ER) (q.d.) became available in 1996 and 2003 respectively [1, 2].

Bupropion is a CNS drug used for major depression, smoking cessation, and seasonal depression [6-9]. Bupropion is a BCS class I drug due to its high permeability and high solubility [10]. It is extensively metabolized to form 3 primary active metabolites; hydroxybupropion and the diastereoisomers threo/ erythrohydrobupropion by Cytochrome P450 2B6 (CYP2B6) and Carbonyl Reductase (CR) respectively [11-14]. Using an animal model, it was shown that these metabolites might exhibit as much as 25-50% potency compared to bupropion [15, 16]. Bupropion is 87% excreted in urine (0.05% unchanged) and 10% eliminated in feces.

To date, there is a gap in comparing these different formulations both in terms of efficacy and its pharmacokinetics [3]. Studies have suggested that these formulations are bioequivalent; however, bupropion has been noted for its high inter-patient variability and differences in plasma concentrations are normally observed [4, 5]. We proposed that if different release profiles caused changes in absorption, metabolism, and were differences in polymorphisms influencing this as well. Therefore, we conducted a clinical trial consisting of a single dose, 6 phase, crossover study where all participants were randomized to one of the formulations at two different doses to

explore aspects relating to absorption and metabolism to see if this variability can be explained.

Using the clinical data samples analyzed by LC-MS, we extensively looked at metabolism by comparing the concentration of bupropion and its major metabolites in plasma for each formulation as well as genotyping these participants for CYP2B6 to see if any variability can be related to polymorphisms in this metabolizing enzyme. Similarly, we examined absorption and the rate of absorption to look at differences amongst these formulations. In typical pharmacokinetics, drug absorption rate is described by a first order process [17]. An alternative to this model is the flip-flop model which is typically observed with modified release products [18]. In this model the drug absorption is slower than elimination, therefore the terminal slope tends to show the absorption phase (k_a) rather than elimination (K_e) [19]. Several papers have highlighted alternative methods for measuring absorptions. One paper specifically highlights atypical absorption profiles aside from first order absorption; including parallel first order absorption, mixed zero-order and first-order absorption, Weibull-type absorption, absorption window with or without Michaelis-Menten, and time-dependent absorption [20]. For the purpose of these studies, we focused on Weibull-type absorption as it allows the absorption rate to change over time.

In our study, we showed that metabolism did not contribute significantly to the variability observed in PK parameters. Bupropion's ER products showed lower relative bioavailability compared to the immediate release products. Finally, we demonstrated that bupropion's absorption rate can be described by Weibull-type absorption and absorption rate for all products were complete by 10 hours or less.

Materials/ Methods

Clinical Trial/ Patient Recruitment

This study was approved by both the Food & Drug Administration Institutional review board (IRB) and the University of Michigan IRB for both the protocol and informed content (HUM00081894). All participants signed an informed content (IC) before drug was administered.

Study Subjects, recruitment, screening, and contentment

The data analysis performed here was with 14 participants who have completed the study (one participant dropped from the study after 2 phases). There were no sex/gender or racial/ethnic group excluded from this study; although healthy participants had to meet the inclusion/ exclusion criteria (see below). To date the demographics our study are outlined in **Supplemental Table 1**.

Details Highlighting Inclusion and Exclusion from Protocol	
Inclusion Criteria	**Exclusion Criteria**
- Healthy volunteers 25 to 55 years old. - Subjects are willing to participate in the study as indicated by giving informed consent. - Volunteers have a BMI within a range of 18.5 to 35. - Willing to be medication and supplement free 2 weeks prior to beginning study, and throughout the study. All forms of birth control are okay. - Willing to abstain from alcohol for duration of study.	- Patients unwilling or unable to comply with the study protocol - Patients unwilling or unable to take bupropion or have an allergy to bupropion - Any medical or surgical conditions which might significantly alter bupropion absorption and pharmacokinetics (e.g., history of malabsorption, liver cirrhosis) - Any medical or surgical conditions which might significantly interfere with the functions of gastrointestinal tract (e.g., gastric/intestinal bypass surgeries, irritable bowel disease, chronic narcotic use)

• Willing to adhere to all other protocol requirements as outlined in the informed consent document. • Not Pregnant	• Individuals with a history of psychiatric or neurological illness, including seizure disorders • Individuals with a documented history of poor adherence to medical treatments and attendance to appointments for medical procedures or clinic visits • Any patient currently receiving known CYP2B6 inhibitors or inducers and unwilling to be medication free for two weeks. • Pregnant or nursing women • Administration of investigational drugs or any medication (prescription or over the counter or herbal) within the proceeding 2 weeks of the study and throughout the study, with the exception of birth control. • Alcohol dependency. • Nicotine dependency.

After prescreen, each subject vitals were obtained to assure participants were considered "healthy" according to our study. This was defined as having normal vital ranges for lipid levels, blood glucose, blood urea nitrogen (BUN), creatinine, passed the urine drug screen, thyroid-stimulating hormone (TSH), complete blood count (CBC), electrolytes, and BMI with in a range of 18.5-35. If subjects met these criteria, they were randomized to start phase I. Each subject who entered the trial went through a 6 phase cross-over study voluntarily with the 6 various phases (3 formulations; immediate release 75 & 100 mg, sustained release 100 & 150 mg, and extended release 150 & 300 mg) of bupropion. Before entering the next phase, each subject had a 10 day wash out period to ensure the drug was completely eliminated. Before the drug was administrated, each subject fasted for at least 10 hours and had to refrain from water

one hour pre- and post- dosing. When drug was administered the participant received 240 mL of water. Blood samples were obtained at the following hours; 0, 0.5, 1, 2, 3, 4, 6, 8, 12 (for ER only), 24, 48, 72, and 96 hours. During each phase, participants reported any adverse events they might have experienced; these were very few and were minor (**Supplemental Figure 2**). After blood samples were taken, they were spun down (2000 g, 10 minutes, 4ºC) to extract plasma. In addition to the pharmacokinetics samples, one whole blood sample was taken for genotyping purposes.

Liquid chromatography/ Mass Spectrometry-Mass Spectrometry

Samples were analyzed by LC-MS/MS; see chapter 3 for a detailed description of the method used for this as well as sample preparation. Briefly, samples were stored at -80 ºC until they were analyzed. Samples were thawed on ice. Samples were prepared with 50 µL of plasma, 50 µL of methanol, and 150 µL of IS (500 nM) in methanol. Calibrations curves (preparation described in chapter 3) were prepared fresh for each batch as well as fresh QC samples (2X low, medium, and high concentrations peranalyte). All samples were vortex and centrifuged at 15,000 rpm. The supernatant was analyzed by LC-MS/MS.

Genotyping Methods

Whole blood was used for DNA extraction using the salt precipitation method [21]. The *CYP2B6* polymorphisms; rs8192709, rs3745274, rs45482602, rs2279343, rs3211371, and rs34223104 were chosen based on a literature review in which specific *CYP2B6* variants were associated with alterations in enzyme activity [14, 22, 23]. Polymorphism rs34223104 (T/C) is located 82 nucleotides upstream of the protein coding portion and

is associated with increased transcription of *CYP2B6* but only has a minor allele frequency (MAF) of 0.012% (from the 1000 genomes project). Other *CYP2B6* selected polymorphisms located on the extronic portion of the allele and allelic frequency varies in different populations [22]. Genotyping was completed by polymerase chain reaction followed by pyrosequencing [24].

Variant Alleles Description

We selected five different *CYP2B6* variant alleles to genotype (see table below). Due to linkage disequilibrium, certain polymorphisms are often inherited together to construct specific variant alleles [25]. The most common *CYP2B6* variant allele observed in previous population studies is CYP2B6 *6, which is comprised of both the K262R and Q172H polymorphisms.

CYP2B6 **variant alleles.** Reported activity changes are noted in the second column when known.			
Variant	Associated SNP	Suggested Phenotype	Allele Frequency % (95% CI) [37]
CYP2B6*1	*1- Wild type (WT) allele, or the NCBI reference allele		54.5 (48-61)
Cyp2B6*2	R22C		5.8 (3.3-9.7%)
Cyp2B6*3	S259R	Found in a small number of Caucasian people	0 (0-1.9%)
Cyp2B6*4	K262R	Increase metabolism	5.0 (2.7-8.7%)
Cyp2B6*5	R487C	Decrease Metabolizer	9.5 (6.2-15%)
Cyp2B6*6	K262R + Q172H-	Occurs with the highest frequency among populations. Suggested that homozygous show	25 (20-31%)

		decrease in activity (but no transcription changes).	
Cyp2B6*7	Q172H, K262R, R487C- MUCH lower frequency than *5 or *6	MUCH lower frequency than *5 or *6	0 (0-1.9%)
Cyp2B6*9	Q172H	Frequency is very low in all populations.	n.a.
Cyp2B6*22	T-82C	Increased expression	n.a.

Data Analysis

Data analysis was performed in Phoenix WinNonlin (6.3) using noncompartment

analysis to estimate the AUC, C_{max}, and T_{max} for each individual for each formulation.

The Weibull function was used to model the absorption rate using non-linear mixed

effect modeling software (NONMEM) version 7.3.0. with a subroutine of ADVAN 6 for

estimate of alpha, beta, CL, and Vd. The Weibull equation (1) was set to estimate K_a in

NONMEM. The differential equations constructed for the ADVAN 6 setting are shown

below (2 & 3). Equation 2 described the disappearance of the drug from the GI and

equation 3 described the appearance of drug in the blood.

$$Ka = \frac{beta}{alpha} * \left(\frac{t}{alpha}\right)^{(beta-1)} * EXP\left(-\frac{t}{alpha}\right)^{beta} \quad (1)$$

$$\frac{dA}{dT} = -Ka * A(1) \quad (2)$$

$$\frac{dA}{dT} = Ka * A(1) - K10 * A(2) \quad (3)$$

The rest of the data analysis to examine the absorption and metabolism was performed in RStudio v0.99.464.

Results

The following analysis was performed with 14 completers who finished all 6 phases for data analysis. Each subject received a single dose of bupropion (IR 75 or 100 mg, SR 100 or 150 mg, or ER 150 or 300 mg) during each phase. All subjects were treated and monitored according to our protocol and informed consent; and any adverse events (AE) were reported to the IRB Committee.

All PK blood samples were drawn and spun down to collect plasma for LC-MS/MS analysis. The LC-MS/MS method was validated according to the FDA bioanalytical method development and validation (see chapter 3). **Figure 1** shows the time vs plasma concentration based off the mean ± standard deviations for each formulation at various doses for bupropion and metabolites. **Table 1** summarizes the area under the curve (AUC) and the percent of coefficient of variation (%CV) associated with each formulation and each analyte. There was a large inter-patient variability observed within each formulation.

We conducted model based drug development analysis with our clinical data to compare the various formulations (IR, SR, and ER). To begin, we examined how bioavailability might vary across different formations. Using the relative bioavailability, we saw that with the ER formulations; there was a decrease in relative bioavailability compared to IR formulations for bupropion (**figure 2**). For the 100 mg IR formulation, the relative bioavailability was 92% of IR 75 using the geometric mean. For the SR

formations, a slight decrease in bioavailability was observed at higher doses, the geometric mean showed 78 & 110% for SR 150 & SR 100, respectively compared to IR 75. However, for the ER formulations geometric mean was 55-64% of the IR75. Likewise, when we looked at the arithmetic mean, we saw a decrease in relative bioavailability for the ER formulations (**table 2**), where the relative bioavailability was 56-64% of the IR 75 AUC. Again, this confirmed that for bupropion's systemic appearance, the ER formulations had lower systemic exposure compared to the IR formulations.

Since these metabolites are thought to exhibit as much as 25-50% potency compared to bupropion, we questioned whether the decrease in bioavailability for ER formulation might be compensated for by the increase in metabolite formation. Therefore, we went on to analyze the AUC (m)/AUC (p) to see if we saw a higher ratio for the ER formulation (**figure 3**). However, due to the high inter-subject variability, we saw no statistical difference in AUC (m)/AUC (p) amongst the formulations for each metabolite. This suggested to us that either regional GI metabolism or increase metabolism due to more exposure in GI tract was not accounting for this difference.

Similarly, we looked at the pharmacogenomics to see if polymorphisms in CYP2B6 produced differences in hydroxybupropion which might be accounting for any of the variability. In **figure 4**, we summarized the different variants of CYP2B6 observed in our population. Our population showed a pretty homogenous expression, without observing much variability in expressing different variants of CYP2B6. In the far column we indicated the potential genotypes of these individuals. As noted, most of our population is thought to be CYP2B6 *5/*6.

90

Next we went on to examine the absorption of the various formulations for bupropion HCl. We applied Weibull type absorption to describe oral absorption (**figure 5**). Here it was shown the rate of absorption for the immediate release product was completed by 2 hours. The SR products absorption was completed by 4-5 hours. Finally, it was shown that for ER products, absorption was completed by 10 hours. This suggested that if any of the ER formulation was released after 10 hours, absorption was minimal or not occurring. Finally, we looked at the accumulation of bupropion absorption (**figure 6**). This demonstrated the amount vs time of bupropion percent absorbed *in vivo*. This was normalized by the relative bioavailability (IR 75 as reference). Altogether, Weibull type absorption was able to accurately describe oral absorption for bupropion and differentiate various release patterns.

Discussion

We observed that bupropion ER products showed a decrease in bioavailability compared to IR products. Increase metabolism for ER formulations or polymorphisms in CYP2B6 was unable to explain differences. There was high variability that was observed in both bupropion and metabolite concentrations. Finally, we showed using Weibull type absorption we were able to describe the various release of the different products and the absorption was near complete by 10 hours or less for all products.

Bupropion is extensively metabolized to form 3 active metabolites. The metabolite formation has been highly studied *in vitro* [13, 14, 26, 27]. Likewise, it has been shown that CYP2B6 is both highly variable in expression and activity which might cause as much as 20-250 fold inter-individual variation [28]. Likewise, it was shown that

hydroxybupropion formation can vary as much as 80 fold *in vitro* using liver microsomes [29]. Therefore, we thought that metabolism might be able to explain the variability that has been associated with bupropion products. However, the AUC (m)/AUC (p) nor polymorphisms in CYP2B6 were able to significantly account for this difference. However, our population for genotyping CYP2B6 was small and might have showed more of an effect with more participants.

Since bupropion HCl has never been dosed IV in human we don't have an absolute bioavailability for bupropion. Therefore, we used the relative bioavailability where all formulations/ doses were referenced to IR 75. The IR formulations are less complex compared to MR formulation; they do not have the complication of a release rate/ mechanism before absorption. Whereas, IR will only be govern by the disintegration, dissolution, and permeability for absorption since this a BCS class I drug [30].

Typically pharmacokinetics explains oral absorption as first order process. However, for MR formulations there has been discrepancy whether first order or flip-flop absorption holds true [34]. In fact, it has been highlighted that flip-flop kinetics hold true to very few drugs and the typical drugs to follow this model are Class 3 or 4 in the biopharmaceutical drug disposition classification system, which bupropion is not [34]. We examined atypical absorption that might occur using the Weibull type absorption. This has been highlighted as an appropriate method for measuring absorption rates for pharmacokinetics especially for absorption that might change overtime [20, 35, 36], as seen in MR formulations. Here we showed using Weibull we were able to describe bupropion absorption rate and absorption amount *in vivo*. We saw that no absorption

92

occurred after 10 hours. This becomes especially important for modified release

formulations which are designed to release beyond 10 hours. Although this phenomena

works well with bupropion, further validation and research toward this idea would need

to be explored.

It has been highlighted that the average transit time for drug in stomach and

small intestinal is on the order of 3.5 hours (0.25 hours in stomach and 199 minutes in

small intestines) [31, 32]; although this can be highly variable and many factors

influences this. One prolonging factor is gastric emptying, which is influenced by many

things including caloric intake, liquid vs solid intake, size of particles, enteric coated or

sustain-release table, and more [17]. In this study, food should not have played an

effect on gastric emptying because the participants were fasted; however, the modified

release formulations may have had slower gastric emptying rates and thus longer time

in the GI tract. In fact, MR products are designed for this purpose. However, we

showed that the absorption for bupropion was attenuate at 10 hours. One can

hypothesize that at this time, the drug may be in large intestines at this point. Drug

absorption occurs at a higher extent in small intestines compared to the large intestines

due the increase surface area from microvilla and villa [33]. Therefore, if the drug is in

the large intestines less absorption may be occurring to cause a decrease in

bioavailability. Another hypothesis is that there is a problem with the drug release

mechanism that may be causing the drug not to be release from the ER formulation.

However, this would further need to be validated before we could draw a conclusion.

In conclusion, these findings illustrate how complex MR products are. Typically

the IR formulation is dosed three times daily, the SR formulation dosed twice daily, and

the ER formulation dosed once a day. However, after normalizing concentration, we demonstrated that these formulations were not equivalent to systemic exposure after a single dose. This is important because this could ultimately affect the efficacy *in vivo* and cause complication when switching amongst formulations. Whether there is accumulation that might occur with multiple dosing or steady state would further need to be validated.

References

1.	Fava, M., et al., *15 years of clinical experience with bupropion HCl: from bupropion to bupropion SR to bupropion XL.* Prim Care Companion J Clin Psychiatry, 2005. **7**(3): p. 106-13.
2.	Settle, E.C., Jr., *Bupropion sustained release: side effect profile.* J Clin Psychiatry, 1998. **59 Suppl 4**: p. 32-6.
3.	Jefferson, J.W., J.F. Pradko, and K.T. Muir, *Bupropion for major depressive disorder: Pharmacokinetic and formulation considerations.* Clin Ther, 2005. **27**(11): p. 1685-95.
4.	Laizure, S.C., et al., *Pharmacokinetics of bupropion and its major basic metabolites in normal subjects after a single dose.* Clin Pharmacol Ther, 1985. **38**(5): p. 586-9.
5.	Preskorn. S., K.S., *Bupropion Plasma Levels Intraindividual and Interindividual Variability.* Annals of Clinical Psychiatry, 1989. **1**(1): p. 59-61.
6.	Dwoskin, L.P., et al., *Review of the pharmacology and clinical profile of bupropion, an antidepressant and tobacco use cessation agent.* CNS Drug Rev, 2006. **12**(3-4): p. 178-207.
7.	Foley, K.F., K.P. DeSanty, and R.E. Kast, *Bupropion: pharmacology and therapeutic applications.* Expert Rev Neurother, 2006. **6**(9): p. 1249-65.
8.	Stahl, S.M., et al., *A Review of the Neuropharmacology of Bupropion, a Dual Norepinephrine and Dopamine Reuptake Inhibitor.* Prim Care Companion J Clin Psychiatry, 2004. **6**(4): p. 159-166.
9.	Vassout, A., et al., *Regulation of dopamine receptors by bupropion: comparison with antidepressants and CNS stimulants.* J Recept Res, 1993. **13**(1-4): p. 341-54.
10.	Paudel. A., P.Y., Shrestha. S., Shrestha. S., *Formulation and In-Vitro Evaluation of Controlled Release Tablet of Bupropion Hydrochloride by Direct Compression Technique and Stability Study.* International Journal of Pharma Sciences and Research, 2014. **5**(05): p. 186-192.
11.	Coles, R. and E.D. Kharasch, *Stereoselective metabolism of bupropion by cytochrome P4502B6 (CYP2B6) and human liver microsomes.* Pharm Res, 2008. **25**(6): p. 1405-11.
12.	Hesse, L.M., et al., *CYP2B6 mediates the in vitro hydroxylation of bupropion: potential drug interactions with other antidepressants.* Drug Metab Dispos, 2000. **28**(10): p. 1176-83.
13.	Molnari, J.C. and A.L. Myers, *Carbonyl reduction of bupropion in human liver.* Xenobiotica, 2012. **42**(6): p. 550-61.
14.	Skarydova, L., et al., *Deeper insight into the reducing biotransformation of bupropion in the human liver.* Drug Metab Pharmacokinet, 2014. **29**(2): p. 177-84.
15.	Bondarev, M.L., et al., *Behavioral and biochemical investigations of bupropion metabolites.* Eur J Pharmacol, 2003. **474**(1): p. 85-93.
16.	Damaj, M.I., et al., *Enantioselective effects of hydroxy metabolites of bupropion on behavior and on function of monoamine transporters and nicotinic receptors.* Mol Pharmacol, 2004. **66**(3): p. 675-82.

17.   Hirtz, J., *The gastrointestinal absorption of drugs in man: a review of current concepts and methods of investigation.* Br J Clin Pharmacol, 1985. **19 Suppl 2**: p. 77S-83S.

18.   Yanez, J.A., et al., *Flip-flop pharmacokinetics--delivering a reversal of disposition: challenges and opportunities during drug development.* Ther Deliv, 2011. **2**(5): p. 643-72.

19.   Byron, P.R. and R.E. Notari, *Critical analysis of "flip-flop" phenomenon in two-compartment pharmacokinetic model.* J Pharm Sci, 1976. **65**(8): p. 1140-4.

20.   Zhou, H., *Pharmacokinetic strategies in deciphering atypical drug absorption profiles.* J Clin Pharmacol, 2003. **43**(3): p. 211-27.

21.   Pistis, G., et al., *Genome wide association analysis of a founder population identified TAF3 as a gene for MCHC in humans.* PLoS One, 2013. **8**(7): p. e69206.

22.   Kirchheiner, J., et al., *Bupropion and 4-OH-bupropion pharmacokinetics in relation to genetic polymorphisms in CYP2B6.* Pharmacogenetics, 2003. **13**(10): p. 619-26.

23.   Zanger, U.M. and K. Klein, *Pharmacogenetics of cytochrome P450 2B6 (CYP2B6): advances on polymorphisms, mechanisms, and clinical relevance.* Front Genet, 2013. **4**: p. 24.

24.   King, C.R. and S. Marsh, *Pyrosequencing of clinically relevant polymorphisms.* Methods Mol Biol, 2013. **1015**: p. 97-114.

25.   Charles, B.A., D. Shriner, and C.N. Rotimi, *Accounting for linkage disequilibrium in association analysis of diverse populations.* Genet Epidemiol, 2014. **38**(3): p. 265-73.

26.   Connarn, J.N., et al., *Metabolism of bupropion by carbonyl reductases in liver and intestine.* Drug Metab Dispos, 2015. **43**(7): p. 1019-27.

27.   Meyer, A., et al., *Formation of threohydrobupropion from bupropion is dependent on 11beta-hydroxysteroid dehydrogenase 1.* Drug Metab Dispos, 2013. **41**(9): p. 1671-8.

28.   Wang, H. and L.M. Tompkins, *CYP2B6: new insights into a historically overlooked cytochrome P450 isozyme.* Curr Drug Metab, 2008. **9**(7): p. 598-610.

29.   Faucette, S.R., et al., *Validation of bupropion hydroxylation as a selective marker of human cytochrome P450 2B6 catalytic activity.* Drug Metab Dispos, 2000. **28**(10): p. 1222-30.

30.   Martinez, M.N. and G.L. Amidon, *A mechanistic approach to understanding the factors affecting drug absorption: a review of fundamentals.* J Clin Pharmacol, 2002. **42**(6): p. 620-43.

31.   Jamei, M., et al., *Population-based mechanistic prediction of oral drug absorption.* AAPS J, 2009. **11**(2): p. 225-37.

32.   Yu. L.X., C.J.R., Amidon G.L., *Compartmental transit and dispersion model analysis of small intestinal transit flow in humans.* International Journal of Pharmaceutics, 1996. **140**(1).

33.   Lin, J.H., M. Chiba, and T.A. Baillie, *Is the role of the small intestine in first-pass metabolism overemphasized?* Pharmacol Rev, 1999. **51**(2): p. 135-58.

34. Garrison, K.L., S. Sahin, and L.Z. Benet, *Few Drugs Display Flip-Flop Pharmacokinetics and These Are Primarily Associated with Classes 3 and 4 of the BDDCS.* J Pharm Sci, 2015.

35. Heikkila, H.J., *New models for pharmacokinetic data based on a generalized Weibull distribution.* J Biopharm Stat, 1999. **9**(1): p. 89-107.

36. Piotrovskii, V.K., *The use of Weibull distribution to describe the in vivo absorption kinetics.* J Pharmacokinet Biopharm, 1987. **15**(6): p. 681-6.

37. Kirchheiner J. et al. *Bupropion and 4-OH-bupropion pharmacokineticsin relation to genetic polymorphisms in CYP2B6.* Pharmacogenomics. 2003. **13** (10): p. 619-26
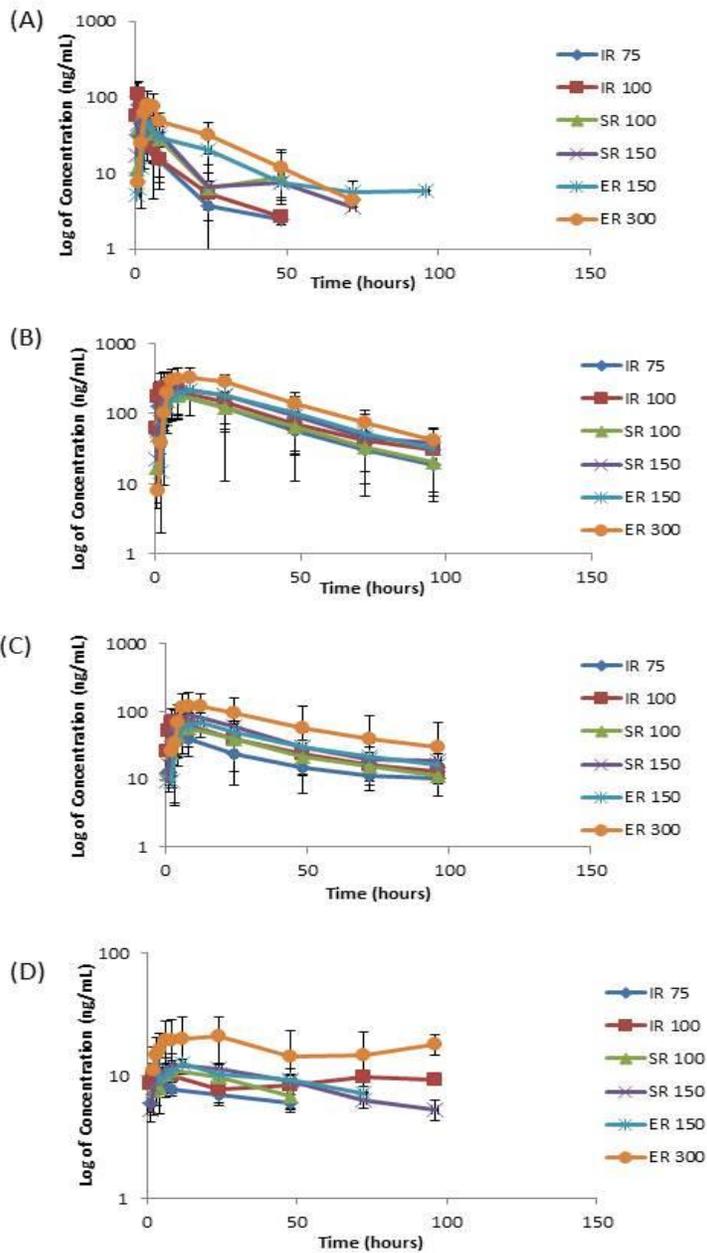
Figure 4-1. **Time vs Concentration Plots.** The following show the mean ± standard deviation for each formulations at the indicated dose (A) bupropion. (B) hydroxybupropion. (C) threohydrobupropion. (D) erythrohydrobupropion. (n=14).
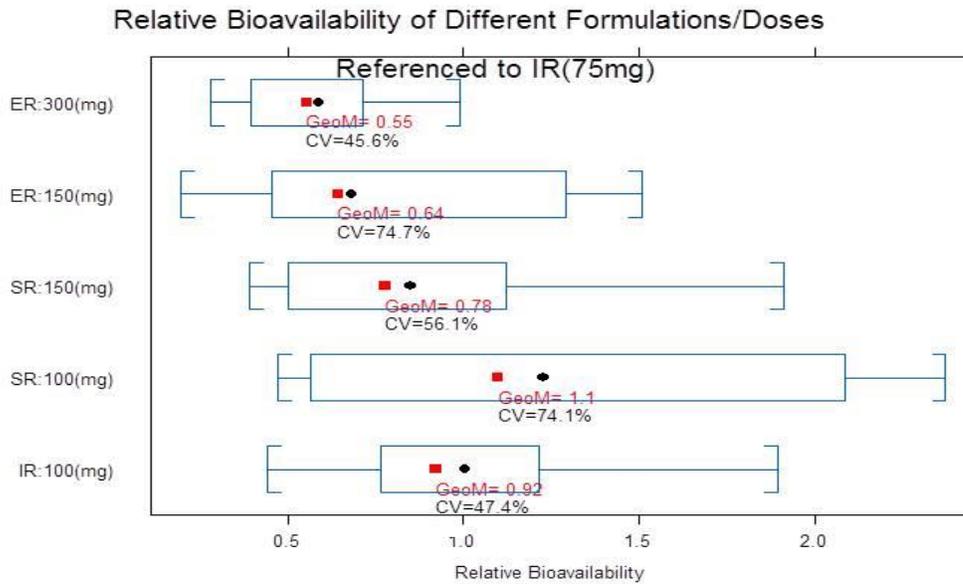
Figure 4-2. **Relative Bioavailability.** Each formulation was dosed normalized to look at the relative bioavailability using IR 75 as a reference. The boxplot shows the 25-75% range. The red dot represents the geometric mean and the black dot represents the median.
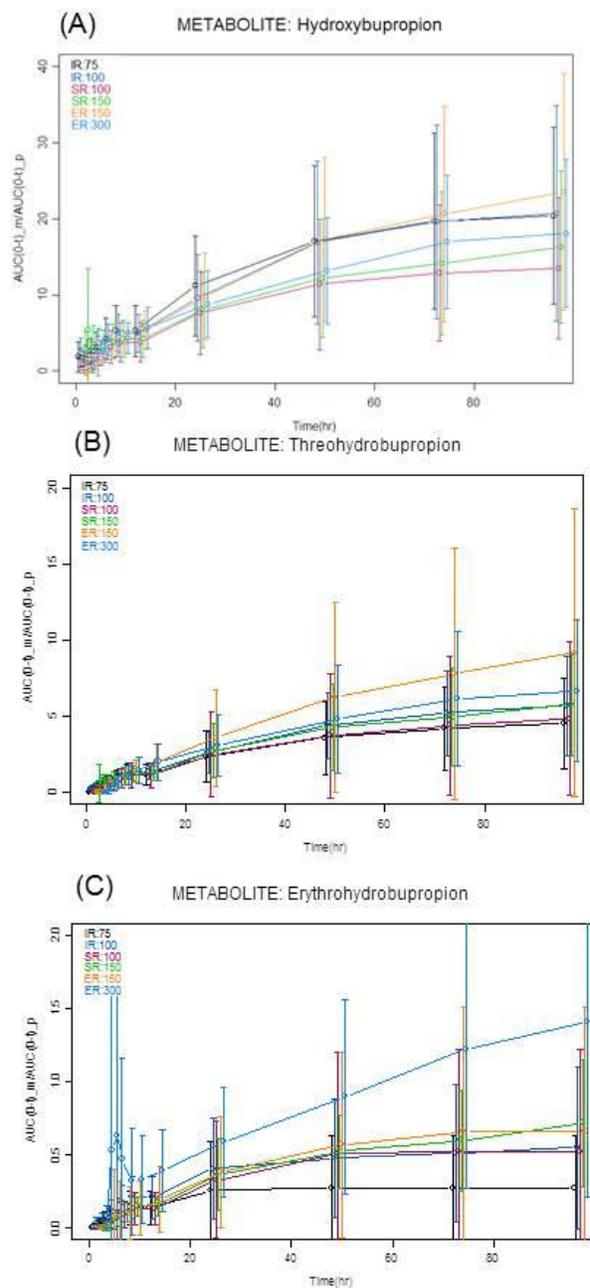
Figure 4-3. **Analysis of Metabolites.** The area under the curve for the metabolites/ area under the curve for parent (AUC(m)/AUC(p)) for each metabolite is shown (A) hydroxybupropion (B) threohydrobupropion (C) erythrohydrobupropion.

	AA sub	R22C	Q172H	S259R	K262R	R487C	*22A	
	SNP	C64T	G516T	C777A	A785G	C1459T	T-82C	
ID	rs #	rs8192709	rs3745274	rs4548260 2	rs2279343	rs3211371	rs34223 104	Genotype
1		CC	AC	GG	GA	TC	AA	*5/*6
2		CC	AC	GG	GA	TC	AA	*5/*6
3		CC	AC	GG	GA	TC	AA	*5/*6
4		CC	AC	GG	GA	TC	AA	*5/*6
5		TC	AC	GG	AA	TC	AA	*2/*7
6		CC	AC	GG	AA	TC	AA	*5/*6
7		CC	AC	GG	GA	TC	AA	*5/*6
8		CC	AC	GG	GA	TC	AA	*5/*6
9		CC	AC	GG	GA	TC	AA	*5/*6
10		TC	AC	GG	GA	TC	AA	*2/*7
11		CC	AA	GG		TC	AA	*5/*6
12		CC	AC	GG	GA	TC	AA	*5/*6
13		CC	AC	GG	AA	TC	AA	*5/*6
14		CC	AA	GG	GA	TC	AA	*5/*9

Figure 4-4. **Pharmacogenomics of CYP2B6.** We genotyped our clinical participants for CYP2B6. Above summarizes the various single nucleotide polymorphisms (SNP) in our population. We show both the amino acid substitution (AA sub) caused by the different SNP and the amino acid position. Also, we show the SNP variant and where the loci are located on the genes. RS# indicated the reference number in the literature. In the far column, each individual person's possible variant is listed.
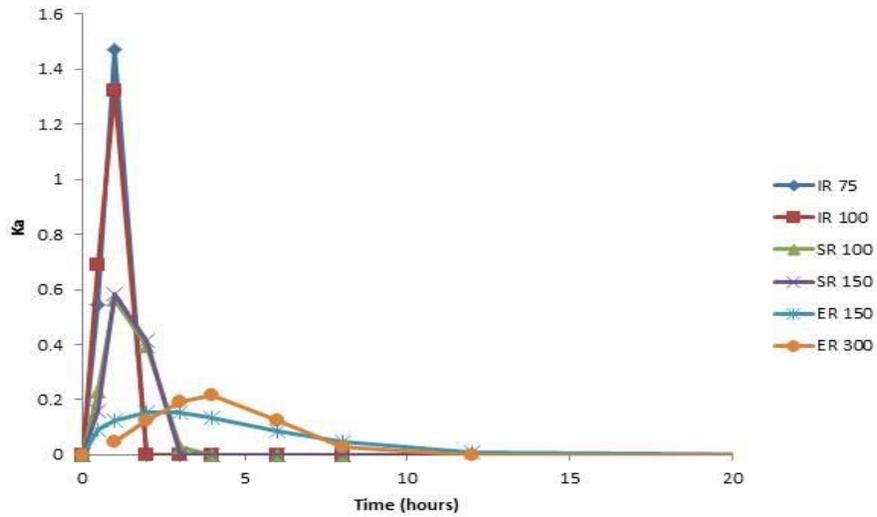
Figure 4-5. **Weibull Absorption Rate.** Using the mean concentration for each formulation, we described the absorption rate for each formulation using Weibull distribution

102
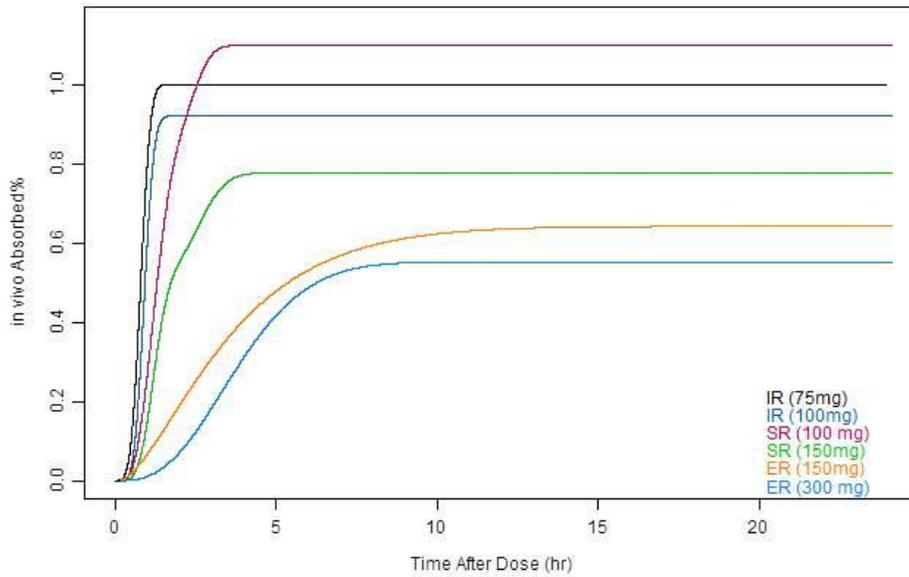
Figure 4-6. **Cumulative Percent Absorbed.** The mean concentrations were used to calculate the percent absorbed *in vivo* vs time for each formulation.

	BUP		H-BUP		T-BUP		E-BUP	
	AUC (hr*ng/mL)	% CV	AUC (hr*ng/mL)	% CV	AUC (hr*ng/mL)	% CV	AUC (hr*ng/mL)	% CV
IR 75	393 ± 217	55%	7253 ± 4099	56.5%	1390 ± 1094	78.6%	106 ± 115	108%
IR 100	502 ± 160	31.9%	9458 ± 7505	79%	2781 ± 1943	70%	184 ± 116.5	63.2%
SR 100	553 ± 279	50%	7894 ± 3950	54%	2643 ± 1564	59%	283 ± 219	78%
SR 150	663 ± 305	48%	11337± 6157	54%	3692 ± 2040	55%	540 ± 366	67%
ER 150	508 ± 292	57.5%	9690 ± 5078	52%	3392 ± 1607	47%	598.8 ± 765	127%
ER 300	887 ± 488	55%	15055 ± 7592	50%	5740 ± 4265	74.3%	1090 ± 847.5	77%

Table 4-1. **Area Under the Curve.** The table shows the AUC ± SD for each formulation and the %CV for each formulation for bupropion and metabolites (n=14).

104

	AUC (hr*ng/mL)	% CV	Relative Bioavailabiliy
IR 75	393 ± 217	55%	100%
IR 100	502 ± 160	31.9%	95.8%
SR 100	553 ± 279	50%	105.5%
SR 150	663 ± 305	46%	84.3%
ER 150	508 ± 292	57.5%	64.6%
ER 300	887 ± 488	55%	56.4%

Table 4-2. **Percent of Relative Bioavailability.** For each formulation the AUC for bupropion is shown using the arithmetic mean, the relative bioavailability was calculated using IR 75 as a reference.

RACE	White: 10 African American: 3 Asian/ Asian America: 2
AGE	25-53
SEX	Females: 7 Males: 8
BMI RANGE	20.5 -33.4

Supplemental Figure 4-1. **Study Demographics.** Summarizes the demographic distribution of race, age, sex, and BMI of the participants who entered our study.

Subject ID	Event Description	Severity	Study Relatedness	Outcome
3154	Injured/ infected thumb	Moderate	Not Related	Outgoing Treatment
3154	Migraine	Mild	Unlikely	Resolve
3122	Rash on both arms	Moderate	Not Related	Resolved

Supplemental Figure 4-2. **Adverse Events.** Above list any adverse events that occurred with our participants in the clinical trial.

Chapter 5
Conclusions

Summary of Findings and Significances

Despite the fact that bupropion was approved clinically in the late 1980's, there

are still uncertainties about its pharmacology and metabolism [1, 2]. Many investigators

still study *in vitro* metabolism of bupropion, even when the issues of bioineequivalence

generic bupropion products surfaced in 2006 [3]. Although the drug product is

prescribed to over 11 million people a year [4], it has been a challenge to figure out

issues that still remain. Although one would think that Bupropion PK should be simple

since it has high permeability, high solubility, and exhibits linear pharmacokinetics at

clinical dosing; it is in fact very complicated. There are 3 formulations (immediate,

sustained, and extended release) that are dosed up to 3 times daily, the drug is highly

metabolized to form multiple metabolites in which the three primary metabolites are

thought to be active [5, 6], and when studying this drug there is no *in vitro* dissolution/

IV/ or solution data for bupropion HCl. Although these challenges remain, we try to

unravel much about the metabolism of bupropion both *in vitro* and *in vivo*.

Chapter 2 highlights many new finding for *in vitro* metabolism. Specifically, it was

thought that bupropion's major metabolite was hydroxybupropion [7, 8]. However, many

previous studies only used a microsomes system in which it is hard to capture the

metabolites formed by carbonyl reductase. A more appropriate system would be to use

an S9 fraction (which contains both microsome and cytosolic fraction) or even better yet hepatocytes. When we used a hepatic S9 fraction, we saw that the formation kinetics for the metabolite threohydrobupropion was similar to the formation of hydoxybupropion. This is important clinically since it is thought that the major metabolites are active. Furthermore, we saw that threohydrobupropion was able to form in the intestines using an *in vitro* system. This concept is important especially pertaining to a modified release product that might have more exposure in GI tract therefore forming more of this metabolite compare to an immediate release product.

Initially when designing our clinical trial, we thought that that metabolism, specifically polymorphs in CYP2B6 could explain a lot of variability that is seen with bupropion's plasma concentrations. In chapter 4, we investigated various formulations (immediate, sustained, extended release) of bupropion in healthy individuals to see how the pharmacokinetics might change (ie from GI regional metabolism). In combination, we looked at genotyping these individual for CYP2B6. Much to our surprise, CYP2B6 could not account for much variability; in fact most of our population had similar expression of CYP2B6 variants.

However, as discussed in chapter 4, we started to perform model based drug development analysis on the plasma concentrations for these various release products for bupropion. Here we found that looking at the relative bioavailability (reference was IR 75), there was a decrease in bioavailability for the ER formulations and 150 mg SR formulation. Despite the heavy emphasis on designing these studies to focus on metabolism, we saw no difference in CYP2B6 polymorphs or AUC(m) / AUC(p) for any formulation or metabolites.

In addition in chapter 4, we highlighted bupropion's absorption rate. Specifically, modified release formulation which may not exhibit either typical first oral absorption or flip-flip kinetics, but rather can be outlined using atypical absorption [9]. Weibull type absorption has been purposed as one way to describe oral absorption [10-12]. By using Weibull we showed that absorption was attenuate after 10 hours. This point becomes important with MR formulations that may be designed to release later than 10 hours. In fact, this concept may be able to explain the decrease in bioavailability. We hypothesize that the decrease in bioavailability for the MR products might not be releasing in the small intestines but instead the large. Or, there may just be a release mechanism problem not allowing these formulations to completely release. However, further investigations would be needed to confirm this.

References

1. Dwoskin, L.P., et al., *Review of the pharmacology and clinical profile of bupropion, an antidepressant and tobacco use cessation agent.* CNS Drug Rev, 2006. 12(3-4): p. 178-207.
2. Fava, M., et al., *15 years of clinical experience with bupropion HCl: from bupropion to bupropion SR to bupropion XL.* Prim Care Companion J Clin Psychiatry, 2005. 7(3): p. 106-13.
3. Woodcock, J., M. Khan, and L.X. Yu, *Withdrawal of generic budeprion for nonbioequivalence.* N Engl J Med, 2012. 367(26): p. 2463-5.
4. Bondarev, M.L., et al., *Behavioral and biochemical investigations of bupropion metabolites.* Eur J Pharmacol, 2003. 474(1): p. 85-93.
5. Damaj, M.I., et al., *Enantioselective effects of hydroxy metabolites of bupropion on behavior and on function of monoamine transporters and nicotinic receptors.* Mol Pharmacol, 2004. 66(3): p. 675-82.
6. Coles, R. and E.D. Kharasch, *Stereoselective metabolism of bupropion by cytochrome P4502B6 (CYP2B6) and human liver microsomes.* Pharm Res, 2008. 25(6): p. 1405-11.
7. Chen, Y., et al., *The in vitro metabolism of bupropion revisited: concentration dependent involvement of cytochrome P450 2C19.* Xenobiotica, 2010. 40(8): p. 536-46.
8. Zhou, H., *Pharmacokinetic strategies in deciphering atypical drug absorption profiles.* J Clin Pharmacol, 2003. 43(3): p. 211-27.
9. Heikkila, H.J., *New models for pharmacokinetic data based on a generalized Weibull distribution.* J Biopharm Stat, 1999. 9(1): p. 89-107.
10. Piotrovskii, V.K., *The use of Weibull distribution to describe the in vivo absorption kinetics.* J Pharmacokinet Biopharm, 1987. 15(6): p. 681-6.
11. Wagner, J.G., *Application of the Wagner-Nelson absorption method to the two-compartment open model.* J Pharmacokinet Biopharm, 1974. 2(6): p. 469-86.
12. Wagner, J.G., *Application of the Wagner-Nelson absorption method to the two-compartment open model.* J Pharmacokinet Biopharm, 1974. **2**(6): p. 469-86.

Appendices

Appendix 1
Introduction to HSP70/ HSP90

1. HSP90

Heat shock protein 90 (HSP90) is a molecular chaperone involved in protein

quality control. In order to perform these functional tasks and maintain protein

homeostasis, HSP90 cooperates with a network of co-chaperones, including

tetratricopeptide repeat (TPR) domain-containing proteins (such as HSP70-HSP90

organizing protein (HOP)). HSP90 is involved in a number of cellular functions such as

kinase, transcription, and steroid receptors which aids in the regulation of apoptosis,

signal transduction, folding, maintenance, degradation, and cell-cycle regulation [1].

HSP90 is conserved throughout most organisms. Prokaryotes have one non-

essential form of HSP90 whereas Eukaryotes have several forms of HSP90 [2].

Different isoforms of the HSP90 are produced by different genes. To begin, two of the

more common forms of HSP90 include the cytosolic forms. The two isoforms of the

cytosolic HSP90 are HSP90α and HSP9β which are encoded by the genes HSP90AA1

and HSP90AB1, respectively [2]. HSP90α and HSP90β share 86% similarity in

sequence, however, HSP90α is an inducible form whereas HSP90β is constitutively

expressed [3]. In addition to the cytosolic form, an endoplasmic reticulum and

113

mitochondrial form exist; these forms are encoded by the genes HSP90B1 and TRAP1, respectively [4]. For the purpose of the studies presented here, we will focus on the cytosolic forms of HSP90 (both α and β).

HSP90 exist as a dimer. For each monomer, HSP90 contains an N-terminal domain that is 25 kDa. Within the N-terminal of HSP90, the ATP binding pocket is located. Following the N-terminal domain is a charged linker which connects the N-terminal domain to the middle domain. The middle domain (40 kDa) of HSP90 is where many substrates bind; the amphipathic loops in the structure of the middle domains allows for substrate binding. Finally, the C-terminal of HSP90, which is about 12 kDa, contains an alternate ATP binding site. The C-terminal is responsible for the dimerization of HSP90 [5]. More importantly, the C-terminal contains the MEEVD region. This highly conserved region of HSP90 is important for many interactions with other proteins including the interactions with an important group of co-chaperones, tetratricopeptides domain (TPR) containing proteins [6]. The MEEVD nucleotide sequence within the C-terminal of HSP90 has been found to be an important binding motif for TPR containing proteins [7-9].

HSP90 interacts with a variety of co-chaperones and client proteins to facilitate maturation. During this process, HSP90's structure goes through different conformational states. In the open state, the N-terminal lids of HSP90 are opened. Upon ATP binding to the N-terminal of HSP90, the lids close and the N-terminal domain rotates 120 degrees blocking the ATP binding site. This causes a transient dimerization

of N-terminal to form a close state. Finally, ATP hydrolysis occurs to return to the open confirmation state again [2]. In addition, co-chaperones assist HSP90 through these conformational states to form an early, intermediate, and mature chaperone complex. In the early complex, the co-chaperones Heat Shock Protein 70 (HSP70) and HSP70-HSP90 Organizing Protein (HOP) are bound together and client proteins are capable to bind to HSP70. In the intermediate complex, HSP90 comes into to the complex and binds with HSP70 with the help of HOP. Client proteins can then be shuffled from HSP70 to HSP90 [10].   Upon an ATP hydrolysis, HSP70 leaves the complex and HSP90 finally forms the mature complex at which point HOP may or may not be replace with an alternative TPR containing protein.   Additionally, at this point, client proteins are folded into a state where they can perform their various functions or client proteins can be marked for ubiquitination and degraded by proteasomes with the help of the co-chaperone, C- terminus of Hsc70 interacting protein (CHIP) [11, 12].

Although HSP90 is critical for normal cellular functions; dysregulation of HSP90 and dysfunction of protein homeostasis is linked to many diseases. For example, HSP90 plays a critical role in the folding and maturing of a number of oncogenic proteins in cancer cells [1]. Furthermore, the expression of HSP90 is increased in cancer cells [13-17]. Currently, it is thought that increased levels of HSP90 sustain cancer growth by protecting oncogenic proteins from degradation, thereby preventing apoptosis [18, 19]. Therefore, HSP90 has emerged as an ideal target in many disease states.

2. Targeting HSP90

HSP90 is highly expressed in stressed cell; in normal cells HSP90 constitutes 1-2% of total cellular protein however, when cells become stressed, HSP90 raises to 4% of total cellular protein [20]. When these cells become stressed, HSP90's expression increases and HSP90 matures mutated or oncogenic client proteins. This dysregulation of the complex has been associated with many disease states including cancer, neurodegenerative disease, metabolic disease, and more [21]. In fact, overexpression of HSPs is partially to blame for the reason resistance to current cancer therapy such as anti-tumor agents and chemotherapy occurs [22]. The exact reason for this is not known to date.

The development of an HSP90 inhibitor has been an attractive area for many years. Specifically targeting HSP90 has been appealing due to the diversity of client proteins that become degraded by proteasomes when inhibiting HSP90. Furthermore, studies have shown that inhibitors targeting HSP90 in cancerous cells have a 100 fold time greater affinity than normal cells containing HSP90 [23], meaning inhibitors would specifically target disease cells leading to reduce toxicity from off target effects. One common attempt of targeting the HSP90 complex has been to inhibit the ATP binding site. Geldanamycin and its derivatives, 17-AAG and 17-DMAG were one of the most promising candidates to target HSP90's ATP binding site. These inhibitors made it to phase III of clinical trials, however due to the hepatotoxicity and poor solubility, the drug was not able to continue through clinical development [22]. Many similar approaches to inhibiting HSP90 have been attempted including targeting various protein-protein

interactions within this complex. Despite many designs, challenges still arise at developing a successful HSP90 inhibitor that can make it through clinical trials.

3. Targeting HSP90 in breast cancer

HSP90 is typically overexpressed in breast cancer. Some common client proteins of HSP90 that are offend found to be mutated or oncogenic are p53, v-SRC, AKT, HER2, EGFR, estrogen/androgen receptor, and NF- κB [24, 25]. Breast cancer is a particularly appealing target since HER2 is one of the most sensitive client proteins [26]. The overexpression of both HSP70 and HSP90 has been associated with poor prognosis in cancer [27, 28]. Additionally, tissue microarrays showed that high expression of HSP90 in breast cancer was associated with poor survival [29]. Therefore, it is thought that inhibiting HSP90 will lead in helping degrade a multitude of signaling pathways for breast cancer therapy as well as the high risk associated with HSP90 itself.

4. Heat Shock Protein 70 (HSP70)

HSP70 is a weak ATPase chaperone protein that is also involved in protein quality control. HSP70 is 70 kDa protein that exists as a monomer. HSP70 has several functions including protein folding, degradation, transport, and aggregation prevention [30-36].

In eukaryotes, there are several different HSP70 proteins. Hsc70 is constitutively expressed and makes up 1-3% of total cellular protein whereas HSP72 is the inducible form of HSP70 that is highly expressed upon stress [37].

HSP70 is regulated by two groups of proteins; one group of proteins, J- domain proteins which help to facilitate substrates binding to HSP70. It is believed that HSP70 exist in two conformational states that is dictated by ADP or ATP. HSP70 is controlled by two domains; nucleotide-binding domain (NBD) and polypeptide substrate-binding domain (SBD). The substrates affinity for binding to the SBD region is highly dependent on which state HSP70 is in. HSP70's N-terminal domain is 45 kDa. Similarly to HSP90, there is an ATPase within the N-terminal of HSP70 which shuffles through ATP and ADP dependent states. When ATP is bound, peptides are able to associate with SBD at high rates but low affinity. After ATP hydrolysis by NBD, the affinity of substrates to SBD is high and the rate of association/dissociation is low [38-41]. Furthermore, another group of proteins, nucleotide exchange factors are also involved to determine the lifetime of the complex [42]. The C-terminal of HSP70 is 25 kDa [43]. The C-terminal of HSP70 also accepts TPR containing proteins. However, instead of the MEEVD nucleotide sequence seen in HSP90, HSP70 TPR motif contains an IEEVD nucleotide sequence motif.

5. Targeting HSP70

Similar to HSP90, HSP70 has been correlated with various disease states. Targeting HSP70 has been an attractive target as well. Like HSP90, there are also similar problems in developing a successful molecule to inhibit HSP70. First, HSP70 has been associated with diseases such as neurodegenerative disorders, cancer, and infectious disease [44-46]. HSP70 interacts with numerous signal transduction pathways, so inhibiting this protein would also aid in regulating a subset of other pathways. Attempts at developing an inhibitor to HSP70 ATPase have been a hot area. Unlike the low affinity compounds towards HSP90s ATPase, compounds towards HSP70 have been on the mid-nanomolar scale [47]. However, the lack of functional effect has been seen with this approach [48]. It has been proposed that targeting protein-protein interactions within HSP70 might be a better option. Specifically targeting HSP70 and TPR contain proteins, J proteins, or nucleotide exchange factors. It was suggested that inhibiting different interaction may lead to different outcomes which might help maintain protein homeostasis [49].

6. Tetratricopeptides Repeat Domains Proteins

The tetratricopeptide repeat (TPR) domain is a tandem repeat of 34 amino acid motif [50-52]. These proteins are highly conserve and many TPR containing proteins are involved in the HSP70 and HP90 complex such as; HOP, CHIP, PP5, CYP40, FKBP52, and FKBP51. There are a variety of TPR containing protein functions including; isomerases, phosphatases, and ligases [52]; it is thought that HSP90 and HSP70 are universal acceptor of TPR domain proteins [3]. The binding site for TPR containing proteins is located in the C-terminal of HSP90 (MEEVD) and HSP70 (IEEVD) [7-9]. TPR proteins can contain multiple TPR domains; such as HOP which has 3 TPR domain sites. Typically the TPR domains are 3 sets of antiparallel alpha helices. Within the TPR domain that contain a "carboxylate clamp" that consists of positive residues such as arginine's and lysine's that bind to the negatively charged residues, MEEVD/IEEVD, regions on HSP90/HSP70 [53].

6.1 Protein Phosphatase 5

Protein Phosphatase 5 (PP5) is one of a number of TPR containing proteins. PP5 is unique to the protein phosphatases family because it's the only one to contain a TPR domain [54]. The TPR domain is located in the N-terminal of PP5. The C-terminal of PP5 contains the catalytic site. Within the catalytic domain lies a nuclear localizing signal. PP5 was first discovered in the nucleus, it was later determined that it was also localized in the cytoplasm [55-57]. In addition, PP5 is an autoinhibitor protein; meaning that its typical expression is of basal level. The alpha J helix located in the C-terminal of PP5 folds over to the N-terminal, where the HSP90 binding region is located. In this

autoinhibitory state, catalytic activity does not occur. It has been shown that HSP90

and fatty acids, such as arachidonic acid can relieve this autoinhibition [58, 59]. At this

point, when HSP90 binds to PP5, PP5 undergoes a conformational rearrangement

which then allows substrates to bind and PP5 can perform phosphatase activity. PP5

has also been shown to have high affinity (on the nanomolar scale) for HSP90 [6, 59].

PP5's function in the HSP90 complex to date is still unclear; however, many studies

show that PP5 does bind to HSP90's MEEVD region [50, 52, 54, 60-62]. PP5 has also

been shown to be involved in numerous signaling pathways, many which are also client

proteins of HSP90 including MAPK, ASK, ATM, cyclinD, p53, steroid receptors, and

more [63-68].

Similar to HSP90, PP5 has also been implemented in cancer, particular breast

cancer. One study has suggested that PP5 causes cell growth in estrogen positive

(ER+) breast cancer [69]. Similarly, another group showed using a xenograph model,

overexpression of PP5 lead to a higher mean tumor diameter [70]. Additionally they

showed that when they stained both invasive ductal carcinoma tumors and ductal

carcinoma tumors, higher levels of PP5 were found in these tissues compared to normal

tissues [70]. These evidences advocate PP5 as a good target in ER+ breast cancer.

6.2 HSP70-HSP90 Organizing Protein (HOP)

HOP, another TPR containing protein is known to bind not only HSP90 but also

HSP70. However, HOP differs from PP5 in that it has 3 TPR domains. The first TPR

domain, TPR1 is important for binding to HSP70. The second TPR domain, TPR2A is

important for binding HSP90. Finally the last TPR domain, TPR2B is undefined to date; however, some evidence show that it might be important to bind to HSP90's N-terminal domain [71]. In addition, there are also two undefined domains of HOP referred to as DP repeat motif due to the aspartic acid (D) and proline (P) repeat motifs [72]. HOP resides in both the cytoplasm and nucleus. The main function of HOP is to link HSP70 and Hp90 together. Many studies have indicated that the affinity of HOP for both HSP70 and HSP90 is on the high nanomolar/ lower micromolar scale depending on the platform of the assay [9, 73, 74].

Likewise, HOP has also been implemented in disease states. Particularly in cancer, it has been shown that increase expression of HOP lead to increase complex formation in human colon tumors [75]. In addition, it has been shown that when HOP was knockdown via RNAi, a decrease in invasive pancreatic cancer proliferation occurred. Furthermore, they also observed client proteins such as HER2, Bcr-Abl, c-MET, and v-Src expression was reduced when HOP was knocked down [76]. Studies have also shown that compounds that were able to inhibit the HOP-HSP90 complex was able to decrease cancer cell viability *in vitro* [77]. This too, suggest targeting this TPR interaction for cancer therapy is ideal.

7. Specific Aims

Our goal is to understand mechanisms as well as discovering and developing inhibitors to the chaperone complex. First, we studied the mechanism of HSP70/90 binding to the tetratricopeptide repeat (TPR) domain of protein phosphatase 5 (PP5). While it is known that HSPs can bind TPR containing proteins, less is known about the HSP70/90-PP5 interaction and their potential roles in protein homeostasis. Therefore, we sought to characterize these protein-protein interactions through various biochemical assays.

In addition, we performed a High Throughput Screen for inhibitors of HSP90-TPR containing proteins. We hypothesized that compounds that block the TPR-HSP interaction will aid in a novel approach for breast cancer therapy.

Aim 1: The Molecular Chaperone Hsp70 Activates Protein Phosphatase 5 (PP5) By Binding the Tetratricopeptide Repeat (TPR) Domain

Aim 2: High Throughput Screen for Small Molecules to Block TPR containing Co-chaperones-Hsp90 Chaperone Complex

References

1.   Theodoraki, M.A. and A.J. Caplan, *Quality control and fate determination of Hsp90 client proteins.* Biochim Biophys Acta, 2012. **1823**(3): p. 683-8.
2.   Hahn, J.S., *The Hsp90 chaperone machinery: from structure to drug development.* BMB Rep, 2009. **42**(10): p. 623-30.
3.   Pratt, W.B. and D.O. Toft, *Steroid receptor interactions with heat shock protein and immunophilin chaperones.* Endocr Rev, 1997. **18**(3): p. 306-60.
4.   Chen, B., et al., *The HSP90 family of genes in the human genome: insights into their divergence and evolution.* Genomics, 2005. **86**(6): p. 627-37.
5.   da Silva, V.C. and C.H. Ramos, *The network interaction of the human cytosolic 90 kDa heat shock protein Hsp90: A target for cancer therapeutics.* J Proteomics, 2012. **75**(10): p. 2790-802.
6.   Cliff, M.J., et al., *Conformational diversity in the TPR domain-mediated interaction of protein phosphatase 5 with Hsp90.* Structure, 2006. **14**(3): p. 415-26.
7.   Chen, S., et al., *Differential interactions of p23 and the TPR-containing proteins Hop, Cyp40, FKBP52 and FKBP51 with Hsp90 mutants.* Cell Stress Chaperones, 1998. **3**(2): p. 118-29.
8.   Ramsey, A.J., et al., *Overlapping sites of tetratricopeptide repeat protein binding and chaperone activity in heat shock protein 90.* J Biol Chem, 2000. **275**(23): p. 17857-62.
9.   Brinker, A., et al., *Ligand discrimination by TPR domains. Relevance and selectivity of EEVD-recognition in Hsp70 x Hop x Hsp90 complexes.* J Biol Chem, 2002. **277**(22): p. 19265-75.
10.   Gallo, L.I., et al., *Differential recruitment of tetratricorpeptide repeat domain immunophilins to the mineralocorticoid receptor influences both heat-shock protein 90-dependent retrotransport and hormone-dependent transcriptional activity.* Biochemistry, 2007. **46**(49): p. 14044-57.
11.   Connell, P., et al., *The co-chaperone CHIP regulates protein triage decisions mediated by heat-shock proteins.* Nat Cell Biol, 2001. **3**(1): p. 93-6.
12.   Murata, S., et al., *CHIP is a chaperone-dependent E3 ligase that ubiquitylates unfolded protein.* EMBO Rep, 2001. **2**(12): p. 1133-8.
13.   Neckers, L., *Hsp90 inhibitors as novel cancer chemotherapeutic agents.* Trends in Molecular Medicine, 2002. **8**(4): p. S55-S61.
14.   Sarto, C., P.A. Binz, and P. Mocarelli, *Heat shock proteins in human cancer.* Electrophoresis, 2000. **21**(6): p. 1218-1226.
15.   Morimoto, R.I., et al., *The heat-shock response: regulation and function of heat-shock proteins and molecular chaperones.* Essays in Biochemistry, Vol 32, 1997, 1997. **32**: p. 17-29.
16.   Hartl, F.U. and M. Hayer-Hartl, *Protein folding - Molecular chaperones in the cytosol: from nascent chain to folded protein.* Science, 2002. **295**(5561): p. 1852-1858.
17.   Parsell, D.A. and S. Lindquist, *The Function of Heat-Shock Proteins in Stress Tolerance - Degradation and Reactivation of Damaged Proteins.* Annual Review of Genetics, 1993. **27**: p. 437-496.

18.   Joly, A.-L., et al., *Dual Role of Heat Shock Proteins as Regulators of Apoptosis and Innate Immunity.* Journal of Innate Immunity, 2010. **2**(3): p. 238-247.

19.   Kim, T.S., et al., *Interaction of Hsp90 with ribosomal proteins protects from ubiquitination and proteasome-dependent degradation.* Molecular Biology of the Cell, 2006. **17**(2): p. 824-833.

20.   Sanchez, E.R., *Chaperoning steroidal physiology: lessons from mouse genetic models of Hsp90 and its cochaperones.* Biochim Biophys Acta, 2012. **1823**(3): p. 722-9.

21.   Peterson, L.B. and B.S. Blagg, *To fold or not to fold: modulation and consequences of Hsp90 inhibition.* Future Med Chem, 2009. **1**(2): p. 267-83.

22.   Khalil, A.A., et al., *Heat shock proteins in oncology: diagnostic biomarkers or therapeutic targets?* Biochim Biophys Acta, 2011. **1816**(2): p. 89-104.

23.   Kamal, A., et al., *A high-affinity conformation of Hsp90 confers tumour selectivity on Hsp90 inhibitors.* Nature, 2003. **425**(6956): p. 407-10.

24.   Picard, D. *HSP90 Interactors*. 2015; Available from: http://www.picard.ch/downloads/Hsp90interactors.pdf.

25.   Whitesell, L. and S.L. Lindquist, *HSP90 and the chaperoning of cancer.* Nat Rev Cancer, 2005. **5**(10): p. 761-72.

26.   Kim, L.S. and J.H. Kim, *Heat shock protein as molecular targets for breast cancer therapeutics.* J Breast Cancer, 2011. **14**(3): p. 167-74.

27.   Nanbu, K., et al., *Prognostic significance of heat shock proteins HSP70 and HSP90 in endometrial carcinomas.* Cancer Detect Prev, 1998. **22**(6): p. 549-55.

28.   Yano, M., et al., *Expression and roles of heat shock proteins in human breast cancer.* Jpn J Cancer Res, 1996. **87**(9): p. 908-15.

29.   Pick, E., et al., *High HSP90 expression is associated with decreased survival in breast cancer.* Cancer Res, 2007. **67**(7): p. 2932-7.

30.   Arndt, V., C. Rogon, and J. Hohfeld, *To be, or not to be--molecular chaperones in protein degradation.* Cell Mol Life Sci, 2007. **64**(19-20): p. 2525-41.

31.   Bercovich, B., et al., *Ubiquitin-dependent degradation of certain protein substrates in vitro requires the molecular chaperone Hsc70.* J Biol Chem, 1997. **272**(14): p. 9002-10.

32.   Frydman, J., *Folding of newly translated proteins in vivo: the role of molecular chaperones.* Annu Rev Biochem, 2001. **70**: p. 603-47.

33.   Hartl, F.U., A. Bracher, and M. Hayer-Hartl, *Molecular chaperones in protein folding and proteostasis.* Nature, 2011. **475**(7356): p. 324-32.

34.   Kettern, N., et al., *Chaperone-assisted degradation: multiple paths to destruction.* Biol Chem, 2010. **391**(5): p. 481-9.

35.   Pratt, W.B. and D.O. Toft, *Regulation of signaling protein function and trafficking by the hsp90/hsp70-based chaperone machinery.* Exp Biol Med (Maywood), 2003. **228**(2): p. 111-33.

36.   Tyedmers, J., A. Mogk, and B. Bukau, *Cellular strategies for controlling protein aggregation.* Nat Rev Mol Cell Biol, 2010. **11**(11): p. 777-88.

37.   Tavaria, M., et al., *A hitchhiker's guide to the human Hsp70 family.* Cell Stress Chaperones, 1996. **1**(1): p. 23-8.

38. Gassler, C.S., et al., *Bag-1M accelerates nucleotide release for human Hsc70 and Hsp70 and can act concentration-dependent as positive and negative cofactor.* J Biol Chem, 2001. **276**(35): p. 32538-44.

39. Pierpaoli, E.V., S.M. Gisler, and P. Christen, *Sequence-specific rates of interaction of target peptides with the molecular chaperones DnaK and DnaJ.* Biochemistry, 1998. **37**(47): p. 16741-8.

40. Schmid, D., et al., *Kinetics of molecular chaperone action.* Science, 1994. **263**(5149): p. 971-3.

41. Takeda, S. and D.B. McKay, *Kinetics of peptide binding to the bovine 70 kDa heat shock cognate protein, a molecular chaperone.* Biochemistry, 1996. **35**(14): p. 4636-44.

42. Mayer, M.P., *Hsp70 chaperone dynamics and molecular mechanism.* Trends Biochem Sci, 2013. **38**(10): p. 507-14.

43. Mayer, M.P. and B. Bukau, *Hsp70 chaperones: cellular functions and molecular mechanism.* Cell Mol Life Sci, 2005. **62**(6): p. 670-84.

44. Broadley, S.A. and F.U. Hartl, *The role of molecular chaperones in human misfolding diseases.* FEBS Lett, 2009. **583**(16): p. 2647-53.

45. Mosser, D.D. and R.I. Morimoto, *Molecular chaperones and the stress of oncogenesis.* Oncogene, 2004. **23**(16): p. 2907-18.

46. Otvos, L., Jr., et al., *Interaction between heat shock proteins and antimicrobial peptides.* Biochemistry, 2000. **39**(46): p. 14150-9.

47. Massey, A.J., *ATPases as drug targets: insights from heat shock proteins 70 and 90.* J Med Chem, 2010. **53**(20): p. 7280-6.

48. Chang, L., et al., *Mutagenesis reveals the complex relationships between ATPase rate and the chaperone activities of Escherichia coli heat shock protein 70 (Hsp70/DnaK).* J Biol Chem, 2010. **285**(28): p. 21282-91.

49. Assimon, V.A., et al., *Hsp70 protein complexes as drug targets.* Curr Pharm Des, 2013. **19**(3): p. 404-17.

50. Smith, D.F., *Tetratricopeptide repeat cochaperones in steroid receptor complexes.* Cell Stress Chaperones, 2004. **9**(2): p. 109-21.

51. Cortajarena, A.L. and L. Regan, *Ligand binding by TPR domains.* Protein Sci, 2006. **15**(5): p. 1193-8.

52. Blatch, G.L. and M. Lassle, *The tetratricopeptide repeat: a structural motif mediating protein-protein interactions.* Bioessays, 1999. **21**(11): p. 932-9.

53. Allan, R.K. and T. Ratajczak, *Versatile TPR domains accommodate different modes of target protein recognition and function.* Cell Stress Chaperones, 2011. **16**(4): p. 353-67.

54. Golden, T., M. Swingle, and R.E. Honkanen, *The role of serine/threonine protein phosphatase type 5 (PP5) in the regulation of stress-induced signaling networks and cancer.* Cancer Metastasis Rev, 2008. **27**(2): p. 169-78.

55. Chen, M.X., et al., *A novel human protein serine/threonine phosphatase, which possesses four tetratricopeptide repeat motifs and localizes to the nucleus.* EMBO J, 1994. **13**(18): p. 4278-90.

56. Ollendorff, V. and D.J. Donoghue, *The serine/threonine phosphatase PP5 interacts with CDC16 and CDC27, two tetratricopeptide repeat-containing*

subunits of the anaphase-promoting complex. J Biol Chem, 1997. **272**(51): p. 32011-8.

57.   Russell, L.C., et al., *Identification of conserved residues required for the binding of a tetratricopeptide repeat domain to heat shock protein 90.* J Biol Chem, 1999. **274**(29): p. 20060-3.

58.   Das, A.K., P.W. Cohen, and D. Barford, *The structure of the tetratricopeptide repeats of protein phosphatase 5: implications for TPR-mediated protein-protein interactions.* EMBO J, 1998. **17**(5): p. 1192-9.

59.   Yang, J., et al., *Molecular basis for TPR domain-mediated regulation of protein phosphatase 5.* EMBO J, 2005. **24**(1): p. 1-10.

60.   Hinds, T.D., Jr. and E.R. Sanchez, *Protein phosphatase 5.* Int J Biochem Cell Biol, 2008. **40**(11): p. 2358-62.

61.   Silverstein, A.M., et al., *Protein phosphatase 5 is a major component of glucocorticoid receptor.hsp90 complexes with properties of an FK506-binding immunophilin.* J Biol Chem, 1997. **272**(26): p. 16224-30.

62.   Richter, K. and J. Buchner, *Hsp90: chaperoning signal transduction.* J Cell Physiol, 2001. **188**(3): p. 281-90.

63.   Ali, A., et al., *Requirement of protein phosphatase 5 in DNA-damage-induced ATM activation.* Genes Dev, 2004. **18**(3): p. 249-54.

64.   Galigniana, M.D., et al., *Hsp90-binding immunophilins link p53 to dynein during p53 transport to the nucleus.* J Biol Chem, 2004. **279**(21): p. 22483-9.

65.   Gasco, M., S. Shami, and T. Crook, *The p53 pathway in breast cancer.* Breast Cancer Res, 2002. **4**(2): p. 70-6.

66.   Sun, H. and Y. Wang, *Novel Ser/Thr protein phosphatases in cell death regulation.* Physiology (Bethesda), 2012. **27**(1): p. 43-52.

67.   Urban, G., et al., *Identification of a functional link for the p53 tumor suppressor protein in dexamethasone-induced growth suppression.* J Biol Chem, 2003. **278**(11): p. 9747-53.

68.   Zhou, G., et al., *Ser/Thr protein phosphatase 5 inactivates hypoxia-induced activation of an apoptosis signal-regulating kinase 1/MKK-4/JNK signaling cascade.* J Biol Chem, 2004. **279**(45): p. 46595-605.

69.   Urban, G., et al., *Identification of an estrogen-inducible phosphatase (PP5) that converts MCF-7 human breast carcinoma cells into an estrogen-independent phenotype when expressed constitutively.* J Biol Chem, 2001. **276**(29): p. 27638-46.

70.   Golden, T., et al., *Elevated levels of Ser/Thr protein phosphatase 5 (PP5) in human breast cancer.* Biochim Biophys Acta, 2008. **1782**(4): p. 259-70.

71.   Schmid, A.B., et al., *The architecture of functional modules in the Hsp90 co-chaperone Sti1/Hop.* EMBO J, 2012. **31**(6): p. 1506-17.

72.   Carrigan, P.E., et al., *Domain:domain interactions within Hop, the Hsp70/Hsp90 organizing protein, are required for protein stability and structure.* Protein Sci, 2006. **15**(3): p. 522-32.

73.   Hernandez, M.P., W.P. Sullivan, and D.O. Toft, *The assembly and intermolecular properties of the hsp70-Hop-hsp90 molecular chaperone complex.* J Biol Chem, 2002. **277**(41): p. 38294-304.

74. Onuoha, S.C., et al., *Structural studies on the co-chaperone Hop and its complexes with Hsp90.* J Mol Biol, 2008. **379**(4): p. 732-44.

75. Kubota, H., et al., *Increased expression of co-chaperone HOP with HSP90 and HSC70 and complex formation in human colonic carcinoma.* Cell Stress Chaperones, 2010. **15**(6): p. 1003-11.

76. Walsh, N., et al., *RNAi knockdown of Hop (Hsp70/Hsp90 organising protein) decreases invasion via MMP-2 down regulation.* Cancer Lett, 2011. **306**(2): p. 180-9.

77. Pimienta, G., K.M. Herbert, and L. Regan, *A compound that inhibits the HOP-Hsp90 complex formation and has unique killing effects in breast cancer cell lines.* Mol Pharm, 2011. **8**(6): p. 2252-61.

78. Odunuga, O.O., V.M. Longshaw, and G.L. Blatch, *Hop: more than an Hsp70/Hsp90 adaptor protein.* Bioessays, 2004. **26**(10): p. 1058-68.

79. Chinkers, M., *Protein phosphatase 5 in signal transduction.* Trends Endocrinol Metab, 2001. **12**(1): p. 28-32.

80. Gray, P.J., Jr., et al., *Targeting the oncogene and kinome chaperone CDC37.* Nat Rev Cancer, 2008. **8**(7): p. 491-5.

81. McDonough, H. and C. Patterson, *CHIP: a link between the chaperone and proteasome systems.* Cell Stress Chaperones, 2003. **8**(4): p. 303-8.

82. Felts, S.J. and D.O. Toft, *p23, a simple protein with complex activities.* Cell Stress Chaperones, 2003. **8**(2): p. 108-13.

83. Erlejman, A.G., M. Lagadari, and M.D. Galigniana, *Hsp90-binding immunophilins as a potential new platform for drug treatment.* Future Med Chem, 2013. **5**(5): p. 591-607.
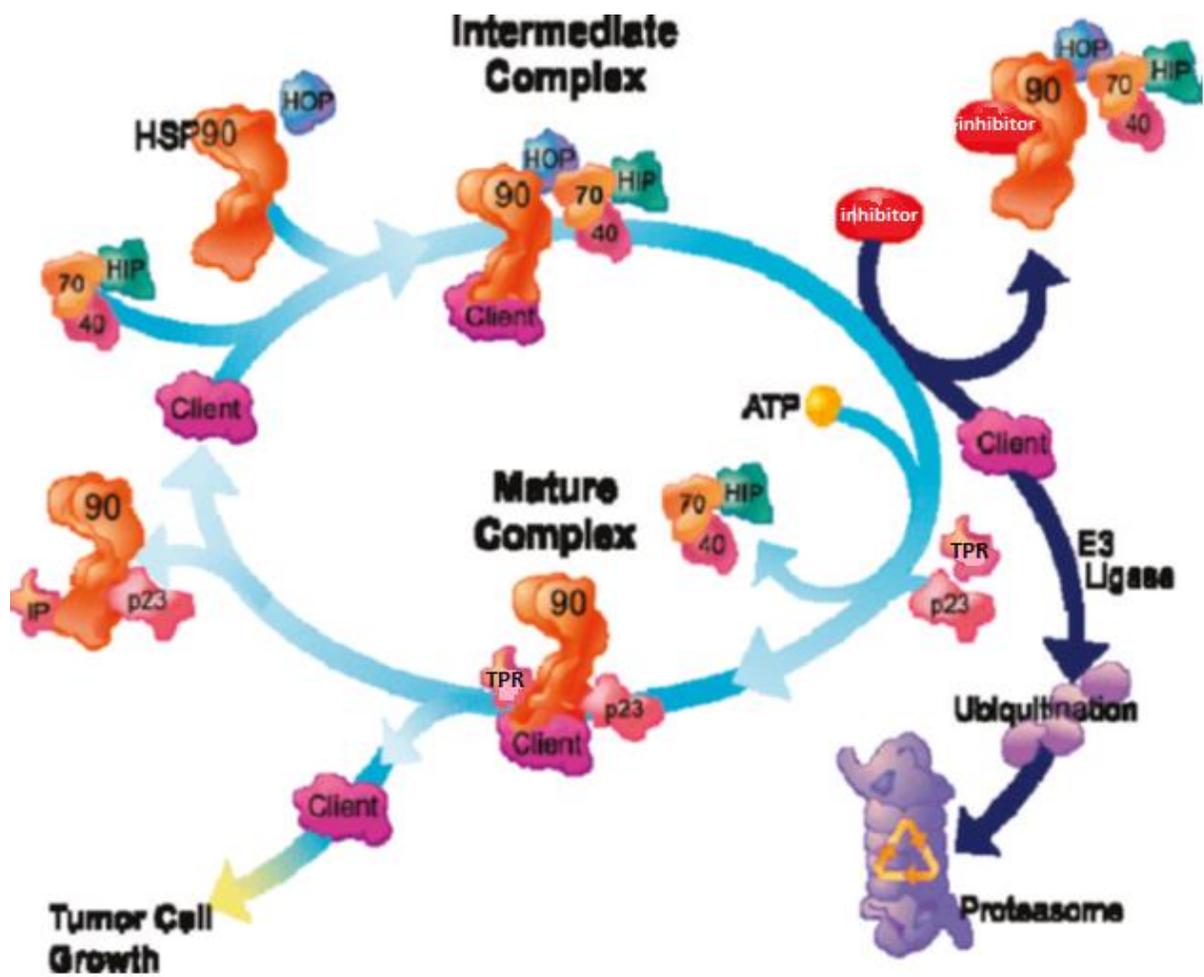
(Adapted from Biamonte M. Heat Shock Proteins 90 Inhibitors in Clinical Trials. J. Med. Chem. 2010, 53, 3–17 3).

Appendix Figure 1-1. **HSP90 Complex.** In a disease state, oncogenic proteins are matured for tumorigenesis. However, if an inhibitor is present, client proteins will be marked for ubiquitination and degraded by proteasomes.

Co-Chaperone	Contains TPR domain?	Binding Site on HSP90	Function
HOP	Yes	C-Terminal	HSP70-HSP90 organizing proteins which helps to link HSP70 and HSP90. Moves back and forth from cytoplasm to nucleus [78].
PP5	Yes	C-Terminal	The exact function involved with the HSP90 complex unknown. Evidence proposes that it might be important for dephosphorylation of kinase. Also it's been suggested that the HSP90-PP5 interaction is important for regulating the steroid receptor [79].
Cdc37	No	N-Terminal	Co-Chaperone that interacts with many kinases. Helps stabilizes and promotes activity of the complex. Important for signal transduction. Cellular location is in the cytoplasm [80].
CHIP	Yes	C-Terminal	E3 ubiquitin protein ligase which marks misfolded substrates to be degraded by proteasomes [81].
P23	No	N-Terminal	Participates in folding HSP90 and a number of cellular regulations. Enters the mature complex and helps with the maturation of client proteins. [82]
Immunophillins (FKB51/52)	Yes	C-Terminal	FKB51/52 are peptidylprolyl isomerase that associates with HSP90 to help intracellular trafficking of the steroid hormone receptor [83].

Appendix Table 1-1. **Co-Chaperones that bind to HSP90.** This summarizes important co-chaperones that bind to HSP90, functions of co-chaperones, and whether they contain TPR domains.

**The Molecular Chaperone Hsp70 Activates Protein Phosphatase 5 (PP5) By
Binding the Tetratricopeptide Repeat (TPR) Domain**

Abstract

Protein phosphatase 5 (PP5) is auto-inhibited by intramolecular interactions with
its tetratricopeptide repeat (TPR) domain. Hsp90 has been shown to bind PP5 to
activate its phosphatase activity. However, the functional implications of binding Hsp70
to PP5 are not yet clear. In this study, we find that both Hsp90 and Hsp70 bind to PP5
using a luciferase fragment complementation assay. A fluorescence polarization assay
shows that Hsp90 (MEEVD motif) binds to the TPR domain of PP5 almost 3-fold higher
affinity than Hsp70 (IEEVD motif). However, Hsp70 binding to PP5 stimulates higher
phosphatase activity of PP5 than the binding of Hsp90. We find that PP5 forms a stable
1:1 complex with Hsp70, but the interaction appears asymmetric with Hsp90, with 1 PP5
binding the dimer. Solution NMR studies reveal that Hsc70 and PP5 proteins are
dynamically independent in complex, tethered by a disordered region that connects the
Hsc70 core and the IEEVD-TPR contact area. This tethered binding is expected to allow
PP5 to carry out multi-site dephosphorylation of Hsp70-bound clients with a range of
sizes and shapes. Together, these results demonstrate that Hsp70 recruits PP5 and
activates its phosphatase activity which suggests dual roles for PP5 that might link
chaperone systems with signaling pathways in cancer and development.

Introduction

Protein phosphatase 5 (PP5) is a member of the PPP family of serine/threonine-specific phosphatases and has been linked to signaling pathways that control growth arrest, apoptosis, and DNA damage repair [1-3]. Specifically, PP5 plays important roles in regulating the dynamic phosphorylation of p53, ASK-1, MAPK and many other signaling components [4-6]. PP5 also has been implicated in the regulation of glucocorticoid receptor, although the mechanism is controversial [1, 7]. Additionally, PP5 levels are elevated in human breast cancer [8]. Together, these studies have suggested that PP5 may be a novel target for anti-cancer therapies [9]. However, the catalytic subunit of PPP phosphatases is highly conserved and it has been difficult to develop selective, competitive inhibitors of these enzymes [10]. In addition to its catalytic domain, PP5 is the only member of the PPP family that contains an N-terminal tetratricopeptide repeat (TPR) domain [11, 12]. TPR domains are assembled from repeats of an amphipathic antiparallel-helix that assemble into superhelical structures bearing a concave central groove [13-16]. PP5 has been shown to interact with the molecular chaperones heat shock protein 70 (Hsp70) and heat shock protein 90 (Hsp90) [17-21]. Specifically, PP5's TPR domain binds to cytoplasmic Hsp90 homologs, Hsp90α (stress inducible) and Hsp90β (constitutively active), through a conserved MEEVD motif that is located at the end of the C-termini of these chaperones [17-20]. Although biochemical data illustrates that an MEEVD peptide has high affinity for PP5's TPR domain (~50 nM), solution phase NMR studies revealed that this interaction is highly dynamic with only few enduring contacts [19, 20]. Comparatively less is known about how PP5 interacts with Hsp70. Co-immunoprecipitation studies suggest that PP5

133

binds Hsp70 [21], but it isn't yet clear how PP5 interacts with this chaperone or whether the TPR domain is involved. Based on the Hsp90-PP5 complex, it is likely that this interaction occurs through the IEEVD motif at the C-termini of the cytoplasmic Hsp70 family members, including heat shock cognate 70 (Hsc70; HSPA8) and heat shock protein 72 (Hsp72; HSPA1A).

PP5 belongs to a family of TPR domain-containing co-chaperones that includes Hop (Hsp70/90 organizing protein), CHIP (carboxyl-terminus of Hsp70 interacting protein) and a number of immunophillins, such as FKBP52 (FK506 binding protein 52kDa). Members of this co-chaperone family bind to Hsp70 and/or Hsp90 at these chaperones' C-terminal EEVD motifs. In turn, the TPR co-chaperones are important regulators of chaperone function [16] [22, 23]. For example, complexes between CHIP and either Hsp70 or Hsp90 are linked to the ubiquitination and therefore the proteasomal degradation of chaperone-bound clients. Likewise, a complex between these chaperones and HOP is critical to the folding of some clients, such as nuclear hormone receptors [24-26]. Additionally, FKBP52 couples clients of Hsp70 and Hsp90 to the cytoskeleton [27]. However, less is known about the Hsp70-PP5 and Hsp90-PP5 complexes and their potential roles in the protein homeostasis network. One important clue comes from observations that the TPR domain and the C-terminal catalytic subunit of PP5 have an auto-inhibitory function, suppressing phosphatase activity. Indeed, binding of Hsp90 to the TPR domain has been reported to weakly activate PP5 [14]. However, it is not yet clear whether Hsp70 also binds the TPR domain or whether this interaction activates PP5.

134

Towards these questions, we characterized the interaction of Hsp70 and Hsp90 with PP5, using a panel of cell-based assays and biophysical methods. These studies confirmed that PP5 binds Hsp70 and Hsp90 through the canonical EEVD motifs. However, we found that C-terminal peptides derived from Hsp90α/β bind to PP5 10-fold tighter than C-terminal peptides derived from Hsc70/Hsp72. Despite Hsp70's weaker affinity for PP5, this chaperone was far more effective at stimulating PP5's phosphatase activity. Additionally, solution phase NMR studies showed that Hsp70 and PP5 move independently of each other in the bound complex, suggesting that the disordered C-terminus of Hsp70 allows the activated PP5 to "sample" a relatively large area around the chaperone. This ultra-structure might be important in allowing PP5 to act on a wide range of chaperone clients. Together, these results suggest that the Hsp70-PP5 complex is a potent phosphatase that might link chaperone systems with signaling pathways in cancer and development.

Material/ Methods

Materials.   Reagents were obtained from the following sources: pLentilox vectors (University of Michigan Vector Core); pMSCG9 vector (Clay Brown, Center for Structural Biology, University of Michigan); restriction endonucleases (New England Biolabs, Ipswich, MA); HEK293 (American Type Culture Collection); Dulbecco's modified Eagle media (Gibco Life Technologies, 11965-092); fetal bovine serum (10082-147); antibiotic-antimycotic (Gibco Life Technologies, 15240-062); 6-well tissue culture plate (BD Falcon, 3046); polybrene linker (Santa Cruz, sc-134220) *Renilla* GLO

Luciferase Kit (Promega, Madison, WI); and pNPP phosphatase substrate kit (Thermo Scientific, 37620).

Plasmid Construction. C-terminal *Renilla* luciferase (CRL, residues 1-229) and full-length Hsp70 or Hsp90 (upstream of CRL) were PCR-amplified and subcloned into a pLentilox RSV-2 dsRed vector using the following restriction site design: BamHI-Hsp72-Xba1-CRL-Not1 and Xma1-HSP90α-BamHI-CRL-Xba1. In these fusion constructs, the stop codon of Hsp70/90 was deleted. Similarly, N-terminal *Renilla* luciferase (NRL, resides 230-311) and full-length PP5 (downstream of NRL) were amplified and subcloned into the pLentilox RSV vector using the following restriction site design: BamHI-NRL-Xba1-PP5-Not1. In this construct, the NRL stop codon was deleted. All fusion constructs (Hsp70/90-CRL and NRL-PP5) contained a GGGGSGGGGS $(G_4S)_2$ peptide linker between the protein of interest and the *Renilla* luciferase reporter [28]. After all sequences were confirmed at University of Michigan DNA sequencing core, lentiviral particles containing these constructs were purchase (University of Michigan Vector Core) in order to create a stable cell lines for additional studies.

Cell Transduction and SRL-PFAC Assay. HEK293 cells were plated using Dulbecco's modified Eagle medium (DMEM) (Gibco Life Technologies) with 10% fetal bovine serum (FBS) and no antibiotics into a 6 well tissue culture plate. Cells were allowed to adhere and grow for 1 day (~70% confluent) before transduction. The next day, fresh media without antibiotics (1.35 mL), 0.15 mL of 10X lentiviral particle (either Hsp70-CRL, Hsp90-CRL, or NRL-PP5), and polybrene linker to a final concentration of 8 µg/mL was

added to each well. After an incubation period of 8 hours at 37 °C and 5% CO_2, the media was replaced with DMEM with 10% FBS and 1% antibiotic-antimycotic. For cells that contained both HSP70/90-CRL and NRL-PP5 viral particles, the above procedure first performed with Hsp90/Hsp70-CRL viral particles. Using these cells, the same procedure was repeated a second time; however, NRL-PP5 lentiviral particle was added. The HSP70/90-CRL and PP5-NRL viral particles contained dsRED and GFP respectively. Cells containing Hsp90-CRL, Hsp70-CRL, NRL-PP5, Hsp90-CRL + NRL-PP5, and Hsp70-CRL + NRL-PP5 constructs were then seeded into a 24 well plate at a density of 5,000 cell/wells and allowed to grow overnight at 37 °C and 5% CO_2. The following day, the media was removed and the cells were washed with phosphate-buffered saline. Luciferase activity determined using the *Renilla*-GLO Luciferase Assay System kit. Briefly, following washing, 100 µL of 1X passive lysis buffer was added to each well and plates were allowed to shake for 15 minutes at room temperature. Afterwards, 1X luciferase substrate was added and the luminescence was measured using Biotek Synergy 2 plate reader.

Protein Purification. Full length PP5 and Hsp90 were expressed in *Escherichia coli* BL21 (DE3) cells from pMCSG9 plasmids. A fresh colony was grown in terrific broth (TB) medium supplemented with 50 mg/L ampicillin at 37 °C with shaking at 250 rpm until OD_{600} reached ~0.8 and protein expression was induced by the addition of IPTG (final concentration of 1 mM). The temperature was reduced to 18 °C and the culture was allowed to shake overnight. Cells were harvested by centrifugation (4000 x g, 10 min, 4 °C). Cell pellets was suspended in lysis buffer (50 mM NaH_2PO_4, 300 mM NaCl,

10 mM Imidazole (pH=8.0)) and sonicated on ice, and clarified by centrifugation at 15,000 x g for 30 min. The His-tagged proteins were purified using a Ni-NTA (Qiagen) column. The eluted protein was subjected to dialysis (PP5 buffer 40 mM Tris-HCL pH 7.4, 10% glycerol, 1mM DTT and HSP90 buffer 20 mM Tris-HCL pH 7.4, 20 mM NaCl, 10% glycerol, 1mM DTT). Proteins were treated with His-tagged tobacco etch virus protease TEV protease (1 µM) overnight at 4 °C to remove tags. This process was repeated a second time prior to extensive dialysis and removal of any residual His-tagged protein by Ni-NTA column. Human Hsp70s (pMCSG7 vector) were expressed in *E. coli* BL21 (DE3) cells using TB medium supplemented with 50 mg/L ampicillin at 37 °C with shaking at 250 rpm until OD_{600} of ~0.8 was reached. Additionally, Hsc70 protein was isotopically labeled for all NMR experiment. For labeled Hsc70, the BL21 cells were grown M9 media with[15]NH_4Cl (Sigma Aldrich). The temperature was reduced to 18 °C and the culture was allowed shake overnight. Cells were harvested by centrifugation (4000 x g, 10 min, 4 °C). All Hsp70s were purified as described [29] and His tags removed *via* TEV protease. Final purification was performed on an ATP agarose column. All protein concentrations were measure using the Pierce BCA protein assay kit according to the manufacturer's protocol. To verify Hsc70 was not aggregated, the raw fluorescence values of the parallel and perpendicular intensity using fluorescence polarization shows no indication of aggregation. In addition, non-binding and binding tracer in fluorescence polarization was also used to confirm Hsc70 was not aggregated. NMR structure showed no sign of Hsc70 aggregation.

Peptide Synthesis. All peptides were synthesized manually or with an ABI 433 peptide synthesizer using Fmoc chemistry with 2-Chlorotrityl resin as the solid support. Either

138

DIC/HOAt or HOBt/HBTU was used as the coupling reagent. Following completion of the peptide, a cleavage cocktail composed of TFA:TIS:H$_2$O (19 mL: 0.5 mL: 0.5 mL) removed the peptide from the resin as well as any side-chain protecting groups. The resulting solution was evaporated and the crude peptide was precipitated with diethyl ether. Peptides were purified via RP-HPLC (Waters, Sunfire Prep C18, 19 mm x 150 mm, 5 μm) and confirmed by electrospray ionization mass spectroscopy (ESI-MS) [30].

Fluorescence Polarization Assay. All fluorescence polarization experiments were conducted in 384-well, black, low volume, round-bottom plates (Corning) using a BioTeck Synergy 2 plate reader (Winooski, VT). For binding experiments, to each well, was added increasing amounts of protein and the 5-carboxyfluorescein (5-Fam) labeled Hsp70/90 C-terminal probe/tracer (20 nM). For competition studies each well had PP5 protein at a concentration equivalent to the K$_d$, 5-FAM labeled peptide was held constant at 20 nM, and varying concentration of unlabeled peptide was added to compete off labeled peptide. All wells had a final volume of 20 uL in the assay buffer (40 mM Tris-HCl, pH=7.4, 10% glycerol, 1mM DTT). The plate was allowed to incubate at room temperature for 5 min to reach equilibrium. The polarization values in millipolarization units (mP) were measured at an excitation wavelength at 485 nm and an emission wavelength at 528 nm. An equilibrium binding isotherm was constructed by plotting the FP reading as a function of the protein concentration at a fixed concentration of tracer (20 nM). All experimental data were analyzed using Prism 5.0 software (Graphpad Software, San Diego, CA) and WinNonlin (version 5.3)).

Protein NMR Experiments. NMR data was collected using an Agilent/Varian NMR System with a room temperature triple resonance probe, interfaced to an Oxford instruments 18.7 T magnet (^{1}H 800 MHz). Backbone assignments for the C-terminus of Hsc70 were previously reported [38]. Experiments for studying the interaction of PP5 with Hsc70 were carried out using full-length PP5 and full length ^{15}N labeled Hsc70 in the following buffer: 50 mM HEPES, 75 mM NaCl, 1 mM ADP, 5 mM MgCl$_2$, 0.02% NaN$_3$, 0.01% Triton pH 7.4, 30°C. The TROSY spectrum with 1:0 Hsc70:PP5 was recorded in 10 hours with a sample of 254 uM Hsc70. The spectrum with 1:1 Hsc70:PP5 was recorded in 22 hours with a sample of 169 uM Hsc70 and 149 uM PP5. The two spectra have the same intrinsic signal to noise ratio ($(254/169)^2 = 2.25$).

Size exclusion chromatography and multi-angle light scattering (SEC-MALS): PP5:Hsp70 and PP5:Hsp90 complexes were formed by incubating proteins at equal molar concentrations (10 µM) in binding buffer (100mM KCl, 20mM HEPES [pH 7.5], 7mM β-mercaptoethanol) at room temperature for 30 min. Identification and molecular weight determination of complexes was achieved through SEC (Wyatt WTC-050S5 and WTC-030S5 columns) with an Akta micro FPLC (GE Healthcare) and in-line DAWN HELEOS MALS and Optilab rEX differential refractive index detectors (Wyatt Technology Corporation). SEC was performed in 100mM KCl, 20mM HEPES [pH 7.5]. Data was analyzed by the ASTRA 6 software package (Wyatt Technology Corporation).The two spectra have the same intrinsic signal to noise ratio ($(254/169)^2 = 2.25$)

p-Nitrophenyl Phosphate Assay. Purified PP5, Hsp70, and Hsp90 were immobilized in 4HBX 96 well plates (thermo-scientific) and diluted with ELISA buffer (BioLegend). Equal molar concentration of protein was added to each well and incubation overnight at 4 degrees. Protein concentrations ranged from 50 uM to 0.5 uM. The following day p-Nitrophenyl Phosphate (pNPP) (Fisher Scientific) was used according to the manufactures protocol. Once pNPP substrates were added to the plates, they were incubated at 37 degrees for 1 hour. After color change, the OD405 was measured on the Biomatrix Plate Reader Synergy 2. The enzymatic activity was calculated using the following equation.

$$Enzyme\ Activity\ \frac{\frac{\mu mol}{\min}}{\mu g} = \frac{Volume * \frac{OD405}{pathlength}}{\varepsilon * enzyme * time\ of\ incubation}$$

Where ε is the molar extinction coefficient which equals 1.78*10^4 M^{-1}*cm^{-1}.

Results

SRL-PFAC confirms that Hsp70 and Hsp90 bind to PP5 in cells.

Previous co-immunoprecipitation studies have suggested that PP5 interacts with both Hsp70 and Hsp90 in cells [21]. To confirm this result, we utilized the SRL-PFAC system, which has proven to be a powerful method for studying protein-protein interactions in cells [31]. In this assay, the full-length *Renilla* luciferase gene is divided into inactive halves, the N-terminal *Renilla* luciferase (NRL, residues 1-229) and the C-terminal *Renilla* luciferase (CRL, residues 230-311). The NRL and CRL will reconstitute

141

functional luciferase if they are brought into close proximity. To explore whether Hsp90 and Hsp70 bind PP5, we created constructs that would express NRL-PP5, Hsp70-CRL or Hsp90-CRL fusion proteins (Figure 1A). We anticipated that a luminescence signal would be detected only if Hsp90 or Hsp70 interacts with PP5 (Figure 1B). When HEK293 cells were transduced with viral vectors expressing either NRL-PP5, Hsp70-CRL or Hsp90-CRL alone, low luciferase activity was measured (Figure 1C). However, co-transduction with either the NRL-PP5 + Hsp70-CRL pair or the NRL-PP5 + Hsp90-CRL pair led to enhanced luciferase activity (Figure 1C), consistent with the interaction of PP5 with both chaperones in cells. We also examined at a control pair (NRL-PP5 + HOP-CRL) if nonspecific complementation would occur. As expected no complementation of two luciferase fragments (NRL and CRL with low luciferase activity) was observed (data not shown).

PP5 binds to the C-terminus of Hsp90 with higher affinity than to Hsp70.

Binding of TPR co-chaperones, such as HOP or CHIP, to Hsp70 and Hsp90 is typically mediated by contacts between the TPR domain and the C-terminal EEVD motif that is shared by both chaperones [32-34]. To explore the affinity of the Hsp90 C-terminus for PP5, we developed a fluorescent MEEVD tracer and measured its binding to PP5 by fluorescence polarization (FP). In this platform, the MEEVD tracer had a K_d value of 0.14 ±0.005 µM (Figure 2B), consistent with literature values [20]. This interaction appeared to be specific, because the reverse tracer (DVEEM) had weak affinity for PP5 (K_d > 10 µM) (Figure 2A). Next, we assessed the ability of an Hsp70-derived IEEVD tracer to bind PP5. This tracer had a ~3-fold weaker affinity for PP5 (K_d

= 0.426 ± 0.06 µM) (Figure 2B). We were then curious to see if the homologs of the chaperones might have different affinities for PP5. We found that 10mer tracers derived from the C-termini of Hsc70 and Hsp72 had comparable affinities for PP5, with K_d values of 1.06 ± 0.34 and 1.55 ± 0.43 µM, respectively (Figure 2C). Additionally, the Hsp90α and Hsp90β tracers bound to PP5 with similar affinities, with K_d values of 0.079 ± 0.02 and 0.077 ± 0.02 µM, respectively (Figure 2C). The longer 10mer tracers also had affinities that were similar to those of their corresponding 5mers, suggesting that most of the affinity of the interaction is engendered by the EEVD motif.

The results of the FP experiments suggested that the methionine of the MEEVD motif in Hsp90α/β may increase affinity for PP5. To test this hypothesis in more detail, we constructed tracers in which this position was mutated. Specifically, the methionine of the Hsp90α tracer was mutated to an isoleucine and the corresponding isoleucine of the Hsp72 tracer was mutated to methionine. As expected, the Hsp72 mutant tracer had higher affinity than the Hsp90α mutant tracer (0.133 ± 0.03 and 0.42 ± 0.02 µM) (Figure 2D). These results clearly showed that the methionine contributed to the greater affinity of Hsp90-derived peptides for PP5.

To further confirm these binding studies, we performed competition studies to compete unlabeled peptide with labeled peptide. The IC_{50} values for the isoforms of HSP90 again showed higher affinity than HSP70 peptides in all 4 tracer competition assays (Figure 3A-D). For these experiments PP5 protein was added at a molar concentration that was equal to the binding affinity (K_d). Therefore, for the competition

assay Hsc70 and Hsp72 contained more PP5 protein compared to Hsp90 α and β due to the lower affinity which can explain the similar IC_{50} among all four tracer assays. However, these results confirmed the binding experiments were correctly portraying the correct affinity.

PP5 binds Hsp70 and Hsp90 in different arrangements.

To better understand how the chaperones bind PP5, we incubated full length Hsp70 or Hsp90 with PP5 and analyzed the complexes by size-exclusion chromatography combined with multi-angle light scattering (SEC-MALS) to obtain an accurate measure of the molecular weight and stoichiometry of the complexes[35]. Additionally, both Hsp70 and Hsp90 are ATPase and they undergo dramatic conformational changes in response to nucleotides [36, 37]. When equimolar PP5 and Hsp70 are incubated and analyzed by SEC-MALS, a single peak predominates and is shifted in elution volume compared to individual runs of Hsp70 and PP5 (Figure 4A), indicating the formation of an Hsp70:PP5 complex. The average molecular weight of this peak was determined to be 145 kDa, and based on comparison with 126 kDa molecular weight calculated from the sequence, this corresponds to a 1:1 complex of Hsp70:PP5. When the Hsp90 dimer and PP5 are incubated together a single, shifted peak is observed as well, with a modest increase in molecular weight, 232 kDa compared to 190 kDa for Hsp90 alone (Figure 4B). This corresponds to an average of less than 1 PP5 bound per Hsp90 dimer indicating the formation of an asymmetric complex of Hp90:PP5 with a 2:1 stoichiometry despite the presence of two MEEVD binding sites in the Hsp90 dimer. Hsp90:PP5 interaction is likely weaker in affinity,

144

resulting in a partial dissociation during the elution, explaining the lower average molecular weight. The presence of saturating amounts of ATP and ADP were tested but resulted in no changes the molecular weight of the Hsp90:PP5 complex. Differences in the average molecular weight measured by SEC-MALS compared to the protein sequence were likely due to minor presence of aggregated PP5 and Hsp90 tetramer species (data not shown). Overall these results demonstrate that PP5 binds full-length Hsp70 and Hsp90 in vitro in different arrangements. Hsp70:PP5 is in a stable 1:1 complex, while Hsp90:PP5 is in a 2:1 arrangement and may be slightly weaker in affinity compared to Hsp70.

Hsc70 and PP5 move independently within the complex.

To explore the Hsp70-PP5 complex in greater detail, we utilized solution-state NMR. A ^{1}H-^{15}N TROSY HSQC spectrum was collected for ^{15}N-labeled Hsc70 (1-646) in the ADP-bound state (Figure 5A in blue). As identified in our previous study where we investigated the interaction of Hsc70 with the highly homologous TPR protein CHIP [38], the middle of the TROSY spectrum (~7.5 to 8.5 ppm) is dominated by intense sharp resonances with a signal-to-noise ratio (SNR) of ~250:1 (Figure 5A). These resonance were assigned using triple resonance experiments to residues 612-646 in C-terminal tail of Hsc70 as well as to a N terminal extension containing a tag [38]. The strong intensity of these resonances, as well as the lack of spectral dispersion, indicated that Hsc70's C-terminal region (612-646), including the IEEVD motif, is a dynamically disordered random coil. Based on comparison with published spectra of the isolated nucleotide-binding domain (NBD) and the substrate-binding domain (SBD), the much weaker

145

signals with SNR ~ 8:1 in the well-dispersed part of the NMR spectrum in Figure 5 originate from the 45 kDa Hsc70 NBD and 25 kDa SBD [38]. In the ADP state, these domains are tethered by a ~10 residue linker and move relatively independently [39-41]. The large difference in peak intensity between the core region and the C-terminus is due to the large difference in TROSY transfer efficiency in molecules with an effective molecular weight of 25 - 45 kDa and a flexible tail with a much smaller effective molecular weight (which one estimates to be ~ 10 kDa on the basis of this intensity difference, see Table 2 and its legend). Increasing the contour level of the spectra focuses on the dynamically disordered region, which included the IEEVD motif (Figure 5B).

The ^{1}H-^{15}N TROSY HSQC spectrum of ^{15}N-labeled Hsc70 with PP5 in a ~1:1 ratio, shown in red in Figure 5 has the same intrinsic SNR as the spectrum of uncomplexed Hsc70 (see materials and methods). With a K_D of Hsc70-PP5 binding of ~ 1 uM (see above), 85% of the 169 uM Hsc70 should be complexed by the 149 uM PP5. Significantly, most of the Hsc70 resonances in the presence of PP5 did not change from those of Hsc70 alone (comparing red and blue overlay, respectively; Figure 5A). This result is unexpected. If the 60 kDa PP5 were to form a rigid 85 kDa complex with the 25 kDa SBD, the SBD TROSY resonance intensities in the complex should drop 180-fold and become invisible; if it were to form a 105 kDa complex with the 45 kDa NBD, the NBD TROSY resonance intensities should drop 160-fold and become invisible; if it were to form a 130 kDa triple complex with SBD and NBD, the latter resonance intensities would drop 7000 and 1500 times, respectively (see Table 2 and its legend for these

146

calculations). In other words, if Hsc70 and PP5 were to form a rigid complex with either SBD or NBD core area's TROSY-HSQC NMR spectrum would become undetectable at the conditions used. In these scenarios, the NMR spectrum of the 15% uncomplexed Hsc70 would also drop below the SNR limit. Hence, as we observe a largely unperturbed NMR spectrum for the Hsc70 core in the complex, we must conclude that the NMR data shows that the core regions of Hsc70 do not form stable complexes with PP5.

The NMR data do show that PP5 interacts with Hsc70's C-terminus. Several resonances in the high-level contour plot (Fig 5b) disappeared and/or shifted in the 1:1 complex with PP5 (red spectrum). In particular, the intense resonances of the IEEVD motif residues disappeared completely from the NMR spectrum (Figures 5B and 5C), without new resonances appearing (also not at lower contour levels). This result is consistent with the dynamic C-terminus of an effective molecular weight of 10 kDa being immobilized by the 58 kDa PP5 protein forming a ~ 70 kDa complex. Table 2 shows that such a change in effective molecular weight results in a 430-fold reduction in TROSY peak intensity, which renders even peaks with an initial SNR of ~ 250:1 invisible. We do not observe resonances for the ~ 15% free Hsc70, which should have an intrinsic ~ 40:1 SNR. It is most likely that the protein concentration estimation is not accurate and that there is no free Hsc70 in the sample.

Very significantly, the NMR spectra also show that the remaining peaks of the C-terminal region (residues 610-640) do not disappear. This strongly suggests that this

area, located between the SBD of Hsc70 and the IEEVD motif, remains a dynamic random coil in the Hsc70-PP5 complex. Thus, the two proteins, while tightly bound through the IEEVD-TPR interaction, appear to move as dynamic, independent units tethered via Hsc70 residues 610-640.

Hsp70 stimulates PP5's phosphatase activity.

In order to further understand the functional consequence of the Hsp70-PP5 interaction, we utilized an *in vitro* phosphatase assay. Previous work illustrates that PP5 maintains a basal level of phosphatase activity, which can be weakly stimulated by Hsp90 [14]. Thus, we assessed the ability of PP5 to hydrolyze the model substrate, p-nitrophenyl phosphate (pNPP) in the presence of Hsp70 or Hsp90. Importantly, neither Hsp70 nor Hsp90 interfered with the assay (Figure 6B), allowing us to determine their effects on PP5. Moreover, PP5 basal activity was very weak (Figure 6A), consistent with previous reports [42]. Interestingly, Hsp70 stimulated PP5's phosphatase activity and this stimulatory activity was much greater than that of Hsp90 (Figure 6A). In addition, we also tested if 10mer C-terminal peptides (Hsp90α, Hsp90β, Hsc70, and Hsp72) would also stimulate PP5 activity. The data showed very little stimulation of PP5 activity when peptides were used (data not shown). These results suggest that full length of Hsp70 may play a significant role in activating PP5's enzymatic activity.

Discussion

The chaperone activities of Hsp90 and Hsp70 are guided by interactions with co-chaperones, including members of the TPR domain family. In turn, Hsp90 and Hsp70 are thought to direct the activity of these co-chaperones towards specific clients. Our

studies confirmed that PP5 is a *bona fide* member of the TPR co-chaperone family and that it binds to both Hsp90 and Hsp70 through its TPR domain. Further, we found that Hsp90α and Hsp90β bind 10-fold tighter than Hsp70 family members. It isn't yet clear whether this difference in affinity has physiological importance. However, our study suggests that methionine plays important role in the affinity. Binding studies showed that most of the affinity of the Hsp70-PP5 and Hsp90-PP5 interactions is engendered by polar contacts with the EEVD motif and NMR studies confirmed that there are no significant stable interactions between other regions of the two proteins.

The independent motion (tethered binding) of Hsp70 and PP5 in the solution complex suggests that the folded regions of these proteins are able to sample a relatively wide area. In the fully extended form, the disordered C-terminus of Hsp70 could be expected to extend nearly 40 Å. We speculate that this flexibility and length might be important in allowing PP5 to find phosphorylated residues in bound Hsp70 clients. Hsp70 clients are thought to include a number of kinases and transcription factors involved in apoptotic signaling. These clients have a wide range of sizes and shapes, so the flexibility of the tethered Hsp70-PP5 complex might be important in bringing activated PP5 in the vicinity of phosphorylated residues on these diverse targets.

Exclusive, tethered binding to the Hsc70 EEVD terminus was recently observed for CHIP, an E3 ubiquitin ligase containing a TPR domain highly homologous to that of PP5 [38]. CHIP mediates broad-spectrum ubiquitination of Hsc70 client proteins

destined for the proteasome. For CHIP, tethered binding was thought to be important to allow the ligase to ubiquitinate diverse Hsp70 clients. Similar mechanisms might also be important in the Hsp90-PP5 complex, because Hsp90 also has a disordered region between its MEEVD motif and the folded portion of its C-terminus.

We found that Hsp70 was a potent stimulator of the phosphatase activity of PP5. It is likely that binding of the IEEVD motif to the TPR disrupts the auto-inhibitory activity of the TPR domain, as has been observed in the Hsp90-PP5 system [14]. This agrees with our observation that PP5 forms a stable 1:1 interaction with Hsp70. Based on our purification methods we expect Hsp70 favors the ADP-bound state in this complex. Because the ADP-bound form of Hsp70 has a tighter affinity for clients, this conformation might provide a way for stimulated PP5 to be held in proximity with Hsp70-bound clients for a length of time that is sufficient to allow dephosphorylation. In turn, this mechanism would limit the phosphatase activity of PP5 once it leaves the chaperone complexes, providing a reversible switch that responds to chaperone activity. Surprisingly, we found that in the context of the full-length protein, Hsp90 interaction appears asymmetric and likely weaker compared to Hsp70. This is in contrast to the 10-fold tighter affinity we identified for the Hsp90 MEEVD motif compared to the Hsp70 IEEVD. Thus, Hsp90 might use a different mechanism potentially involving client interactions or Hsp90 conformational changes that enable accessibility to the MEEVD to enhance PP5 interactions with phosphorylated clients.

Finally, these results point to the Hsp70-PP5 and Hsp90-PP5 protein-protein interactions as potential drug targets. PP5 has been proposed as an anti-tumor target [9], but the active sites of PPP family phosphatases are highly conserved and it has proven difficult to identify selective inhibitors. Based on our results, inhibitors of the PPIs between PP5 and the molecular chaperones might be an attractive alternative. Specifically, inhibitors of these PPIs might be expected to dysregulate kinase-phosphatase balance through multiple mechanisms, disconnecting PP5 from a major activation pathway and disrupting its chaperone-mediated ability to locate clients.

References

1. Zuo, Z., et al., *Ser/Thr protein phosphatase type 5 (PP5) is a negative regulator of glucocorticoid receptor-mediated growth arrest.* Biochemistry, 1999. **38**(28): p. 8849-57.

2. Morita, K., et al., *Negative feedback regulation of ASK1 by protein phosphatase 5 (PP5) in response to oxidative stress.* Embo Journal, 2001. **20**(21): p. 6028-6036.

3. Ali, A., et al., *Requirement of protein phosphatase 5 in DNA-damage-induced ATM activation.* Genes & Development, 2004. **18**(3): p. 249-254.

4. Morita, K., et al., *Negative feedback regulation of ASK1 by protein phosphatase 5 (PP5) in response to oxidative stress.* EMBO J, 2001. **20**(21): p. 6028-36.

5. Zhou, G., et al., *Ser/Thr protein phosphatase 5 inactivates hypoxia-induced activation of an apoptosis signal-regulating kinase 1/MKK-4/JNK signaling cascade.* J Biol Chem, 2004. **279**(45): p. 46595-605.

6. Zuo, Z., N.M. Dean, and R.E. Honkanen, *Serine/threonine protein phosphatase type 5 acts upstream of p53 to regulate the induction of p21(WAF1/Cip1) and mediate growth arrest.* J Biol Chem, 1998. **273**(20): p. 12250-8.

7. Chen, M.S., et al., *The tetratricopeptide repeat domain of protein phosphatase 5 mediates binding to glucocorticoid receptor heterocomplexes and acts as a dominant negative mutant.* J Biol Chem, 1996. **271**(50): p. 32315-20.

8. Golden, T., et al., *Elevated levels of Ser/Thr protein phosphatase 5 (PP5) in human breast cancer.* Biochimica Et Biophysica Acta-Molecular Basis of Disease, 2008. **1782**(4): p. 259-270.

9. Golden, T., M. Swingle, and R.E. Honkanen, *The role of serine/threonine protein phosphatase type 5 (PP5) in the regulation of stress-induced signaling networks and cancer.* Cancer and Metastasis Reviews, 2008. **27**(2): p. 169-178.

10. McConnell, J.L. and B.E. Wadzinski, *Targeting Protein Serine/Threonine Phosphatases for Drug Development.* Molecular Pharmacology, 2009. **75**(6): p. 1249-1261.

11. Bollen, M. and W. Stalmans, *THE STRUCTURE, ROLE, AND REGULATION OF TYPE-1 PROTEIN PHOSPHATASES.* Critical Reviews in Biochemistry and Molecular Biology, 1992. **27**(3): p. 227-281.

12. Cohen, P.T.W., *Novel protein serine/threonine phosphatases: Variety is the spice of life.* Trends in Biochemical Sciences, 1997. **22**(7): p. 245-251.

13. Zhang, M.H., et al., *Chaperoned ubiquitylation - Crystal structures of the CHIPU box E3 ubiquitin ligase and a CHIP-Ubc13-Uev1a complex.* Molecular Cell, 2005. **20**(4): p. 525-538.

14. Yang, J., et al., *Molecular basis for TPR domain-mediated regulation of protein phosphatase.* Embo Journal, 2005. **24**(1): p. 1-10.

15. Wang, L., et al., *Molecular Mechanism of the Negative Regulation of Smad1/5 Protein by Carboxyl Terminus of Hsc70-interacting Protein (CHIP).* Journal of Biological Chemistry, 2011. **286**(18).

16. Scheufler, C., et al., *Structure of TPR domain-peptide complexes: Critical elements in the assembly of the Hsp70-Hsp90 multichaperone machine.* Cell, 2000. **101**(2): p. 199-210.

17. Chen, L., et al., *Purification and properties of human cytosolic folylpoly-gamma-glutamate synthetase and organization, localization, and differential splicing of its gene.* J Biol Chem, 1996. **271**(22): p. 13077-87.

18. Silverstein, A.M., et al., *Protein phosphatase 5 is a major component of glucocorticoid receptor.hsp90 complexes with properties of an FK506-binding immunophilin.* J Biol Chem, 1997. **272**(26): p. 16224-30.

19. Cliff, M.J., et al., *Conformational diversity in the TPR domain-mediated interaction of protein phosphatase 5 with Hsp90.* Structure, 2006. **14**(3): p. 415-426.

20. Cliff, M.J., et al., *Molecular recognition via coupled folding and binding in a TPR domain.* Journal of Molecular Biology, 2005. **346**(3): p. 717-732.

21. Zeke, T., et al., *Human protein phosphatase 5 dissociates from heat-shock proteins and is proteolytically activated in response to arachidonic acid and the microtubule-depolymerizing drug nocodazole.* Biochem J, 2005. **385**(Pt 1): p. 45-56.

22. Hohfeld, J., D.M. Cyr, and C. Patterson, *From the cradle to the grave: molecular chaperones that may choose between folding and degradation.* Embo Reports, 2001. **2**(10): p. 885-890.

23. Mayer, M.P. and B. Bukau, *Hsp70 chaperones: Cellular functions and molecular mechanism.* Cellular and Molecular Life Sciences, 2005. **62**(6): p. 670-684.

24. Connell, P., et al., *The co-chaperone CHIP regulates protein triage decisions mediated by heat-shock proteins.* Nature Cell Biology, 2001. **3**(1): p. 93-96.

25. Qian, S.B., et al., *CHIP-mediated stress recovery by sequential ubiquitination of substrates and Hsp70.* Nature, 2006. **440**(7083): p. 551-555.

26. Chen, S.Y. and D.F. Smith, *Hop as an adaptor in the heat shock protein 70 (Hsp70) and Hsp90 chaperone machinery.* Journal of Biological Chemistry, 1998. **273**(52): p. 35194-35200.

27. Heinlein, C.A. and C.S. Chang, *Role of chaperones in nuclear translocation and transactivation of steroid receptors.* Endocrine, 2001. **14**(2): p. 143-149.

28. Paulmurugan, R., et al., *Molecular imaging of drug-modulated protein-protein interactions in living subjects.* Cancer Res, 2004. **64**(6): p. 2113-9.

29. Chang, L., et al., *Mutagenesis Reveals the Complex Relationships between ATPase Rate and the Chaperone Activities of Escherichia coli Heat Shock Protein 70 (Hsp70/DnaK).* Journal of Biological Chemistry, 2010. **285**(28): p. 21282-21291.

30. Amblard, M., et al., *Methods and protocols of modern solid phase Peptide synthesis.* Mol Biotechnol, 2006. **33**(3): p. 239-54.

31. Jiang, Y.Q., et al., *Split Renilla Luciferase Protein Fragment-assisted Complementation (SRL-PFAC) to Characterize Hsp90-Cdc37 Complex and Identify Critical Residues in Protein/Protein Interactions.* Journal of Biological Chemistry, 2010. **285**(27): p. 21023-21036.

32. Wu, S.J., et al., *Different combinations of the heat-shock cognate protein 70 (hsc70) C-terminal functional groups are utilized to interact with distinct tetratricopeptide repeat-containing proteins.* Biochemical Journal, 2001. **359**: p. 419-426.

33. Liu, F.H., et al., *Specific interaction of the 70-kDa heat shock cognate protein with the tetratricopeptide repeats.* Journal of Biological Chemistry, 1999. **274**(48): p. 34425-34432.

34. Russell, L.C., et al., *Identification of conserved residues required for the binding of a tetratricopeptide repeat domain to heat shock protein 90.* Journal of Biological Chemistry, 1999. **274**(29): p. 20060-20063.

35. Southworth, D.R. and D.A. Agard, *Client-Loading Conformation of the Hsp90 Molecular Chaperone Revealed in the Cryo-EM Structure of the Human Hsp90:Hop Complex.* Molecular Cell, 2011. **42**(6): p. 771-781.

36. Revington, M., et al., *NMR investigations of allosteric processes in a two-domain Thermus thermophilus Hsp70 molecular chaperone.* Journal of Molecular Biology, 2005. **349**(1): p. 163-183.

37. Krukenberg, K.A., et al., *Conformational dynamics of the molecular chaperone Hsp90.* Quarterly Reviews of Biophysics, 2011. **44**(2): p. 229-255.

38. Smith, M.C., et al., *The E3 Ubiquitin Ligase CHIP and the Molecular Chaperone Hsc70 Form a Dynamic, Tethered Complex.* Biochemistry.

39. Swain, J.F., et al., *Hsp70 chaperone ligands control domain association via an allosteric mechanism mediated by the interdomain linker.* Mol Cell, 2007. **26**(1): p. 27-39.

40. Bertelsen, E.B., et al., *Solution conformation of wild-type E. coli Hsp70 (DnaK) chaperone complexed with ADP and substrate.* Proc Natl Acad Sci U S A, 2009. **106**(21): p. 8471-6.

41. Zuiderweg, E.R., et al., *Allostery in the Hsp70 chaperone proteins.* Top Curr Chem, 2013. **328**: p. 99-153.

42. Chen, M.X. and P.T.W. Cohen, *Activation of protein phosphatase 5 by limited proteolysis or the binding of polyunsaturated fatty acids to the TPR domain.* Febs Letters, 1997. **400**(1): p. 136-140.
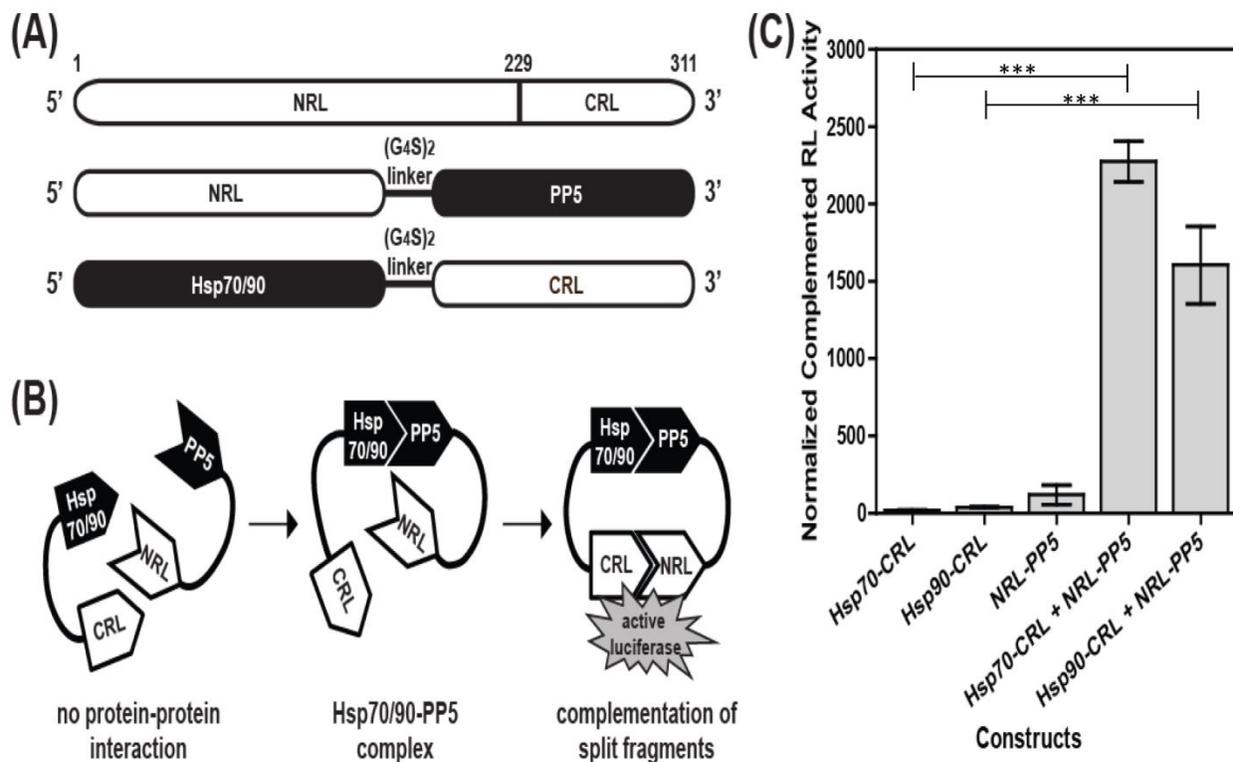
Appendix Figure 2-1. **SRL-PFAC confirm that both Hsp70-PP5 and Hsp90-PP5 interact.** (A) Schematic diagram of plasmid constructs. The two interacting proteins Hsp70/90 and PP5 are fused to NRL (amino acids 1–229) and CRL (amino acids 230–311) portion of the RL, respectively through a $(G_4S)_2$ peptide linker. (B) Schematic diagram of the SRL-PFAC system for monitoring complex formation between Hsp70/90 and PP5. Interactions between Hsp70/90 and PP5 bring CRL and NRL in close proximity, ultimately resulting in the complementation of RL enzyme activity and photon production in the presence of the substrate coelenterazine. (C) SRL-PFAC system is sensitive for monitoring complex formation of Hsp70/90 and PP5 and shows highly complemented RL activity and low background. HEK293 cells were transduced with either Hsp70-CRL, Hsp90-CRL, NRL-PP5, Hsp70-CRL + NRL-PP5, or Hsp90-CRL + NRL-PP5. Data are presented as mean ± S.D. ($n = 3$). *** p<0.001 compared to control
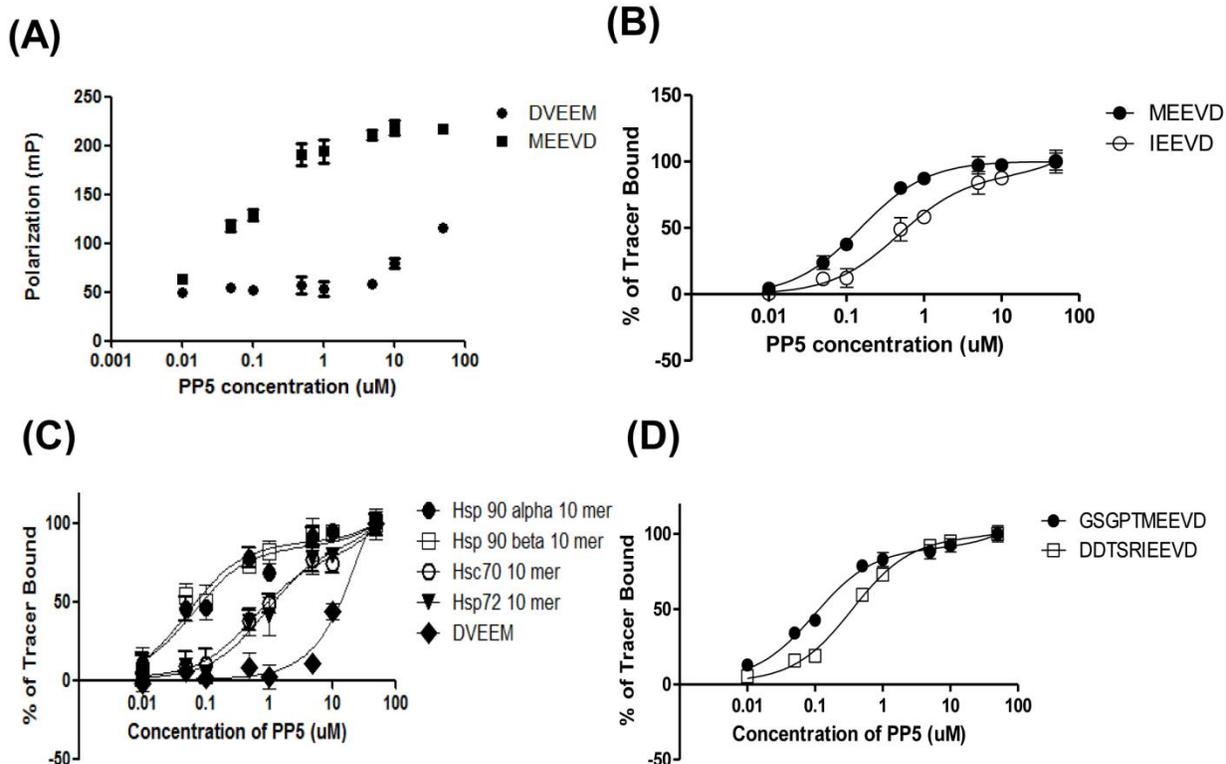
Appendix Figure 2-2. Fluorescence polarization confirms that Hsp90-PP5 has higher affinity than Hsp70-PP5. (A) Raw mP values were plotted with control peptide. No binding was observed with increasing concentrations of PP5 and control peptide at 20nM. (B) Direct binding was measured with increasing concentration of PP5 and 5mer peptides (20nM) (C) Direct binding was measured using increasing concentrations of purified full length PP5 with 5FAM 10mer labeled peptide (20 nM). (D)To see how the residues M and I contribute affinity to PP5, HSP70-90 peptides were synthesis so that HSP90 10mer peptide contained an I instead of an M and HSP70 10mer peptide contained an M instead of an I. FP was performed with increasing concentrations of PP5 and both peptides were held constant at 20 nM. Data are presented as mean ± S.D. ($n = 3$).

(A), **(B)**, **(C)**, **(D)**
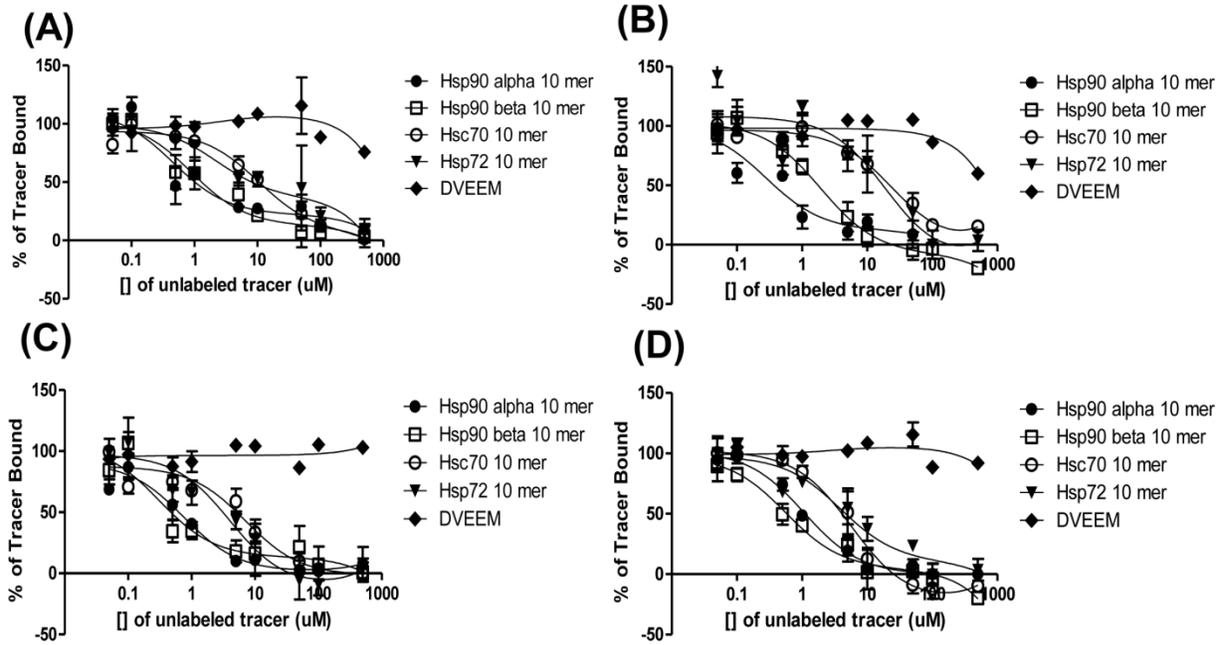
|	Hsp90 α	Hsp90 β	Hsc70	Hsp72
5FAM- Hsp90α	1.23 ± 0.95 μM	1.51 ± 0.53 μM	13.7 ± 2.9 μM	12.87 ± 4.6 μM
5FAM- Hsp90β	1.612 ± 0.76 μM	2.19 ± 1.13 μM	20.4 ± 5.37 μM	20.3 ± 11.69 μM
5FAM- Hsc70	1.0 ± 0.24μM	1.0 ± 025 μM	5.19 ± 2.0 μM	2.94 ± 1.25 μM
5FAM-Hsp72	0.507 ± 0.12 μM	0.7 ± 0.17 μM	4.97 ± 0.7 μM	4.27 ± 2.2 μM

Appendix Figure 2-3. **Competition studies confirm binding data.** (A) Competition of 5FAM-HSP90α (20nM) with increasing concentrations of unlabeled tracer (HSP90α, HSP90β, HSC70, HSP72 peptides). (B) Competition of 5FAM-HSP90β (20nM) with increasing concentrations of unlabeled tracer (HSP90α, HSP90β, HSC70, HSP72 peptides). (C) Competition of 5FAM-HSC70 (20nM) with increasing concentrations of unlabeled tracer (HSP90α, HSP90β, HSC70, HSP72 peptides). (D) Competition of 5FAM-HSP72 (20nM) with increasing concentrations of unlabeled tracer (HSP90α, HSP90β, HSC70, HSP72 peptides). Data are presented as mean ± S.D. (n = 3).

157
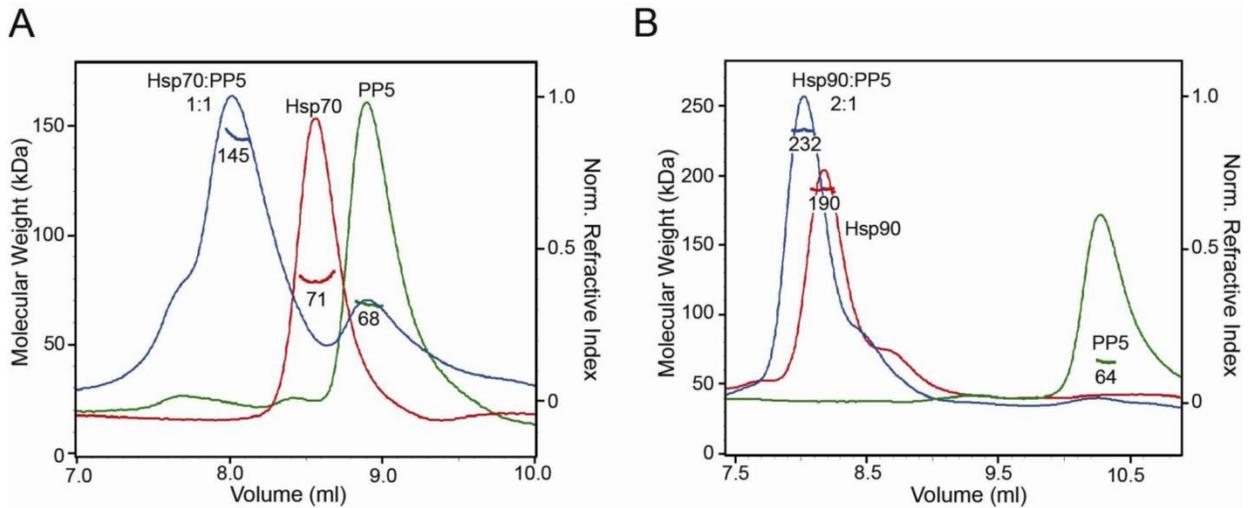
Appendix Figure 2-4. **Hsp70-PP5 and Hsp90 interact with different stoichemetries.** PP5 binds intact Hsp70 and Hsp90. (A) SEC-MALS analysis of Hsp70:PP5 (blue) shows elution volume shift and molecular weight of 145 kDa, indicating stable 1:1 complex compared to Hsp70 (red) and PP5 (green) alone. (B) Hsp90:PP5 (blue) is shifted in elution volume and determined to be a 2:1 complex at 232 kDa compared Hsp90 dimer alone (red). Molecular weights determined from the Raleigh ratio, measured by static light scattering, and the protein concentration (right Y-axis), measured by a refractive index detector are indicated. Molecular weights based on sequence are: 70 (Hsp70), 56 (PP5) and 170 (Hsp90 dimer). SEC columns WTC-030S5 and WTC-050S5 (Wyatt Technology) were used to optimally separate free Hsp70 and Hsp90 from PP5 complexes, respectively.
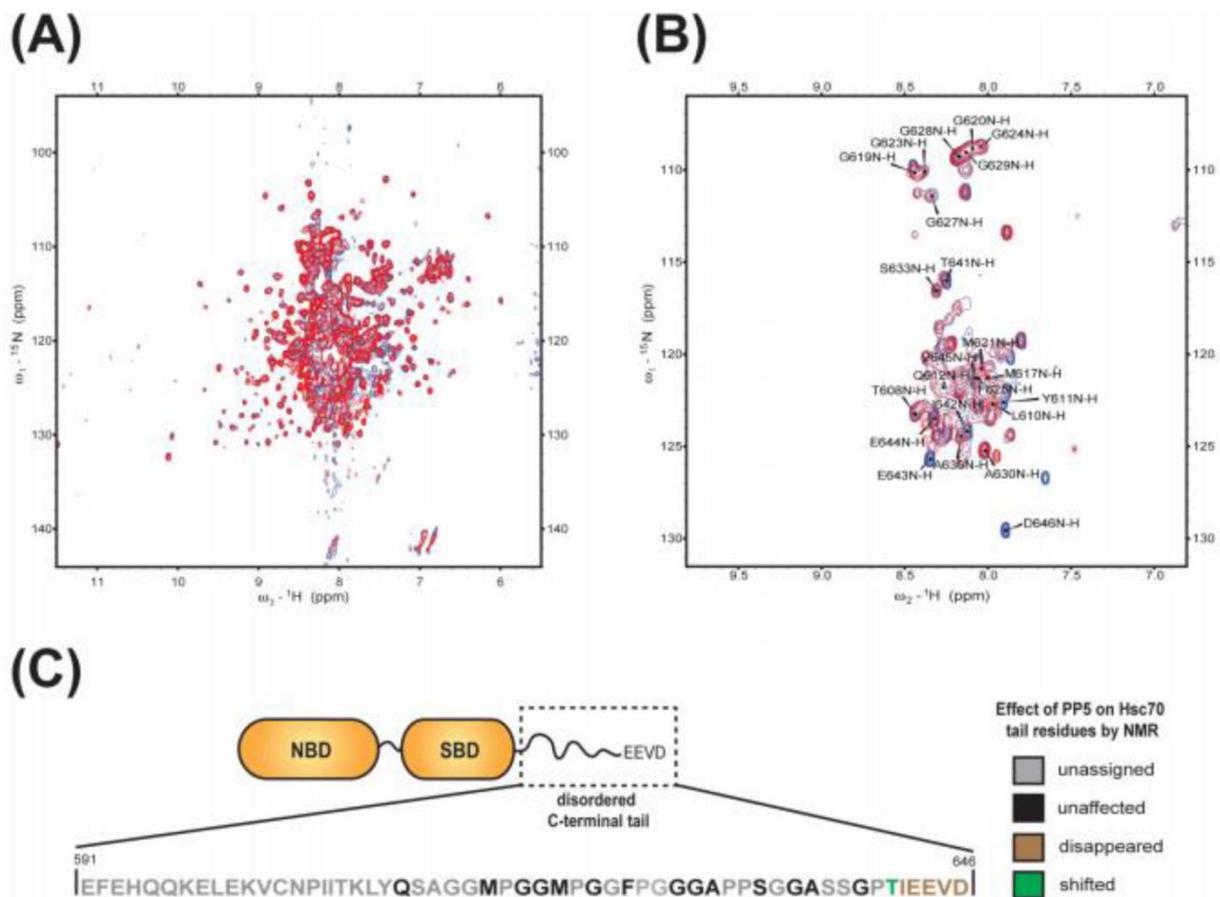
Appendix Figure 2-5. **C-terminal residues of Hsc70 bind PP5**. (a) Full 800 MHz TROSY spectra of 15N-labeled Hsc70 alone (blue) and in a 1:1 mixture with PP5 (red). (b) High-contour view of spectra with resonance assignments. (c)Schematic diagram of the disordered C-terminal tail of Hsc70. Unassigned residues are shown in gray. Residues from Hsc70 that are unaffected by binding the binding of PP5 are depicted in black; those that disappear or shift are shown in brown and green, respectively.
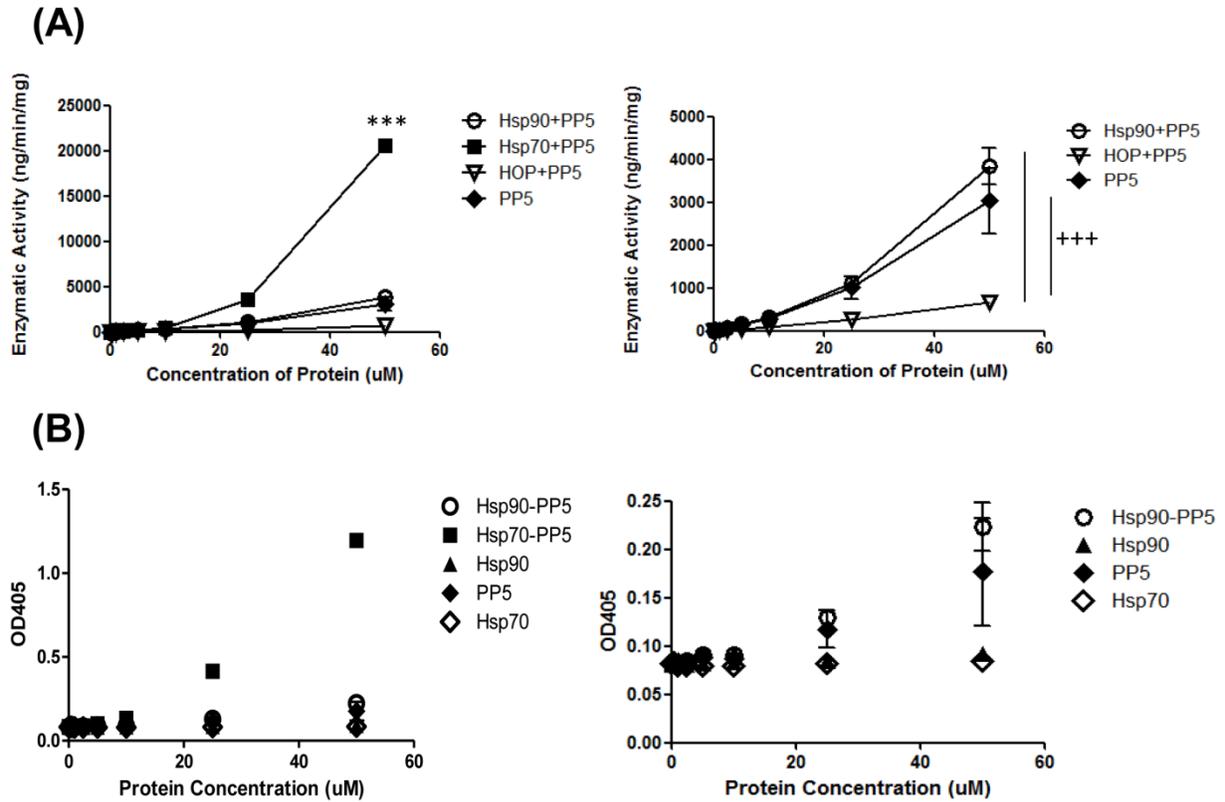
Appendix Figure 2-6. **Hsp70 preferentially stimulates PP5's phosphatase activity.** p-nitrophenylphosphate substrate was added at a concentration of 4.5mM to each well. (A) Represents enzymatic activity. (B) Represent the raw OD values; this confirms that the phosphatase is not due to ATPase from Hsp70 or Hsp90 alone. Data are presented as mean ± S.D. (n = 3). *** $p<0.001$ compared to Hsp90-PP5. +++ $p<0.001$ compare to Hop-PP5.

160

C-terminal Peptide Sequences	Corresponding Human Chaperones
MEEVD	Hsp90α/β
IEEVD	Hsc70 and Hsp72
DDTSRMEEVD	Hsp90α
EDASRMEEVD	Hsp90β
SSGPTIEEVD	Hsc70
GSGPTIEEVD	Hsp72
DVEEM	reverse peptide control
DDTSRIEEVD	Hsp90α mutant
GSGPTMEEVD	Hsp72 mutant

Appendix Table 2-1. **Peptides used in fluorescence polarization assay.** Hsp70/90 C-terminal peptides used in fluorescence polarization assays. For binding experiments, each peptide tracer/probe contained an amino-terminal 5-carboxyfluorescein (5FAM) labeled. Labels were connected to peptides through an aminohexanoic acid (AHX) linker. Additionally, for competitive binding experiments, each unlabeled peptide competitor contained a free amino-terminal end. Mutant residues in the C-terminal tracer are highlighted in gray.

Domain	MW	τ_c @ 30 C[a]	^{1}HN HSQC LW[b]	^{1}HN TROSY LW[b]	^{15}N TROSY LW[b]	TROSY transfer efficiency[c]	Rel. peak height[d]
	kDa	ns	Hz	Hz	Hz	%	a.u.
tail	10	7	20	16	0.5	39	1.0E+00
SBD	25	14	40	32	0.9	15	1.9E-01
NBD	45	23	65	51	1.5	4.7	3.8E-02
Hsc70	70	40	112	90	2.5	0.5	2.3E-03
PP5+tail	70	40	112	90	2.5	0.5	2.3E-03
PP5+SBD	85	45	126	100	2.8	0.3	1.1E-03
PP5+NBD	105	55	154	122	3.5	0.07	2.4E-04
PP5+Hsc70	130	70	196	156	4.4	0.01	2.6E-05

TABLE 2 **Summary of NMR of Hsc70-PP5**

Appendix Table 2-2. **Summary of NMR**. (a) The rotational correlation time τ_c was estimated from the molecular weight following reference [43]. (b) The average amide proton and nitrogen linewidths (LW) at 800 MHz were calculated from coordinates of the crystal structure of ubiquitin as a model, using different rotational correlation times. The calculations took into account all dipole-dipole interactions with all magnetic nuclei in the molecule, and ^{1}H CSA or ^{15}N CSA relaxation. ^{1}H-^{15}N dipolar / ^{1}H CSA or ^{1}H-^{15}N dipolar / ^{15}N CSA cross correlated R_2 relaxation was taken into account for the columns marked "TROSY". We assumed uniform ^{15}N labeling, no ^{13}C or ^{2}H labeling. (c) In TROSY there are three transfer periods with ^{1}HN coherence, that all are tuned to $1/2J_{NH}$ (5 ms). The transfer efficiency is reduced by ^{1}H R_2 relaxation. In total, $I=I_0 (exp(-3.1416*LW*0.005))^3$. The relevant linewidths during these transfers are listed in the column marked "^{1}HN HSQC LW". (d) The peak height for 10 kDa was taken as a standard. The peak heights for other molecular weights were computed by taking the ratio of the relevant transfer efficiencies divided by the ratio of the relevant ^{1}H TROSY linewidths (the latter affects peak height during data acquisition). The effect of increasing ^{15}N linewidth on the TROSY peak intensity is minimal because of the short ^{15}N acquisition time used, and was not included in the calculation.

Appendix 3
High Throughput Screening for Small Molecules to Block TPR containing Co-chaperones- Hsp90 Chaperone Complex

Abstract

Heat Shock Protein 90 (Hsp90) is involved in a complex which facilitates the maturation of many oncogenic client proteins. For this reason, targeting this complex for cancer therapy has been an interest for many. In this study we performed a high throughput screen (HTS) to identify small molecules to inhibit this complex. A subset of co-chaperone proteins, known as tetratricopeptide domain (TRP) proteins, are known to bind to Hsp90 to aid in client folding and help HSP90 carry out its function. Therefore, we believed that if we inhibit these Hsp90-TPR domain containing proteins, it would provide a novel approach at targeting cancer. In this study, we screened two different protein-protein interactions; Hsp90-PP5 and Hsp90- HOP. We optimized our screen using a fluorescence polarization platform and looked at over 140,000 small molecules with these two interactions at the University of Michigan Center for Chemical Genomics (CCG). Our findings suggested that the TPR containing proteins -Hsp90 interactions are difficult to target and to find a specific yet druggable molecule for therapeutic purposes. Perhaps a peptidomimetics would be a better option for targeting this interaction.

Introduction

Hsp90 interacts with co-chaperones to form a complex which regulates the maturation and activity of many oncogenic proteins in disease states. To date, various Hsp90 inhibitors that bind to Hsp90 at its ATP-binding pocket have reached preclinical and clinical trials [1-4]. However, many limitation of these compounds for clinical use have failed due to toxicity [5]. Therefore, alternative strategies in inhibiting Hsp90 function should be explored. One innovative approach is targeting protein-protein interactions (PPI) between TPR contain proteins that bind with Hsp90 [6, 7]. The C-terminal residues, MEEVD of Hsp90 has been recognized to bind to co-chaperones that contain TPR domains [8-10]. Therefore, we hypothesized inhibiting the MEEVD-TPR interactions would alter Hsp90 function and degrade a subset of oncogenic proteins, which would provide more specificity and selectivity against cancer cells.

TPR containing proteins are highly conserved having tandem repeats of 34 amino acids. Both Hsp70 and Hsp90 are found to be "universal acceptors" for TPR proteins [11]. Co-chaperones that interact with Hsp90 that contain TPR domains are Protein Phosphatase 5 (PP5), Hsp70-Hsp90 Organizing Protein (HOP), Carboxy terminus of Hsp70-interacting protein (CHIP), and FK506 binding protein 51 kDa and 52kDa (FKBP51 and FKBP52) [11-16]. The presences and mechanisms of many of these protein interactions remain unclear. However, there has been an association between these TPR containing protein malfunction and disease states [12].

Both PP5 and HOP are two TPR containing co-chaperone proteins that interact with the complex. The function to date of PP5 is unknown and controversial. However,

it has been shown in many studies that it is involved in cell signal transduction [17-19]. Furthermore, PP5 possesses auto-inhibitory domain and maintains low basal activity. In order to relieve this autoinhibition, studies have concluded that Hsp70, Hsp90, or arachondonic acid needs to bind to PP5 [20-24]. HOP's function is still not fully understood to date, but it has been shown that HOP facilitates Hsp70 and Hsp90 binding as well as shuffle client proteins between the two chaperones [25]. Similarly to Hsp90 in the disease states, both HOP and PP5 expression have been positively correlated in cancer. PP5 has been shown to be overexpressed in human breast cancer tissue as well as its expression aiding in breast cancer cell growth (in a MCF-7, an ER+ breast cancer cell line) [26, 27]. In addition, the role of HOP has also been implemented to be important in a disease state. In one study, it was shown that knock down of HOP using siRNA in colon cancer cell lines decreased cell viability [28]. These studies provided evidence for the importance to inhibit Hsp90-TPR domain containing interactions.

Although the affinity of these interactions vary, many of these TPR proteins bind to Hsp90 similarly through the positive residues of lysine and arginine, known as the carboxylate clamp [20]. Therefore, we proposed that inhibitors to TPR co-chaperone-Hsp90 interaction will ultimately be an effective way at targeting the Hsp90 complex. Our hypothesis is that small molecules to block the TPR-Hsp90 interaction will ultimately decrease cancer cell viability by degrading oncogenic client proteins that rely on maturation from this PPI.

Material/ Methods

Reagents

The peptide expressing Hsp90 10 C-terminal peptide (5FAM-DDTSRMEEVD) was purchased from Biomatik (SPR001). Black 96 well plates and 384 well plates were purchased from Corning (3792 and 3676). Follow up compounds were purchased from ChemDiv (cat #: D077-0329, 2039-0579, G756-0219, N025-0039, G756-0234, G617-0103, 4984-0429, 3389-1518, and 8407-0790). The following compounds were also ordered; Trans-2-phenylcyclopropylamine HCl (Sigma p8511), dihydrotanshinone I (Sigma D0947), and suramin (Calbiochem 574625).

Fluorescence Polarization Assay:

All fluorescence polarization (FP) experiments were conducted in 384-well black, low volume, round-bottom plates (Corning 3676) using a BioTeck Synergy 2 plate reader (Winooski, VT). For binding experiments, to each well, we added increasing concentration of full length protein and the 5-carboxyfluorescein (5-FAM) labeled Hsp90 C-terminal probe/tracer. For screening compounds each well had PP5 protein at 100 nM or HOP protein at 4 μM concentration (equivalent to the K_d), 5-FAM Hsp90 10-mer peptide was held constant at 6 nM for PP5 or 3 nM for HOP, and compounds or DMSO were pin tooled into each well. All wells had a final volume of 20 μL in the assay buffer (for PP5 the assay buffer was 40 mM Tris-HCl, pH=7.4, 10% glycerol, 1mM DTT, 0.1% tween 20 and for HOP the assay buffer was 20 mM Tris-HCl pH= 8.0, 50 mM NaCL, 1mM DTT, 10% glycerol, and 0.1% tween 20). The plate was allowed to incubate at room temperature for 30 minutes to reach equilibrium. The polarization values,

millipolarization units (mP) was measured at an excitation wavelength at 485 nm and an emission wavelength at 528 nm.

High Throughput Screening:

All screening was performed at the Center of Chemical Genomics (CCG) at the University of Michigan. For PP5; the screening libraries included the biofocus NCC, focused collection, and MS spectrum which totaled to 4160 compounds. For HOP, 100,000 compounds were screened in the ChemDiv library.

The FP assays were optimized in the CCG laboratory with detergent and DMSO. For primary screen (n=1), each compound was pin tooled using at Biomek FX liquid handling robot into the wells at 10 µM (0.2 µL). For the positive control on each plate, 5-FAM was used alone for the negative control 5-FAM, protein and DMSO was used. The positive and negative controls were used to calculate the Z' factor for the assay (see equation below); each plate assays was considered acceptable if the Z'> 0.5. Compounds that showed activity and were at least 3 standard deviations (3SD) above the negative control were next analyzed in a dose response curves (DRC).

$$Z' = 1 - \frac{3(Xp + Xn)}{SDp - SDn}$$

Where Xp is the average of the positive control, Xn is the average of the negative control, SDp is the standard error of the positive control, and SDn is the average of the negative control.

DRC compounds were added to wells ranging from concentrations of 100 µM to 1 nM, compounds were ran in triplicate for DRC to eliminate any false positives. Each compound was added to each well using a TTP Labtech Mosquito X1. Each well was verified that signal detection was not a result of quench signal or that the compound was fluorescent. Leads from the DRC were repurchased for confirmation and secondary assays.

Results

Optimization of the Fluorescence Polarization Assay

A fluorescence polarization (FP) assay which relies on the rotation of the protein/ protein complex was established for full length HOP and full length PP5 proteins with a 10-mer peptide (DDTSRMEEVD) corresponding to the C-terminal of Hsp90. The FP assay depends on the labeled peptide to measure the fluorescence; when the labeled peptide is free (no binding); rotation of the peptide in solution occurs at a higher rate which produces a low mP measurement. Whereas, when the labeled peptide is able to bind to the protein, the larger complex slows down in rotation corresponding to a high mP reading. To demonstrate that the Hsp90 was indeed able to bind both HOP and PP5, a dose response curve was established for this interaction using increasing concentrations of HOP or PP5. **Figure 1A** verified that the binding affinity for PP5-Hsp90 10-mer was on the low nanomolar scale (66 nM), which provided an ideal binding affinity for screening small molecules. This result was confirmed using a competition assay; the unlabeled peptide of Hsp90 10-mer (DDTSRMEEVD) was able to compete away 5-FAM labeled Hsp90 10-mer peptide at an IC_{50} of 19 µM (**Figure 1B**).

In addition, we established the FP assay with HOP-Hsp90. **Figure 1C** showed

the binding affinity for HOP-Hsp90 peptide was 4.8 μM. Similarly, we validated this

platform by performing competition studies with HOP-Hsp90; however, because HOP

has 3 TPR domains that essentially can bind the Hsp90 peptide, this was a little more

difficult to confirm (**Figure1D**). Whether this curve represents a composite binding

affinity or just the affinity to TPR2A is unknown. We continued screening because we

thought that having multiple TPR domains would be beneficial for discovering an

inhibitor to this interaction. Although this affinity was slightly higher than PP5-Hsp90

interaction, the affinity was still in an acceptable range for screening purposes. We

optimized both platforms with DMSO and detergents.

Primary Screens for HOP-Hsp90 & PP5-Hsp90

After optimization, a high throughput screen (HTS) was performed. To begin with

we started screening using a primary assay for small molecules from the biofocus NCC,

focused collection, and MS spectrum library at the CCG. In the primary screen, each

small molecule was tested once at a single concentration using various libraries.

Figure 2A shows all the compounds screened for the PP5-Hsp90 interaction in

terms of the percent inhibition for each small molecule and **figure 2B** shows all the

small molecules screened for HOP-Hsp90. The positive control consisted of wells that

only contained 5FAM only (indicated by red dots). The negative control contained

5FAM, PP5 protein, and DMSO (indicated by the blue dots). Finally each of the small

molecules that were screened is indicated by the green dots. Compounds were

considered to be a lead for further pursuit if they were 3 standard deviations (3SD) away

from the negative control (indicated by the solid red line). **Table 1** summarizes this data

by libraries screened including; hit rates, total hit compounds for each protein

interaction, as well as the breakdown of each inhibition for each compound. For the

PP5-Hsp90 interaction, we screened about 3391 compounds and had a hit ratio

between 3.65-6.14% which was about 165 hits total for this interaction. For the HOP-

Hsp90 interaction, we screened a lot more compounds, about 100,000 however, how

the hit ratio was way less ~0.27% equaling about 269 hits.

Dose Response Curves Testing

A total of 434 compounds that were considered a hit and were also above 3SD

from the negative control were carried on to dose response curves (DRC). Here,

compounds were run in triplicate at concentrations ranging from 0.1 nM – 100μM.

Figure 3 shows 14 compounds that produced a dose response curve. During the DRC

testing, we also verified that none of these compounds were fluorescing or quenching.

In order to do this, 5-FAM was added to the plate first and the fluorescent values were

read. Directly following, compounds were added to see if the fluorescent values were

quenched compared to the original reading of the 5-FAM label alone. Finally, protein

was added for the final analysis. **Figure 4** shows the 14 compounds structures that had

pAC50 of >5, meaning the log of the activity (in this case inhibition or IC_{50}) were on the

sub-micromolar. These fourteen lead compounds did not show any quenching or

fluorescent effects instead retained activity of pAC50> 5 (**Table 2**).

The top leading compounds from the DRC that still showed inhibition and fairly

good activity (pAC50 of 4 or 6) were then purchased, made fresh, and retested in the

FP platform. We ordered 14 of these compounds to prepare fresh in DMSO solution at 10 mM and retested in the FP platform. The final percentage of DMSO was less than 0.02% for each well. The only compound that retained activity after being test after being freshly prepared was suramin. The rest of the compounds showed no activity in either the PP5-Hsp90 or HOP-Hsp90 platform.

Suramin inhibition of Hsp90-TPR containing proteins

Suramin was the only compound that remained a lead when retested fresh in FP platform for Hsp90-PP5. This compound showed an IC_{50} value of 6.2 ±0.6 µM. (**Figure 5**). Since many TPR containing proteins- Hsp90 have similar binding, via the positive lysine and arginine residues in the carboxylate clamp, we were curious to look at the specificity of this interaction compared to other Hsp90-TPR containing proteins. Therefore, we used full length HOP and Hsp90 10-mer peptide as well as full length CHIP and Hsp90 10-mer peptide to see if suramin also was able to block this interaction. As suspected, it was able to block the interaction at an IC_{50} of 8.7 ± 0.37 µM and 7.43 ± 0.47 µM respectively.

Optimizing Suramin

Although, suramin showed inhibition against TPR-Hsp90 interactions, suramin was far from a drug like molecule. Two apparent issues from just the structure alone were that it was highly charged and has a large molecular weight which would make it difficult for this compound to cross cell membranes (**Figure 6A**). We therefore decided that we would try to modify the compound and see if we could retain activity. **Figure 6B** shows several analogs that were synthesize. Since suramin is a dimer we tried to

171

synthesize the monomer version (**figure 6B i and ii**) and we also tried to keep the dimer but reduce the charge (**figure 6B iii**). However, when these changes were made, activity for blocking Hsp90-PP5 activity was lost (as well as activity for HOP-Hsp90 and CHIP-Hsp90).

Discussion

Targeting Hsp90 chaperone complex has been a challenge for many years. Initially targeting the ATPase of Hsp90 with geldanamycin and derivatives seemed ideal; however, after entering clinical trials it was soon realized that these compounds tend to have low affinity, high toxicity, and solubility issues. Alternative approaches to target Hsp90 are to target PPI. This too presents many problems. In this study we have presented work that targets a group of proteins that interact with Hsp90 called tetratricopeptides domain containing proteins, specifically Hsp90-PP5 and Hsp90-HOP. We found that these interactions are difficult to find a specific inhibitor that selectively binds to the TPR domains.

In this study we screened over 140,000 compounds in which none were able to specifically inhibit TPR containing proteins-Hsp90 interaction. In addition, Lynn Reagan's group had already performed a HTS screen with Hsp90 and the tetratricopeptides containing proteins, HOP [30]. Although this was performed, we still felt that we could find a new chemical entity. The previous screen with HOP consisted of an alpha screen of the TPR2A domain of HOP and the C-terminal of Hsp90. The binding affinity for this interaction was slightly higher than the FP binding affinity used in this study (11 µM vs of 4 µM). In addition, we were screening with full length HOP

instead of one domain (TPR2A), this opened up the possibility for finding compounds that could block either TPR1 and/or TPR2A domains of HOP or a compound specific to TPR2A. Finally, the screen performed previously with HOP by Regean's group was done at the National Cancer Institute- NIH Chemical Genomic Center (NCI NCGC). Comparing the NCI NCGC chemical library with the Center of Chemical Genomics (CCG) at the University of Michigan, there was only a 5% overlap in compounds. Regean's group screened nearly 97,000 compounds. Together, these screens suggest that the Hsp90-TPR containing proteins are not ideal for targeting Hsp90.

Unfortunately, the results that are suggested from our data were unsuccessful at targeting these PPI. These results suggest two things; one being that the small molecules in the Center for Chemical Genomics (CCG) may not be suitable for these PPI. We screened close to 140,000 compounds, in which only one compound, suramin was able to show any type of activity *in vitro* when fresh compound was prepared. Our lab did performed extensive follow ups with this compound. As mentioned and seen, this compound is highly charged and has a large molecular weight. Although this is obviously, we still try to treat several breast cancer cell lines with this compound using an MTS assay in hopes to see efficacy by decreasing in cell viability. However, when treating cells with this compound up to 100 μM, no difference in cell viability was seen compared to control (data not shown). In addition to suramin being highly charged and having a large molecular weight, this compound has been found to be highly promiscuous meaning that this compound hits in many other PPI screens. Due to the fact that Suramin violated many of Lipinski's rules, this was not surprising to us. This

led us to believe that suramin could possibly be a protein aggregated due to it being highly charge and having a big bulky molecular structure.

The second suggest for obtaining unsuccessful results in this screen is the nature of the binding pockets on these TPR containing proteins. Despite having relatively good affinity for Hsp90, both HSP90 and PP5 have hard pockets to target. After performing some modeling simulation it was clear that these pockets are shallow and surfaced expose making it difficult for molecules to bind in these binding pockets.

Although those results were not what we hoped for, there are many other co-chaperones that associate with Hsp90 that may be ideal for targeting PPI within this complex such as Hsp90-p23 or Hsp90-Cdc37. Or an alternative to a small molecule would be a peptidomics of the residues MEEVD for delivery purposes.

References

1. Biamonte, M.A., et al., *Heat Shock Protein 90: Inhibitors in Clinical Trials.* Journal of Medicinal Chemistry, 2010. **53**(1): p. 3-17.
2. Janin, Y.L., *ATPase inhibitors of heat-shock protein 90 second season.* Drug Discovery Today, 2010. **15**(9-10): p. 342-353.
3. Biamonte, M.A., et al., *Heat shock protein 90: inhibitors in clinical trials.* J Med Chem. **53**(1): p. 3-17.
4. Janin, Y.L., *ATPase inhibitors of heat-shock protein 90, second season.* Drug Discov Today. **15**(9-10): p. 342-53.
5. Gorska, M., et al., *Geldanamycin and its derivatives as Hsp90 inhibitors.* Frontiers in bioscience : a journal and virtual library, 2012. **17**: p. 2269-77.
6. Ardi, V.C., et al., *Macrocycles That Inhibit the Binding between Heat Shock Protein 90 and TPR-Containing Proteins.* Acs Chemical Biology, 2011. **6**(12): p. 1357-1366.
7. Cortajarena, A.L., F. Yi, and L. Regan, *Designed TPR modules as novel anticancer agents.* Acs Chemical Biology, 2008. **3**(3): p. 161-166.
8. Chen, S.Y., et al., *Differential interactions of p23 and the TPR-containing proteins Hop, Cyp40, FKBP52 and FKBP51 with Hsp90 mutants.* Cell Stress & Chaperones, 1998. **3**(2): p. 118-129.
9. Ramsey, A.J., et al., *Overlapping sites of tetratricopeptide repeat protein binding and chaperone activity in heat shock protein 90.* Journal of Biological Chemistry, 2000. **275**(23): p. 17857-17862.
10. Brinker, A., et al., *Ligand discrimination by TPR domains - Relevance and selectivity of EEVD-recognition in Hsp70 center dot Hop center dot Hsp90 complexes.* Journal of Biological Chemistry, 2002. **277**(22): p. 19265-19275.
11. Das, A.K., P.W. Cohen, and D. Barford, *The structure of the tetratricopeptide repeats of protein phosphatase 5: implications for TPR-mediated protein-protein interactions.* EMBO J, 1998. **17**(5): p. 1192-9.
12. Allan, R.K. and T. Ratajczak, *Versatile TPR domains accommodate different modes of target protein recognition and function.* Cell Stress Chaperones, 2011. **16**(4): p. 353-67.
13. Blatch, G.L. and M. Lassle, *The tetratricopeptide repeat: a structural motif mediating protein-protein interactions.* Bioessays, 1999. **21**(11): p. 932-9.
14. Cortajarena, A.L. and L. Regan, *Ligand binding by TPR domains.* Protein Sci, 2006. **15**(5): p. 1193-8.
15. Cortajarena, A.L., F. Yi, and L. Regan, *Designed TPR modules as novel anticancer agents.* ACS Chem Biol, 2008. **3**(3): p. 161-6.
16. D'Andrea, L.D. and L. Regan, *TPR proteins: the versatile helix.* Trends Biochem Sci, 2003. **28**(12): p. 655-62.
17. Morita, K., et al., *Negative feedback regulation of ASK1 by protein phosphatase 5 (PP5) in response to oxidative stress.* EMBO J, 2001. **20**(21): p. 6028-36.
18. Zhou, G., et al., *Ser/Thr protein phosphatase 5 inactivates hypoxia-induced activation of an apoptosis signal-regulating kinase 1/MKK-4/JNK signaling cascade.* J Biol Chem, 2004. **279**(45): p. 46595-605.

19. Zuo, Z., N.M. Dean, and R.E. Honkanen, *Serine/threonine protein phosphatase type 5 acts upstream of p53 to regulate the induction of p21(WAF1/Cip1) and mediate growth arrest.* J Biol Chem, 1998. **273**(20): p. 12250-8.

20. Cliff, M.J., et al., *Conformational diversity in the TPR domain-mediated interaction of protein phosphatase 5 with Hsp90.* Structure, 2006. **14**(3): p. 415-26.

21. Cliff, M.J., et al., *Molecular recognition via coupled folding and binding in a TPR domain.* J Mol Biol, 2005. **346**(3): p. 717-32.

22. Connarn, J.N., et al., *The molecular chaperone Hsp70 activates protein phosphatase 5 (PP5) by binding the tetratricopeptide repeat (TPR) domain.* J Biol Chem, 2014. **289**(5): p. 2908-17.

23. Yang, J., et al., *Molecular basis for TPR domain-mediated regulation of protein phosphatase 5.* EMBO J, 2005. **24**(1): p. 1-10.

24. Zeke, T., et al., *Human protein phosphatase 5 dissociates from heat-shock proteins and is proteolytically activated in response to arachidonic acid and the microtubule-depolymerizing drug nocodazole.* Biochem J, 2005. **385**(Pt 1): p. 45-56.

25. Chen, S. and D.F. Smith, *Hop as an adaptor in the heat shock protein 70 (Hsp70) and hsp90 chaperone machinery.* J Biol Chem, 1998. **273**(52): p. 35194-200.

26. Golden, T., et al., *Elevated levels of Ser/Thr protein phosphatase 5 (PP5) in human breast cancer.* Biochim Biophys Acta, 2008. **1782**(4): p. 259-70.

27. Urban, G., et al., *Identification of an estrogen-inducible phosphatase (PP5) that converts MCF-7 human breast carcinoma cells into an estrogen-independent phenotype when expressed constitutively.* J Biol Chem, 2001. **276**(29): p. 27638-46.

28. Walsh, N., et al., *RNAi knockdown of Hop (Hsp70/Hsp90 organising protein) decreases invasion via MMP-2 down regulation.* Cancer Lett. **306**(2): p. 180-9.

29. Scheufler, C., et al., *Structure of TPR domain-peptide complexes: critical elements in the assembly of the Hsp70-Hsp90 multichaperone machine.* Cell, 2000. **101**(2): p. 199-210.

30. Yi, F., et al., *An AlphaScreen-based high-throughput screen to identify inhibitors of Hsp90-cochaperone interaction.* J Biomol Screen, 2009. **14**(3): p. 273-81.
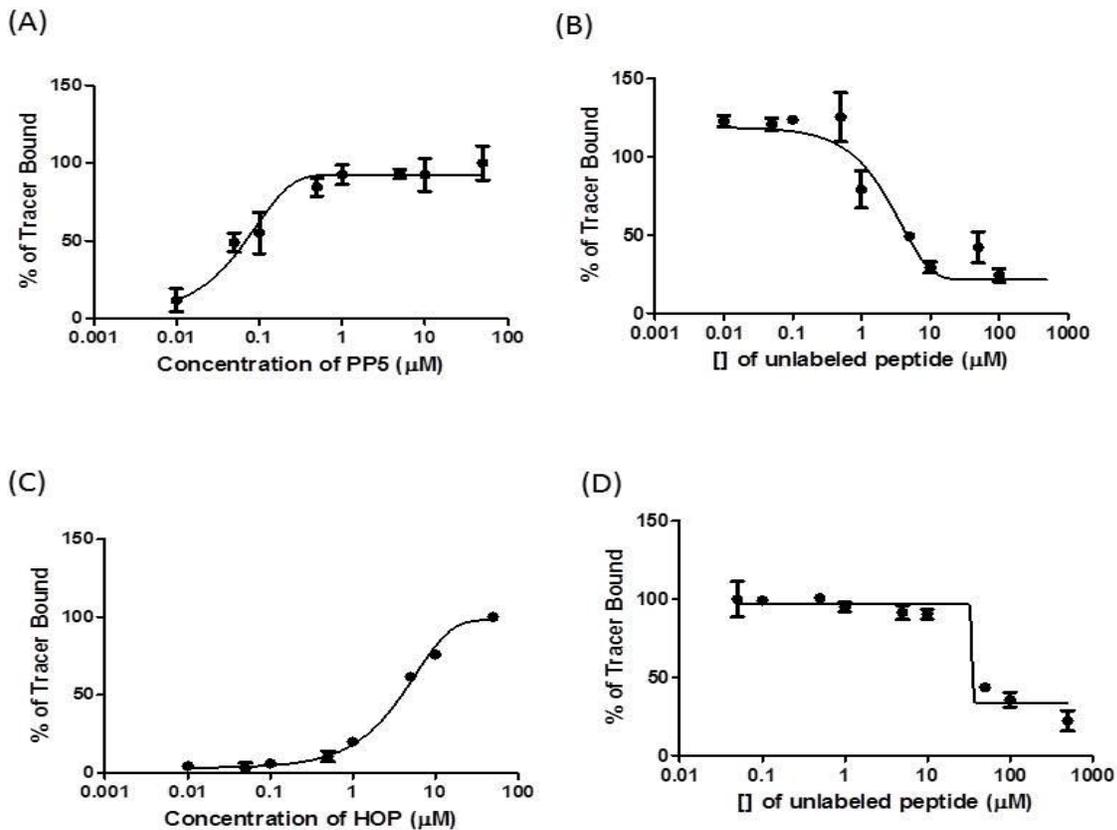
Appendix Figure 3-1. **Fluorescence Polarization Assay.** (A) FP was performed with increasing amounts of full length PP5. 5FAM-Hsp90 10mer peptide was held constant at 6 nM. (B) Full length PP5 (at 100 nM) and 5FAM-Hsp90 peptide (6 nM) interaction was competed away with increasing concentrations of unlabeled peptide. (C) FP was performed with increasing amounts of full length HOP. 5FAM-Hsp90 10mer peptide was held constant at 3 nM. (D) Full length HOP (4 µM) and 5FAM-Hsp90 peptide (3 nM) interaction was competed away with increasing concentrations of unlabeled peptide. Data represents as a mean ± standard deviation (n=3).

(A)

(B)
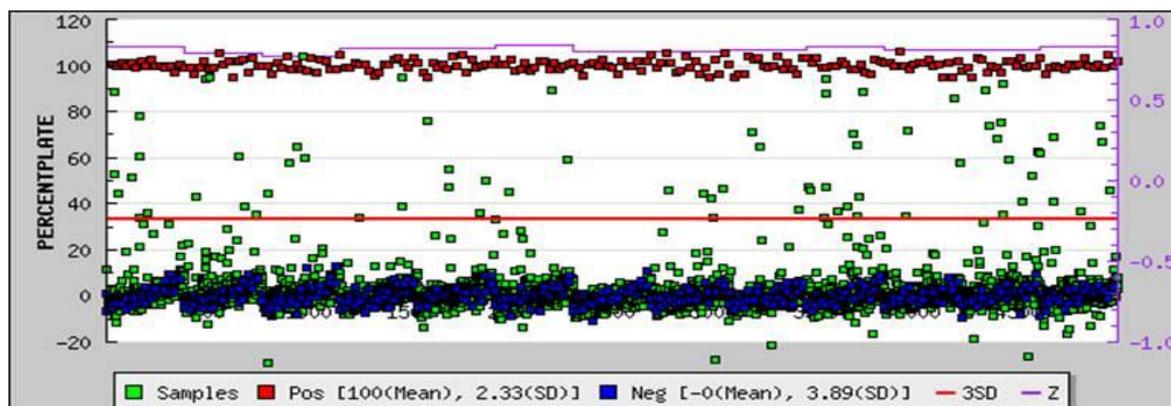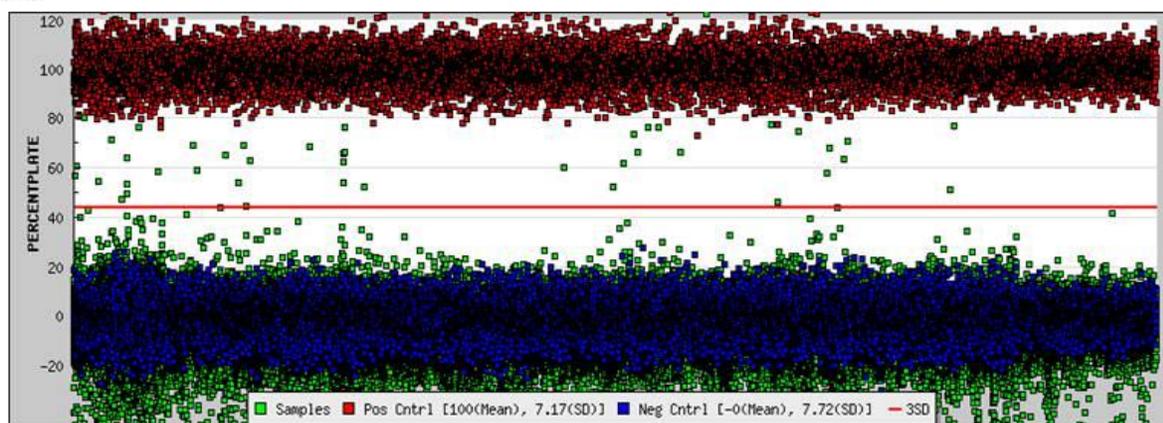
Appendix Figure 3-2. **Primary Screen of TPR containing proteins-Hsp90 peptide.** (A) Primary Assay for Hsp90-PP5. (B) Primary Assay for Hsp90-HOP. The negative control is indicated as the blue dots, the positive control is indicated as the red dots, the solid red line indicates 3SD way from negative control, and the green dots indicate the small molecules screened.

178

(A)

(B)
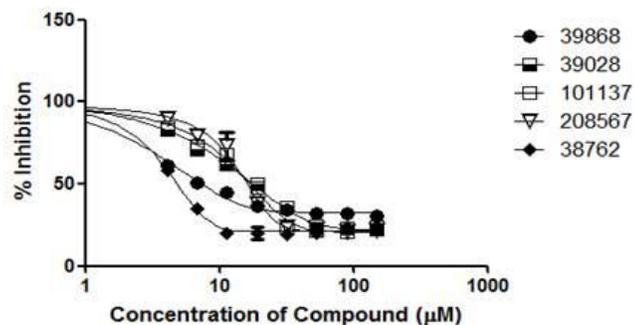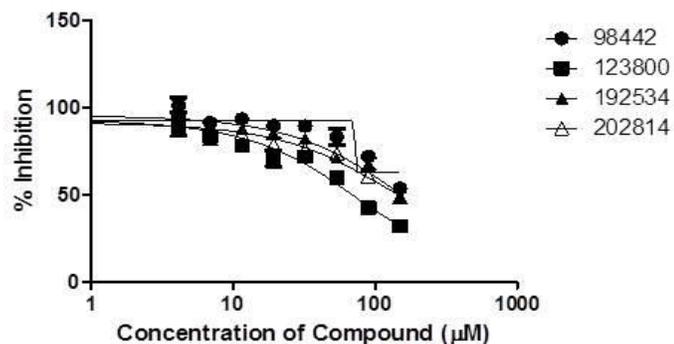
Appendix Figure 3-3. **Dose Response Curves from Hit Compounds.** The data reflects the average dose response curves with inhibitors against (A) Hsp90-PP5 interaction or (B) Hsp90-HOP interaction

179

CCG-100829   CCG-101137   CCG-38762   CCG-207955

CCG-208008

CCG-68895   CCG-202814

CCG-192534   CCG-190358   CCG-113447

CCG-123800

CCG-13232   CCG-107745   CCG-98442
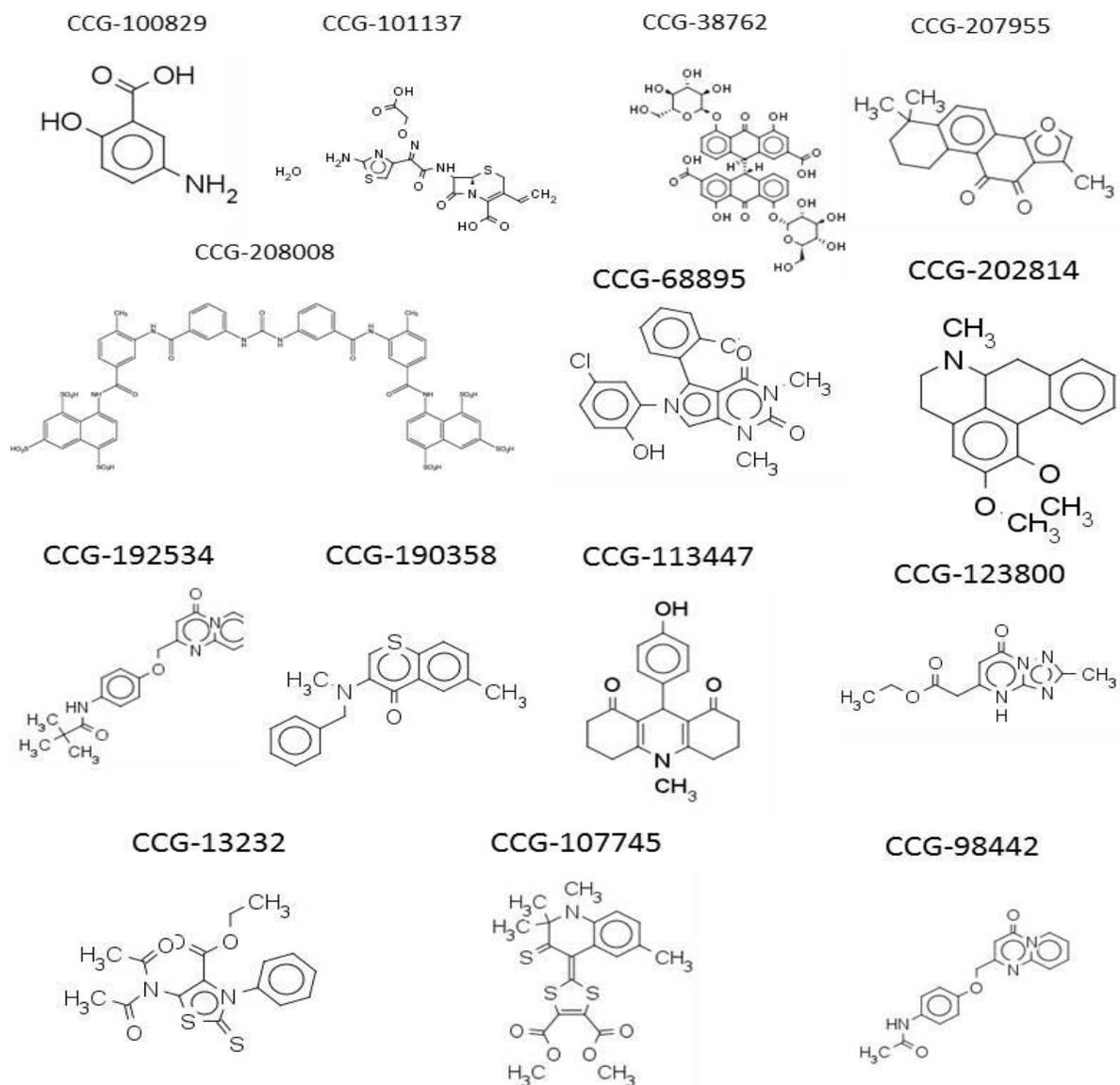
Appendix Figure 3-4. Hits from DRC. Compounds that were still leads after DRC and maintained activity of pAC50>4 (n=3).

**Suramin inhibition on TPR containing Proteins**
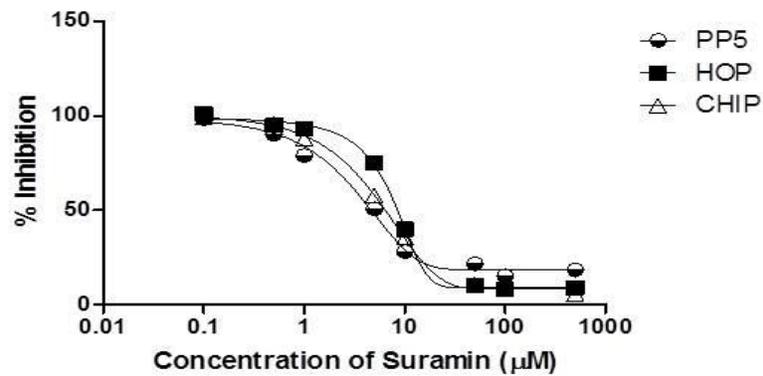
TPR protein	IC50
PP5	6.2 ± 0.6 µM
HOP	8.7 ± 0.37 µM
CHIP	7.43 ± 0.47 µM

Appendix Figure 3-5. **Suramin inhibits TPR containing proteins-Hsp90.** Increasing concentrations of suramin was used to measure the percent inhibition between TPR contain proteins and Hsp90.

(A)

(B)

i.

Chemical Formula: $C_{21}H_{15}N_3O_6$
Molecular Weight: 405.37

ii.

Chemical Formula: $C_{21}H_{17}N_3O_4$
Molecular Weight: 375.38

iii.

Chemical Formula: $C_{43}H_{32}N_6O_9$
Molecular Weight: 776.76
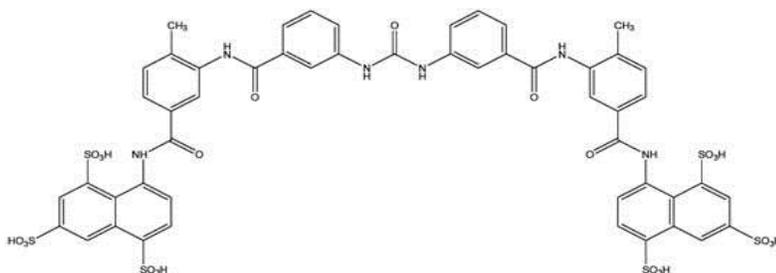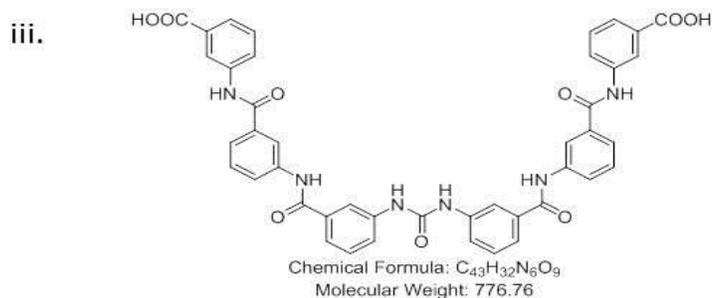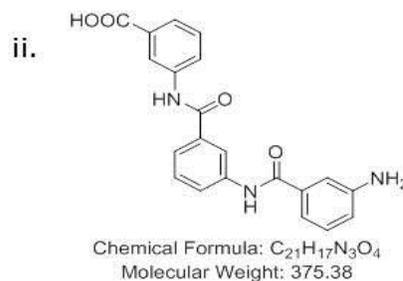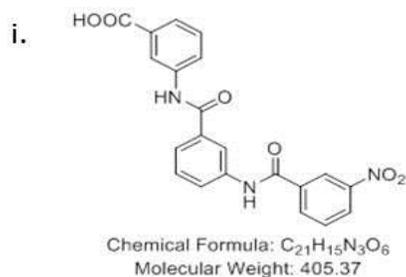
Appendix Figure 3-6. **Sumarin and Analogs for inhibiting Hsp90-TPR containing proteins**. (A) Suramin was made in a fresh stock solution and the FP assay was repeated. Suramin was able to block the Hsp90-PP5 interaction at an IC_{50} of 9.06 μM. (B) Analogs of suramin to eliminate charge and mass were produced.

(A) PP5-HSP90 Primary Screen

Avg Plate Z	Hits	< 0%	0 - 19 %	20 - 39 %	40 - 59 %	60 - 79 %	80 - 99 %	>= 100 %	TOTAL	Outliers
0.81	165	1982	2060	46	23	18	11	11	4160	0

Library	Hits	Total Screened	Hit Ratio
BioFocus NCC	20	446	4.48 %
Focused_Collections	58	945	6.14 %
MS Spectrum 2000	73	2000	3.65 %

(B) HOP-HSP90 Primary Screen

Avg Plate Z	Hits	<-20%	-20 to 0%	0 - 19%	20 - 39%	40 - 59%	60 - 79%	80 - 99%	100 - 120%	> 120%	TOTAL
0.55	269	5907	64941	29346	329	22	26	9	9	21	100800

Library	Hits	Total Screened	Hit Ratio
ChemDiv_100K	269	100000	0.27 %

Appendix Table 3-1. **Summary of Primary Screen for TPR-Hsp90.** (A) Indicated that hits, percent inhibition for each hit, and library for each small molecule for the Hsp90-PP5 interaction. (B) Indicated that hits, percent inhibition for each hit, and library for each small molecule for the Hsp90-HOP interaction.

183

Library	Actives	pAC50 < 4	4 - 5	5 - 6	6 - 7	pAC50 > 7
MS Spectrum 2000	16	17	12			
BioFocus NCC	2	4	1			
Focused_Collections	6	5	4			
MS2000_NCC_Focused	49	58	29	5		
ChemDiv 1000	7					

Appendix Table 3-2. **Summary of Dose Response Screen for TPR domain- Hsp90 peptide.** MS Spectrum2000, BioFocusNCC, Focused_Collection, and MS2000_NCC_Focused were screened against the Hsp90-PP5 interaction. The ChemDiv 1000 was screened against the Hsp90-HOP interaction.